AD-A073 342 TRW DEFENSE AND SPACE SYSTEMS GROUP REDONDO BEACH CA F/G 17/2
DESIGN AND ANALYSIS OF 777 'FLY-BY-WIRE' CONTROL SYSTEM.(U)
APR 76 H C OSBORNE F04701-75-C-0257
UNCLASSIFIED TRW-TR-28600-AR-011-01 SAMSO-TR-79-14 NL

1 OF 2
AD A073342

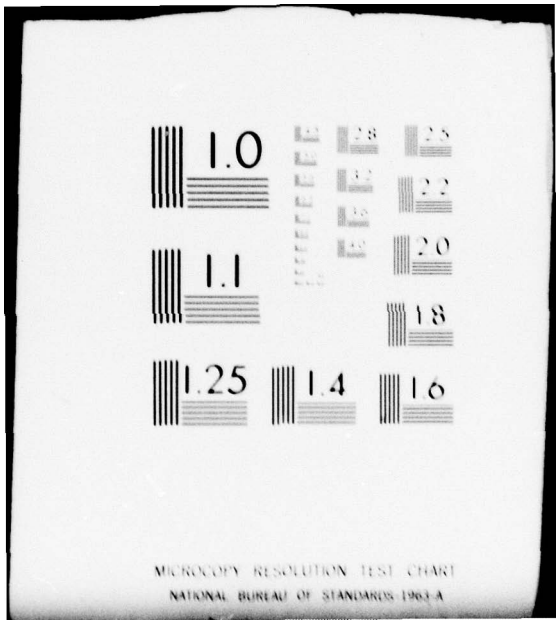
1.0
1.1
1.25
1.4
1.6
2.2
2.0
1.8
MICROCOPY RESOLUTION TEST CHART
NATIONAL BUREAU OF STANDARDS 1963-A

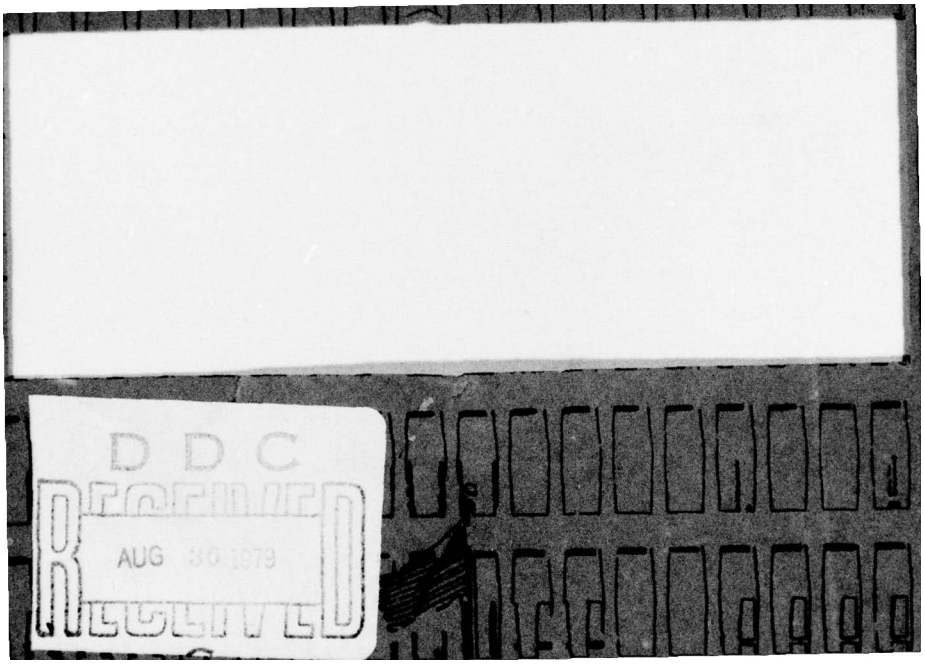

SAMSO-TR-79-14

(2)

DESIGN AND ANALYSIS
OF
777 "FLY-BY-WIRE" CONTROL SYSTEM

28600-AR-011-01

9 April 1976

PREPARED: H. C. Osborne
H. C. Osborne

APPROVED:
R. H. Alborn
Assistant Project Manager
777 Orbital Operations

APPROVED:
A. M. Frew, Manager
Design, Analysis and
Simulation Department

APPROVED:
D. E. Kendall
Manager
Project 777

Prepared for
Department of the Air Force Headquarters
Space and Missile Systems Organization (AFSC)
CDRL Sequence Number A009
Contract F04701-75-C-0257

TRW Systems Group
One Space Park
Redondo Beach, California 90278

This final report was submitted by TRW Defense and Space Systems Group, One Space Park, Redondo Beach, CA 90278, under Contract F04701-75-C-0257, with the Space and Missile Systems Organization, Deputy for Space Communications Systems, P.O. Box 92960, Worldway Postal Center, Los Angeles, CA 90009.

Captain G. D. Nordley, SAMSO/SKD, was the Project Officer for Space Communications Systems.

This report has been reviewed by the Information Office (OI) and is releasable to the National Technical Information Service (NTIS). At NTIS, it will be available to the general public, including foreign nations.

This technical report has been reviewed and is approved for publication. Publication of this report does not constitute Air Force approval of the report's findings or conclusions. It is published only for the exchange and stimulation of ideas.

Gerald D. Nordley
GERALD D. NORDLEY, Capt, USAF
Project Officer,
Deputy for Space Comm Systems

Lawrence A. Barlock
LAWRENCE A. BARLOCK, Lt Col, USAF
Director of Engineering, DSCS II
Deputy for Space Comm Systems

FOR THE COMMANDER

James E. Freytag
JAMES E. FREYTAG, Col, USAF
System Program Director, DSCS
Deputy for Space Comm Systems

UNCLASSIFIED

SECURITY CLASSIFICATION OF THIS PAGE (When Data Entered)

REPORT DOCUMENTATION PAGE	READ INSTRUCTIONS BEFORE COMPLETING FORM
1. REPORT NUMBER: SAMSO-TR-79-14	2. GOVT ACCESSION NO. / 3. RECIPIENT'S CATALOG NUMBER
4. TITLE (and Subtitle): DESIGN ANALYSIS OF 777 "FLY-BY-WIRE" CONTROL SYSTEM	5. TYPE OF REPORT & PERIOD COVERED: Final Report
	6. PERFORMING ORG. REPORT NUMBER: TRW-TR-28600-AR-011-01
7. AUTHOR(s): H. C. Osborne	8. CONTRACT OR GRANT NUMBER(s): F04701-75-C-0257
9. PERFORMING ORGANIZATION NAME AND ADDRESS: TRW Systems Group, One Space Park, Redondo Beach, CA 90278	10. PROGRAM ELEMENT, PROJECT, TASK AREA & WORK UNIT NUMBERS
11. CONTROLLING OFFICE NAME AND ADDRESS: Space and Missile Systems Organization, Air Force Systems Command, Los Angeles, Calif, 90009	12. REPORT DATE: 9 April 1976 13. NUMBER OF PAGES: 99
14. MONITORING AGENCY NAME & ADDRESS (if different from Controlling Office)	15. SECURITY CLASS. (of this report): Unclassified 15a. DECLASSIFICATION/DOWNGRADING SCHEDULE

16. DISTRIBUTION STATEMENT (of this Report)

Approved for public release; distribution unlimited.

17. DISTRIBUTION STATEMENT (of the abstract entered in Block 20, if different from Report)

18. SUPPLEMENTARY NOTES

19. KEY WORDS (Continue on reverse side if necessary and identify by block number)

Satellite
Fly-By-Wire Control System

20. ABSTRACT (Continue on reverse side if necessary and identify by block number)

This document describes the design and implementation of the "fly-by-wire" despin control system for Program 777. Two designs for the ground loop controller are considered - one using proportional control only and one using proportional plus rate control. It is recommended that the spacecraft be operated at the lower RPM's. Also, recommended are counter limits to minimize transient overshoots to large torque disturbances.

DD FORM 1473 (FACSIMILE)

409637

UNCLASSIFIED

SECURITY CLASSIFICATION OF THIS PAGE (When Data Entered)

TABLE OF CONTENTS

LIST OF FIGURES

LIST OF FIGURES (CONT'D)

LIST OF FIGURES (CONT'D)

LIST OF TABLES

ABSTRACT

This document describes the design and implementation of the "fly-by-wire" despin control system for Program 777. In this configuration, the spacecraft will be operated in the search mode with additional commands (i.e., counts) sent up from the ground. The problem with operating the spacecraft in the normal mode is that when the platform is knocked off the earth by large torque disturbances, the on-board logic is programmed so that after 3 invalid signals, the controller goes into standby. To recover the spacecraft, operator intervention involving much time and effort is required.

The advantage of the "fly-by-wire" design is that even if the platform loses earth lock, the controller will continue to send commands to the motor and thus reasonably continuous operation of the spacecraft can be maintained. The use of the narrow coverage antennas is precluded, although the 1 to 2.5 degree pointing accuracy achievable by the "fly-by-wire" technique is more than adequate to allow the use of the earth coverage antenna.

Two designs for the ground loop controller are considered - one using proportional control only and one using proportional plus rate control. Linear analyses, backed up by nonlinear simulation results, show that the best performance is achieved at the lower RPM, because higher position gains can be tolerated. In effect the position gains selected are roughly 1 count per 1 degree error at 40 RPM, and 1 count per 2 1/2 degree error at 75 RPM. The addition of the rate loop produced no improvement in the steady-state performance, but did result in somewhat smaller transients in response to large disturbances at the higher RPM.

It is thus recommended that the spacecraft be operated at the lower RPM's. In addition it is also recommended that the control system first be tested using only the position loop. If this is satisfactory, the rate term need not be included. It is further recommended that the

counter be limited to ± 1 count; this minimizes the transient overshoots to large torque disturbances. The recommended gains are tabulated below.

Recommended Ground Loop Gains

RPM	Gain State	Bias Counts/ Telemetry Counts	Degree Error When 1 Count Sent
		Position Gain A	
40	6	.010	.73°
60	8	.0075	1.5°
75	8	.0063	2.2°
		Rate Gain C	
40	6	.019	
60	8	.025	
75	8	.036	

1.0 INTRODUCTION

The 777 spacecraft #9433 despin control system was originally designed to point the platform to the earth with an accuracy of .15 degree. In August, 1975, large pointing errors of 1.5 degrees were observed, and sometime later, the spacecraft lost lock with the earth. Since then, repeated attempts have been made to bring the spacecraft back into normal mode, but each time, sometimes even after successful operation of several hours or more, the spacecraft is knocked off the earth, and normal mode control is lost. (The problem with the normal mode is that the onboard logic is programmed so that if three successive platform signals are received outside the scanned earth chord, the controller goes into standby.) To bring the spacecraft back into normal mode requires operator intervention, and in recent months this activity has taken a considerable amount of time.

The cause of this anomalous performance has been the subject of much study in the past few months (Reference 1). Basically the anomaly is characterized by an increase in the constant running friction ($\approx$ 100 in-oz) across the rotor-platform interfaces, accompanied by occasional torque transients. It was concluded that the anomaly was most likely due to poor lubrication in the DMA, although the lubrication supply system is not very well understood.

It has recently been suggested that an attempt be made to operate the spacecraft in the rate/search mode, with a ground commandable loop to the spacecraft. In doing so, it was realized that the pointing accuracy would be degraded, but the advantage in this type of operation is that even if the platform is knocked off the earth, the controller can be programmed so that it will not automatically "quit" as in the case of the normal mode, but will continue issuing commands to the motor. Thus, reasonably continuous operation of the spacecraft can be maintained.

This document examines the possibilities of the ground loop in the control system, and suggests a control system that can keep the steady-state

pointing accuracy to within 1 to 2 1/2 degrees. There are three main obstacles to finer pointing accuracy by using the rate/search mode and a ground loop. The first is the rate quantization already existing in the rate loop in the control system of the spacecraft. The other two are concerned with the ground loop - first, the transport lag which is currently estimated at between 2-6 seconds, and second, there is quantization in the ground loop as well. That is, only an integer number of counts can be sent from the ground to the spacecraft, and this quantization turns out to be quite large.

In order to fully understand the effects of quantization, a brief look is taken at the control system with no delay in the ground loop. This is done in Section 2.0, and the ground loop control system consists simply of proportional control. The effect of varying the spin speed (40 to 75 RPM) is also considered. Then in Section 3.0, the effect of the transport lag in the ground position loop is studied. Finally, in Section 4.0, a ground loop consisting of proportional plus rate control is examined. Implementation considerations of the ground loop are discussed in Section 5.0. Conclusions and Recommendations are discussed in Section 6.0. Appendix A is a summary of the results of an analysis of the time delays to be expected in the ground loop, and Appendix B describes the simulation used in this document.

2.0 A "ZERO-DELAY" SYSTEM

This section examines the control system in the rate/search mode with a ground commandable loop which consists only of a gain, K_p, times position. The Z-plane transfer function will be determined in order to compute the range of K_p for stable operation. Then, some non-linearities of the system are examined, with time traces plotted for various RPM. All this will be done assuming zero-delay in both the rate loop and the position loop.

2.1 Z-Plane Analysis of the Linear System

A linear model of the despin controller in the rate/search mode with the ground loop in is shown in Figure 2-1. The open loop transfer function L(s) assuming zero transport lag is

$$L(s) = \frac{k_2(1-e^{-T_s s})}{s} \cdot \frac{k_c'(s+B)}{s} \cdot k_s k_m \cdot \frac{1}{I_p s^2} [K_R T^2 s + K_p]$$

$$= \frac{k_s k_2 k_c' k_m K_R T^2 (1-e^{-T_s s}) (s+B) (s + K_p/(K_R T^2))}{I_p s^4}$$

$$= \frac{K_o T^2 (1-e^{-T_s s}) (s+B) (s+A)}{s^4} \qquad (2\text{-}1)$$

where

$$K_o = \frac{k_s k_2 k_c' k_m K_R}{I_p}$$

$$A = K_p/(K_R T^2)$$

T = spin period (= 1 sec at 60 RPM)

T_s = 2T = sampling period

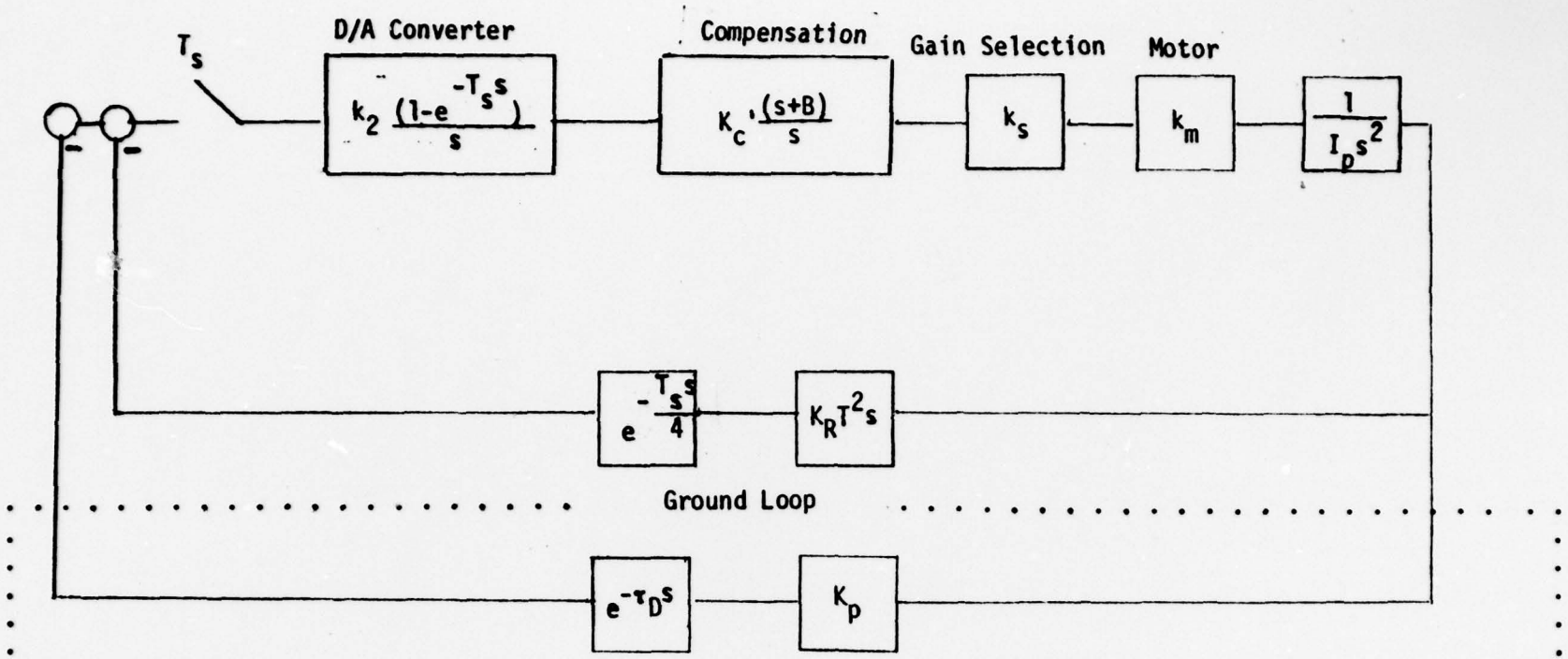

T = spin period
T_s = 2T = sampling period
τ_D = delay in ground loop
K_p = ground position loop gain
$K_R T^2$ = rate loop gain (K_R = 261)
k_s = selectable gain

Figure 2-1. Linear Model of Despin Controller - Search Mode with Ground Connection

Table 2-1. Parameter Values for Figure 2-1

Variable	Value	Description
B	.0667	Filter breakpoint (rad/sec)
I_p	72	Platform inertia (slug-ft^2)
k_2	.00586	D/A converter gain (volts/count)
k_s	G.S. 1 1.00 G.S. 2 1.39 G.S. 3 2.01 G.S. 4 2.82 G.S. 5 3.98 G.S. 6 5.65 G.S. 7 7.97 G.S. 8 11.32	Selectable gain (volts/volt)
k_m	.4	Motor gain (ft-lb/volt)
k'_c	5.51	Compensation gain (volt/volt)
T	40 RPM - 1.5 60 RPM - 1.0 75 RPM - .8	Spin period (sec)
T_s	2T	Sampling period
τ_D	See Appendix A (2-6 sec)	Delay in ground loop

The Z-transform of L(s) is determined by partial fraction expansion. Without the measurement delay, the controllers' open loop Z-plane transfer function is

$$L(z) = Z\,[L(s)]$$

$$= K_o T^2 \frac{z-1}{z} Z\left[\frac{(s+B)(s+A)}{s^4}\right]$$

$$= K_o T^2 \frac{z-1}{z} Z\left[\frac{c_1}{s} + \frac{c_2}{s^2} + \frac{c_3}{s^3} + \frac{c_4}{s^4}\right] \qquad (2\text{-}2)$$

$$= K_o T^2 \frac{z-1}{z}\left[\frac{c_1 z}{z-1} + \frac{c_2 T_s z}{(z-1)^2} + \frac{c_3 T_s^2 z(z+1)}{2(z-1)^3} + \frac{c_4 T_s^3 z(z^2+4z+1)}{6(z-1)^4}\right]$$

where

$$c_4 = AB$$

$$c_3 = A + B$$

$$c_2 = 1$$

$$c_1 = 0$$

so

$$L(z) = K_o T^2 \frac{z-1}{z}\left[\frac{6T_s z(z^2-2z+1) + (3A+3B)T_s^2 z(z^2-1) + ABT_s^3 z(z^2+4z+1)}{6(z-1)^4}\right]$$

$$= K_o T^2 \left[\frac{z^2(6T_s + (3A+3B)T_s^2 + ABT_s^3) + z(-12T_s + 4ABT_s^3) + 6T_s - (3A+3B)T_s^2 + ABT_s^3}{6(z-1)^3}\right]$$

$$= K_Z T^2 \left[\frac{(z-\beta)(z-\alpha)}{(z-1)^3}\right] \qquad (2\text{-}3)$$

where $K_Z T^2$ = root locus gain in the Z-plane.

The two zeros of the Z-plane transfer function are β and α. The zero β which is associated with the S-plane filter breakpoint B, ($\beta = e^{-BT_s}$) is independent of A. The second Z-plane zero, α, is plotted in Figure 2-2 as a function of A (at 60 RPM, or T=1). The zero α approaches e^{-AT_s} as A becomes small.

The Z-plane root locus associated with the transfer function at 60 RPM (T=1) is shown in Figure 2-3. Very roughly, the root locus (the portion off the axis) is a circle with a radius equal to $1-\alpha$. It is thus evident that in order for most of the root locus to be inside the unit circle, that α be > 0. From Figure 2-2 this implies that A be <1 (for 60 RPM).*

Similar plots of α as a function of A were made at 75 RPM (T=.8, or T_s = 1.6) and 40 RPM (T = 1.5, T_s = 3). These are shown in Figure 2-4. These show that at the lower RPM's the S-plane zero A must be reduced.

It is worthwhile at this point to digress for just a moment to consider what the value of A (the S-plane zero) really means, in terms of the ground commandable loop. The gain K_p in this position loop is

$$K_p = A \cdot K_R T^2 \qquad (2\text{-}4)$$

which means that K_p counts should be sent for every AK_RT^2 radians of error. Since K_R = 261, this means that

$$K_p = 261\ A\ T^2 \qquad (2\text{-}5)$$

or in terms of degrees, $4.56\,AT^2$ counts should be sent for every degree of error. At 60 RPM (T=1) typical values of A turn out to be on the order of .1 or .2. A value of A = .1 means .456 counts for every degree of error, or since only an integer number of counts can be sent, 1 count should be sent

* This turns out to be a large upper bound; in fact values of A = .1 and .2 were used.

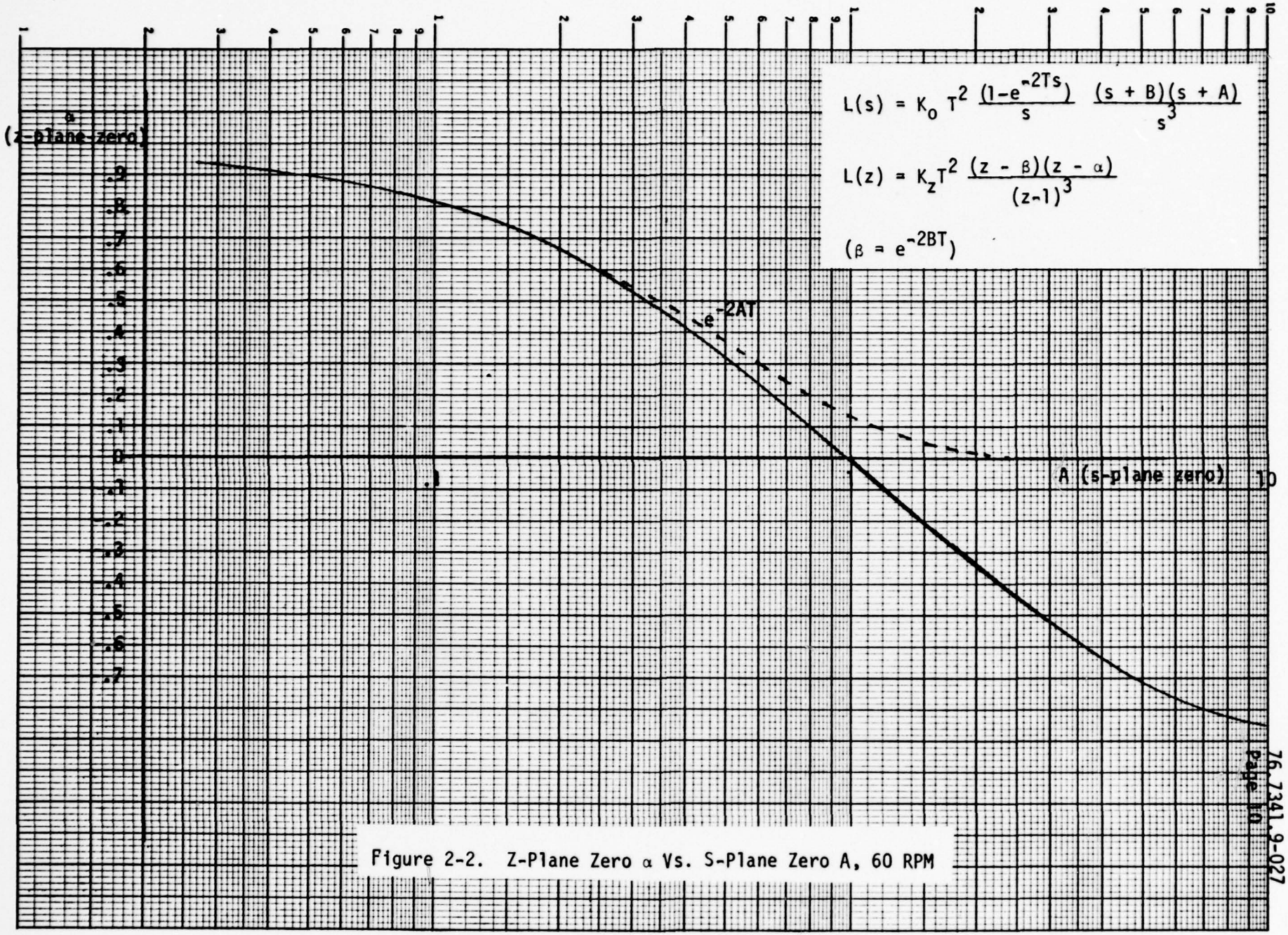

Figure 2-2. Z-Plane Zero α Vs. S-Plane Zero A, 60 RPM

$$L(z) = K_z T^2 \frac{(z - \beta)(z - \alpha)}{(z - 1)^3}$$

$\beta = e^{-2BT} = .875$ (60 RPM)

(α taken from Figure 2-2)

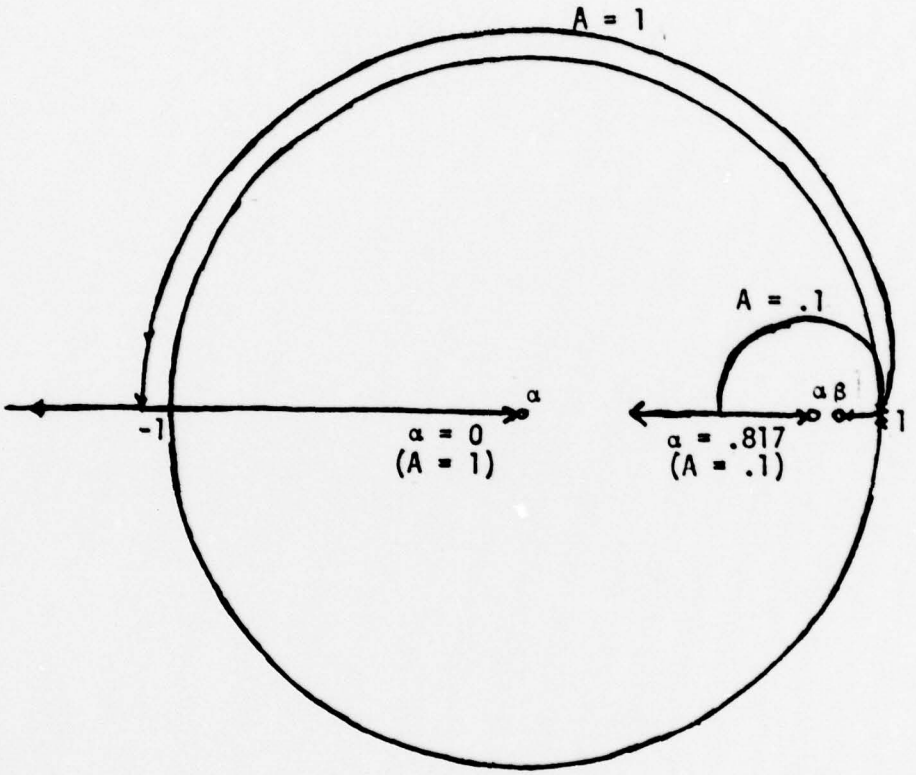

Figure 2-3. Z-Plane Root Locus for Zero-Delay Transfer Function (60 RPM), for Two Values of A. (A is the S-Plane Zero)

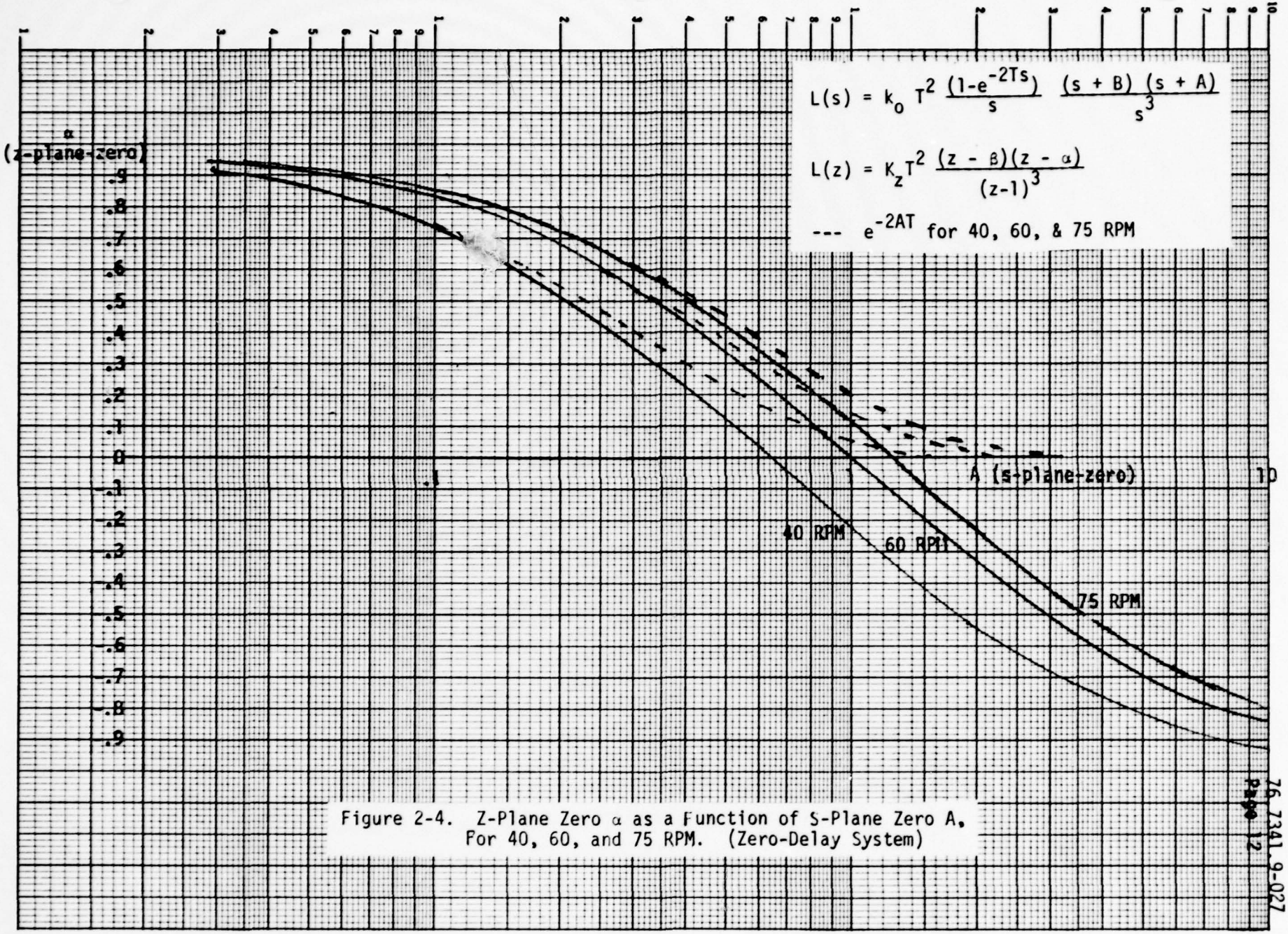

Figure 2-4. Z-Plane Zero α as a Function of S-Plane Zero A, For 40, 60, and 75 RPM. (Zero-Delay System)

for every 2 degrees of error. It has been shown that at the lower RPM, the value of A decreases, but since T increases, the effect on K_p is not obvious at this point. Clearly, however, the accuracy to be expected from this type of system is going to be on the order of degrees, and not fractions of degrees.

A gain phase plot of the system with A = .1 and A = .5 is shown in Figures 2-5 and 2-6 for 60 RPM (0 delay). These two figures show that, at 60 RPM a higher value of A is possible if the gain state is increased. In other words, A is dependent on the gain state chosen, and in order to calculate the "best A", one should choose the optimum gain state for each RPM. This suggests formulating a new problem, where A is the overall gain in the characteristic equation. Thus a root locus will be plotted where the parameter A is the variable gain. The approach used will be to rewrite the characteristic equation

$$1 + L_R(z) + A\,L_p(z) = 0 \qquad (2\text{-}6)$$

where

$L_R(z)$ is the rate loop transfer function

and $AL_p(z)$ is the position loop transfer function

as
$$1 + \frac{A\,L_p(z)}{1 + L_R(z)} = 0 \qquad (2\text{-}7)$$

so that the new "open loop" transfer function to be plotted is $H(z) = \dfrac{A\,L_p(z)}{1 + L_R(z)}$

With no delay, the transfer function of the inner rate loop is

$$L_R(z) = K_o T^2 \left[\frac{z-1}{z}\right] \cdot Z\left[\frac{1}{s^2} + \frac{B}{s^3}\right]$$

$$= K_o T^2 \frac{z-1}{z} \cdot \left[\frac{T_s z}{(z-1)^2} + \frac{B\,T_s^2 z\,(z+1)}{2\,(z-1)^3}\right]$$

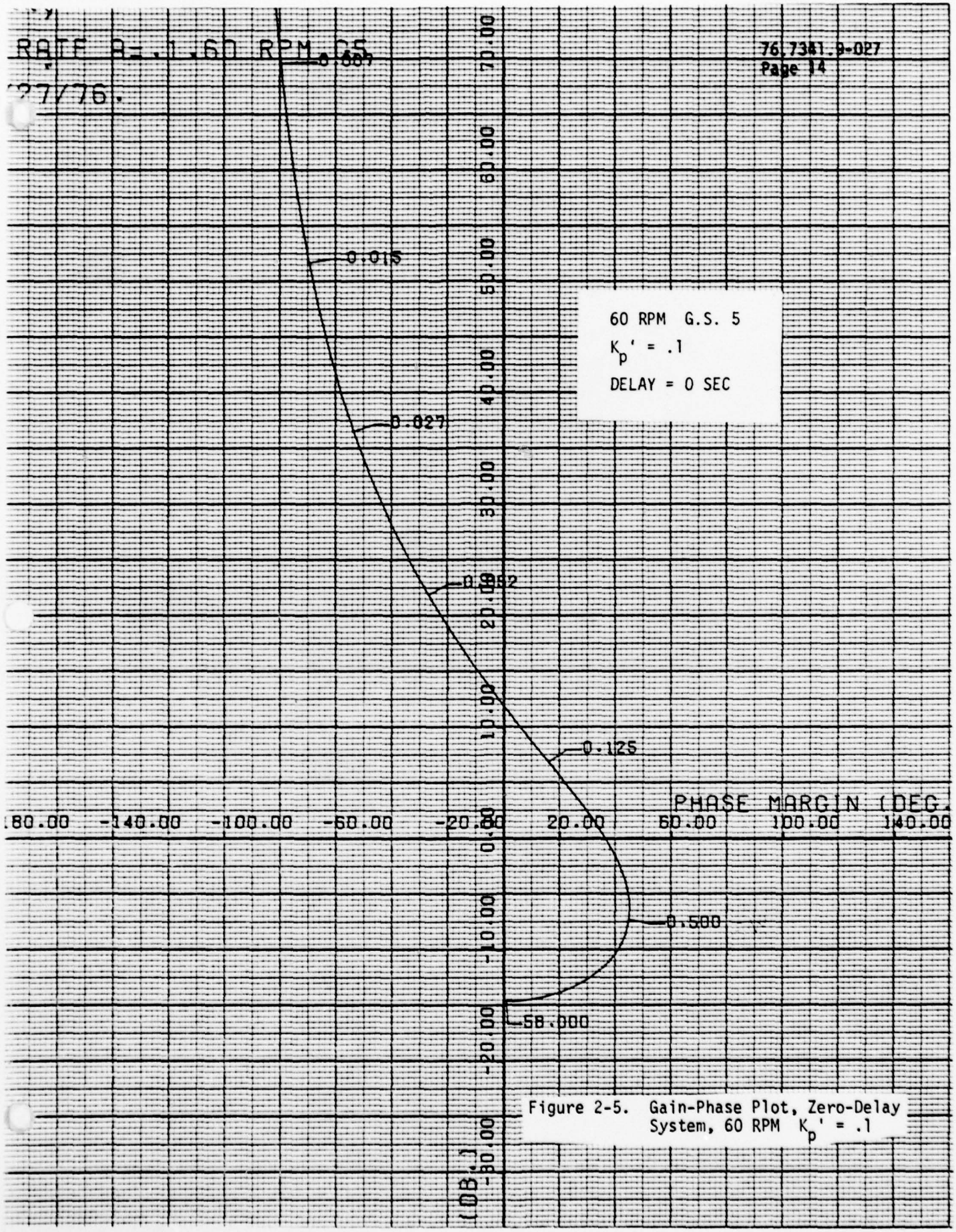

Figure 2-5. Gain-Phase Plot, Zero-Delay System, 60 RPM K_p' = .1

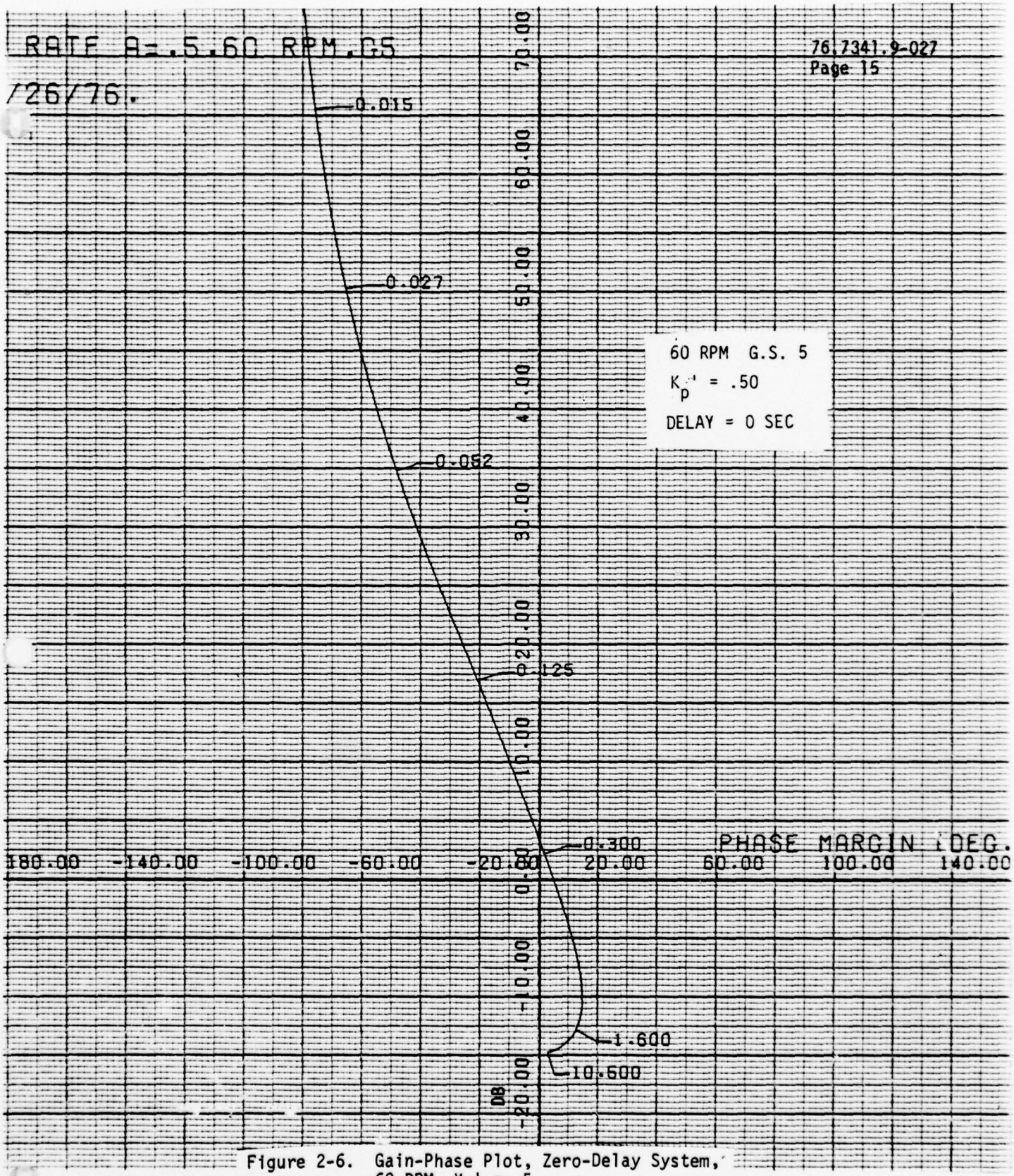

Figure 2-6. Gain-Phase Plot, Zero-Delay System, 60 RPM K_p' = .5

$$= K_o T^2 \left[\frac{2T_s(z-1) + BT_s^2(z+1)}{2(z-1)^2} \right]$$

$$= K_o T^2 \left[\frac{z\,(BT_s^2 + 2T_s) - 2T_s + BT_s^2}{2(z-1)^2} \right]$$

or

$$L_R(z) = K_o T^2 \left[\frac{\sigma_2 z + \sigma_1}{2(z-1)^2} \right] \qquad (2\text{-}8)$$

where

$$\sigma_2 = BT_s^2 + 2T_s$$

$$\sigma_1 = BT_s^2 - 2T_s$$

The Z-transform of the position loop is

$$AL_p(z) = K_o T^2 A \frac{z-1}{z} Z\left(\frac{s+B}{s^4}\right)$$

$$= K_o T^2 A \frac{(z-1)}{z} Z\left[\frac{1}{s^3} + \frac{B}{s^4}\right]$$

$$= K_o T^2 A \frac{(z-1)}{z} \left[\frac{T_s^2 z\,(z+1)}{2(z-1)^3} + \frac{B\,T_s^3\, z\,(z^2 + 4z+1)}{6(z-1)^4} \right]$$

$$= K_o T^2 A \left[\frac{3T_s^2(z^2-1) + BT_s^3(z^2+4z+1)}{6(z-1)^3} \right]$$

or

$$AL_p(z) = K_o T^2 A \left[\frac{\mu_2 z^2 + \mu_1 z + \mu_o}{6\,(z-1)^3} \right] \qquad (2\text{-}9)$$

where

$$\mu_2 = 3T_s^2 + BT_s^3$$
$$\mu_1 = 4BT_s^3$$
$$\mu_0 = BT_s^3 - 3T_s^2$$

The characteristic equation is

$$1 + L_R(z) + AL_p(z) = 0 \qquad (2\text{-}10)$$

or substituting in the expressions for $L_R(z)$ and $L_p(z)$,

$$1 + K_o T^2 \left[\frac{\sigma_2 z + \sigma_1}{2(z-1)^2}\right] + K_o T^2 A \left[\frac{\mu_2 z^2 + \mu_1 z + \mu_o}{6(z-1)^3}\right] = 0 \qquad (2\text{-}11)$$

Multiplying through by $6(z-1)^3$ gives

$$6(z-1)^3 + K_o T^2\, 3(z-1) \cdot [\sigma_2 z + \sigma_1] + K_o T^2 A\, [\mu_2 z^2 + \mu_1 z + \mu_o] = 0 \qquad (2\text{-}12)$$

This must be rewritten in the form of $1+AH(z) = 0$

so

$$1 + \frac{A K_o T^2 [\mu_2 z^2 + \mu_1 z + \mu_o]}{(z-1)[6(z-1)^2 + 3 K_o T^2 (\sigma_2 z + \sigma_1)]} = 0$$

$$1 + \frac{A K_o T^2 [\mu_2 z^2 + \mu_1 z + \mu_o]}{(z-1)[6 z^2 + (3K_o T^2 \sigma_2 - 12) z + 3 K_o T^2 \sigma_1 + 6]} = 0 \qquad (2\text{-}13)$$

It is clear from this transfer function, that the value of A depends on K_o (i.e., the gain state) and T^2.

It will be useful at this point to reintroduce the parameter K_p, which is the ground position loop gain, since the parameter A is somewhat artificial. Recall that A was the S-plane zero in the zero delay system; however, when the characteristic equation is written as above, it makes little sense to isolate A, since the position gain K_p is dependent on the product AT^2.* Let the variable K_p' be defined as

$$K_p' = K_p/K_R = AT^2 \tag{2-14}$$

and substitute K_p' for AT^2 in the above equation. Then the characteristic equation becomes

$$1 + \frac{K_o K_p' [\mu_2 z^2 + \mu_1 z + \mu_o]}{(z-1)[6z^2 + (3K_o T^2 \sigma_2 - 12)z + 3_o T^2 \sigma_1 + 6]} = 0 \tag{2-15}$$

Figure 2-7 contains the root locus of H(z) for 60 RPM (T=1) for gain states 5-8. The zeros are independent of the gain state chosen. One of the zeros is the zero associated with the S-plane break frequency B (i.e., $z = e^{-BT_s}$) while the other is located in the left half plane just outside the unit circle on the real axis. There are 3 Z-plane poles - one at z=1, and two dependent on the gain state chosen. One of these latter poles approaches the Z-plane zero at e^{-BT_s}, while the other moves to the left with increasing gain state. As Figure 2-7 shows, a higher value of K_p' is possible at the higher gain states. However, the association of a higher value of K_p' with a higher gain state is true only up to a point. Figure 2-8 shows the root loci at 40 RPM for various gain states, and as can be seen in gain state 7 (and also in 8), the system is unstable for all values of K_p'. This is because the Z-plane pole has moved so far to the left that it has passed the Z-plane zero outside the unit circle.

* In addition, in the next section, when the system is considered with different delays in each loop, the parameter A loses its significance as the S-plane zero, and it retention only leads to confusion.

$$\text{Transfer Function } H(z) = \frac{K_p' K_o (\mu_2 z^2 + \mu_1 z + \mu_o)}{(z-1)\left[6z^2 + (3K_o T^2 \sigma_2 - 12)\, z + 3K_o T^2 \sigma_1 + 6\right]} \quad *$$

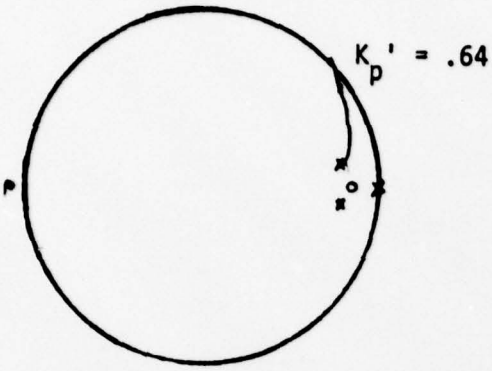

poles - (.80, ± .10), (1,0)
GAIN STATE 5

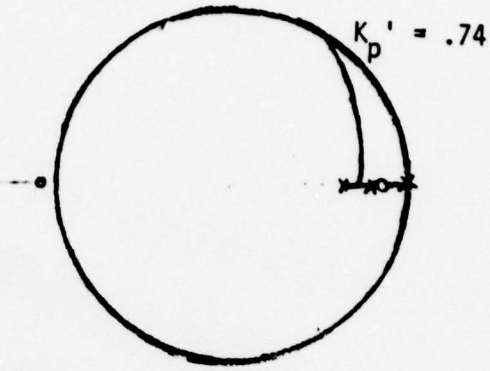

poles - (.81, 0), (.62, 0), (1, 0)
GAIN STATE 6

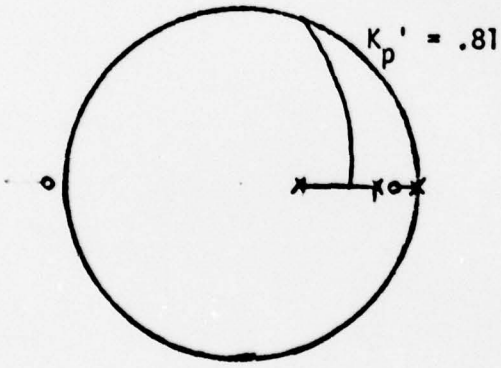

poles - (.84, 0), (.36, 0), (1,0)
GAIN STATE 7

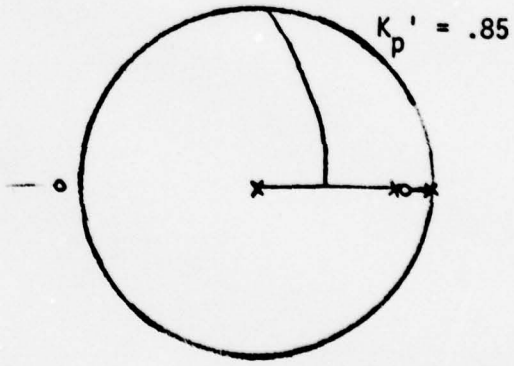

poles - (.86, 0), (.01, 0), (1, 0)
GAIN STATE 8

* Zeros at (.88, 0), (-1.05, 0)

Figure 2-7. Root Locus of H(z) as a Function of Gain State, 60 RPM

$$\text{Transfer Function } H(z) = \frac{K_p' K_o (\mu_2 z^2 + \mu_1 z + \mu_o)}{(z-1)[6z^2 + (3K_o T^2 \sigma_2 - 12) z + 3K_o T^2 \sigma_1 + 6]} \quad *$$

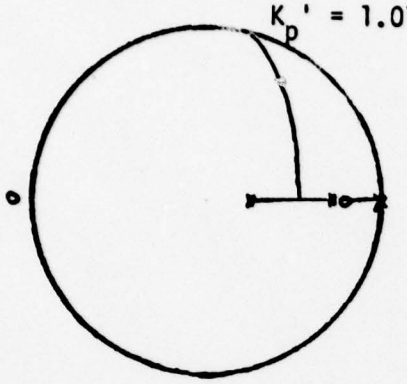

poles - (.76, 0), (.25, 0), (1, 0)
GAIN STATE 4

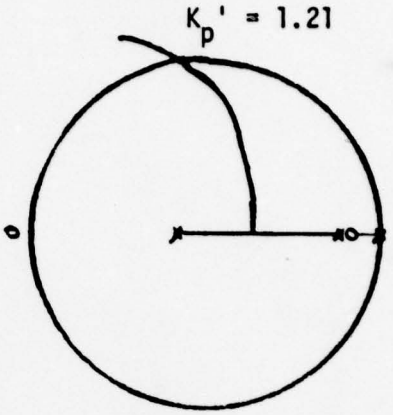

poles - (.78, 0), (-.16, 0), (1, 0)
GAIN STATE 5

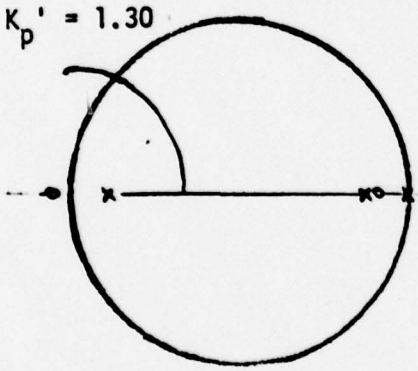

poles - (.79, 0), (-.76, 0), (1, 0)
GAIN STATE 6

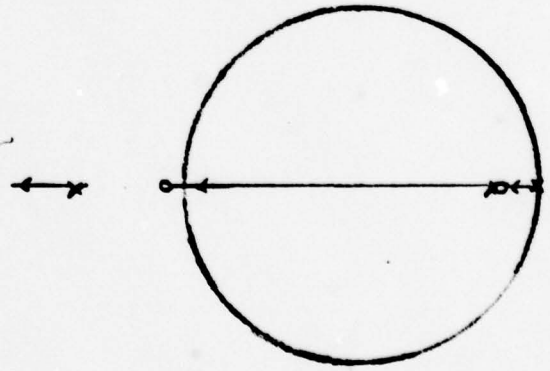

poles - (-1.57, 0), (.804, 0), (1, 0)
(Unstable for all K_p')
GAIN STATE 7

* Zeros at (-1.07, 0), (.81, 0)

Figure 2-8. Root Locus of H(z) as a Function of Gain States, 40 RPM

Figure 2-9 shows the maximum values of $K_p' = K_p/K_R$ plotted as a function of the gain states, for various RPM. This answers one of the questions posed earlier in the section regarding the position gain $K_p = 261\ K_p'$. The gain K_p meant that $4.56\ K_p'$ counts should be sent for every degree of error, or conversely, since only an integer number of counts can be sent, 1 count should be sent for every $1/4.56\ K_p'$ degrees of pointing error. Figure 2-9 shows that at the lower RPM, a higher value of K_p' is possible. This suggests that finer control can be obtained at the lower RPM's. However, it should also be noted that at the lower RPM's, the control signal is sent less often. These effects will be tested by simulation at the end of this section.

Figure 2-9 also shows that at 60 and 75 RPM the spacecraft should be operated in the rate/search mode at gain states 7/8 while using the ground loop, and at 40 RPM, somewhat lower gain states (perhaps 5 or 6) should be used. More will be said about this when the gain phase plots are drawn.

This linear analysis could be carried out even further to determine the ideal damping ratio and its dependence on A, etc., but before carrying on an extensive analysis, it is worthwhile to examine some of the non-linearities in the system to see how they affect the system's performance.

2.2 Non-Linearities in 777 Simulation

Figure 2-10 is a diagram of the nonlinear control system. The significant nonlinearities are discussed below to determine their effect on the systems linear model.

2.2.1 Counter Quantization - Rate Loop

In the rate loop, one count is sent for every $.22/T^2$ deg/sec rate error. This means that the effective rate quantization is as follows:

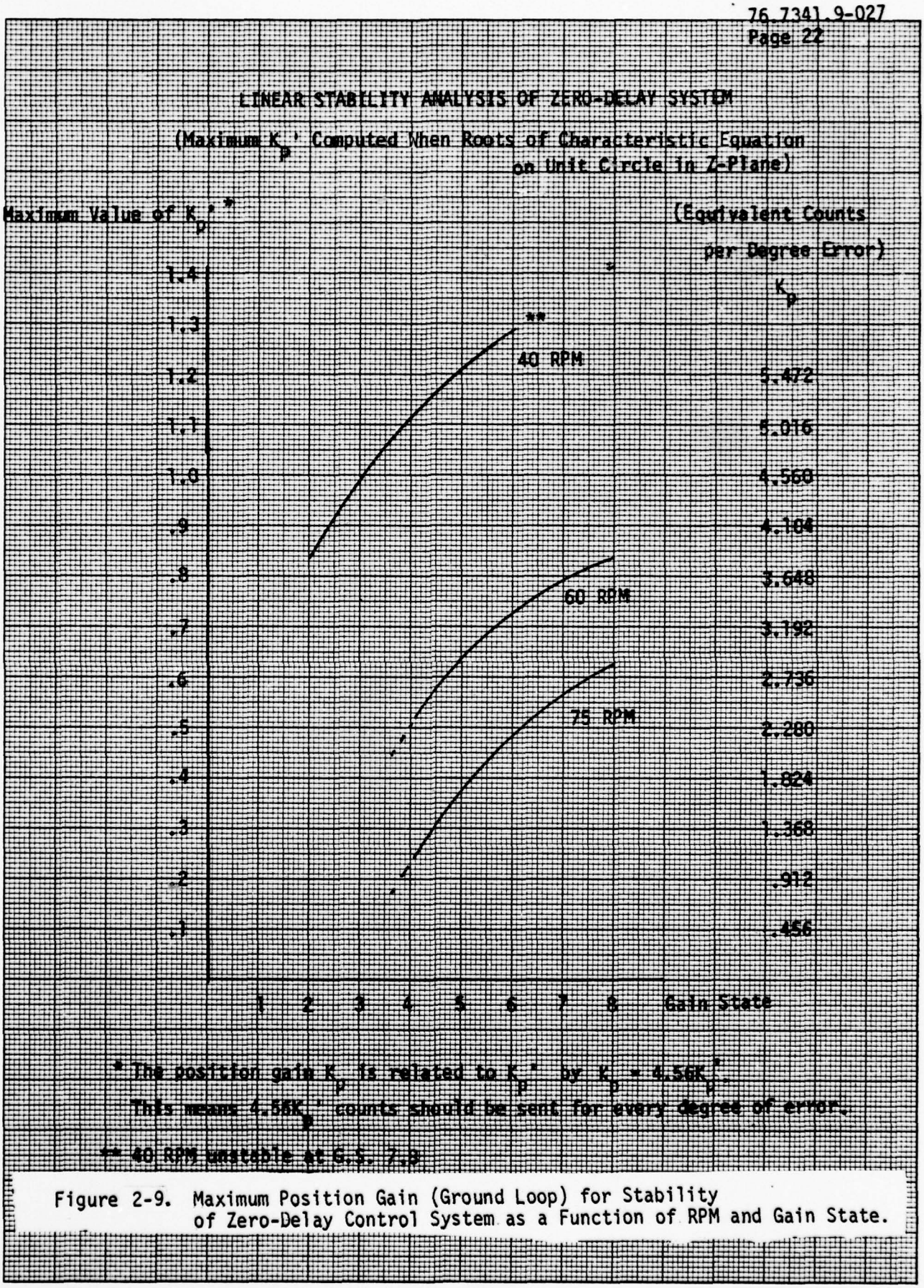

Figure 2-9. Maximum Position Gain (Ground Loop) for Stability of Zero-Delay Control System as a Function of RPM and Gain State.

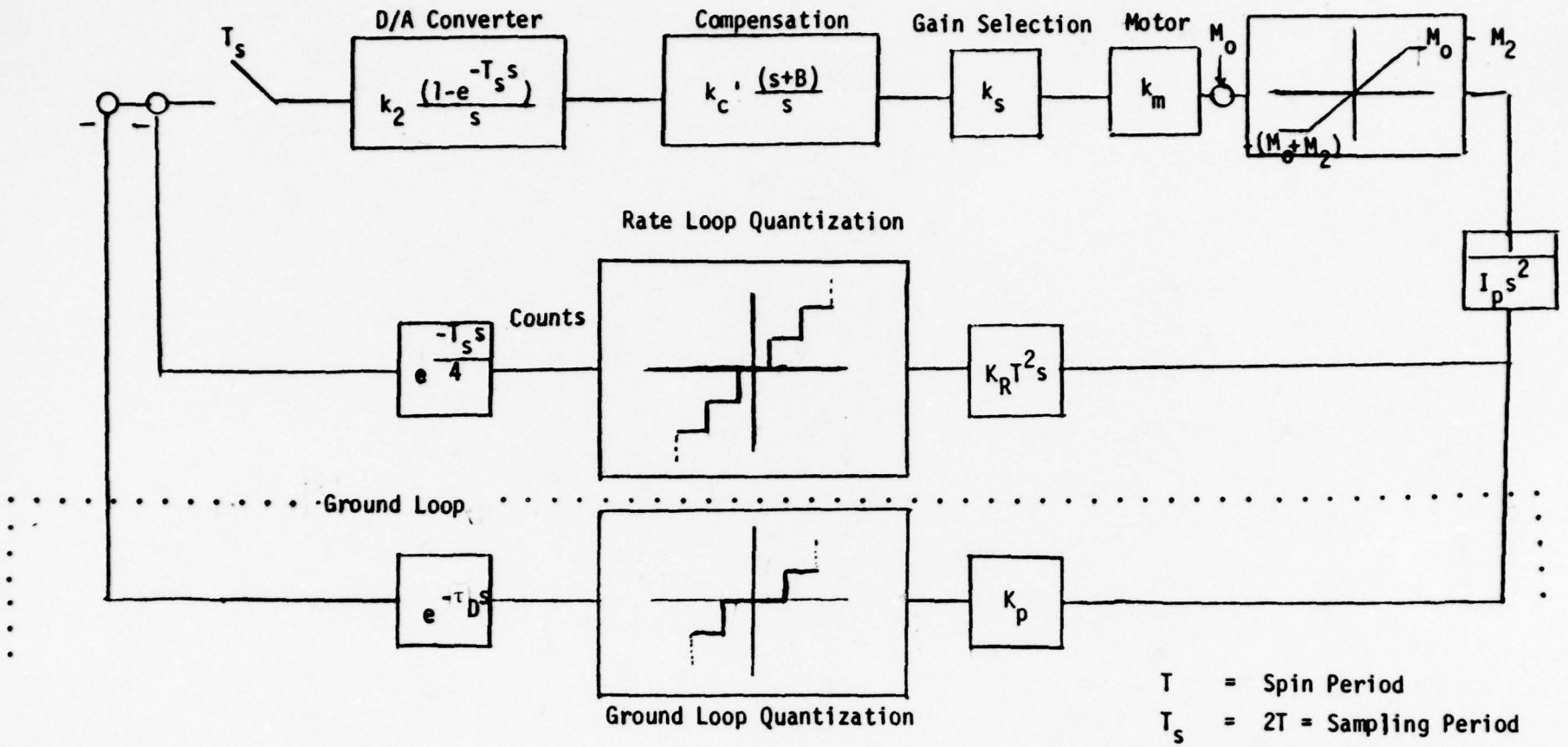

T = Spin Period

T_s = 2T = Sampling Period

τ_D = Delay in Ground Loop

K_p = Ground Position Loop Gain

$K_R T^2$ = Rate Loop Gain (K_R = 261)

k_s = Selected Gain

M_o = Motor Capability

M_2 = Back emf

Figure 2-10. Despin Controller - Search Mode with Ground Connection

RPM	T	
75 RPM	0.8	1 count = $.22/(.80)^2$ = .34 deg/sec
60 RPM	1.0	1 count = .22/1 = .22 deg/sec
40 RPM	1.5	1 count = $.22/(1.5)^2$ = .098 deg/sec

With this large rate quantization, it means that it will be impossible for the pointing error of the spacecraft to settle down and converge as in the normal mode. What can be hoped for, however, is that the steady-state error can be kept within a limit cycle on the order of 1 or 2 degrees. The above table also shows that at the lower RPM, since the rate quantization is smaller, finer pointing error control can be maintained.

2.2.2 Position Loop Quantization

The other significant nonlinearity in the control system is the quantization in the position loop which has already been discussed in Section 2-1. Only an integer number N of counts can be sent from the ground computer, and this number is

$$N = 4.56\ K_p'\ \text{counts/degree of error}$$

or similarly

$$1\ \text{count for every } 1/4.56\ K_p'\ \text{degrees of error.}$$

It is interesting to study the effects of these nonlinearities on the control system. Figure 2-11 is a plot at 60 RPM of the response to a torque disturbance of 10 in-oz for 20 sec. (There was no delay in either loop in this test case.) With no position loop quantization or rate quantization, the error settles down to zero as in the normal mode. With the position quantization in (but still no rate quantization) there is a steady-state error no larger than $1/4.56\ K_p'$ degrees. However, with no position quantization, but with rate quantization, we see the oscillatory response previously predicted. What this means is, with the present spacecraft even

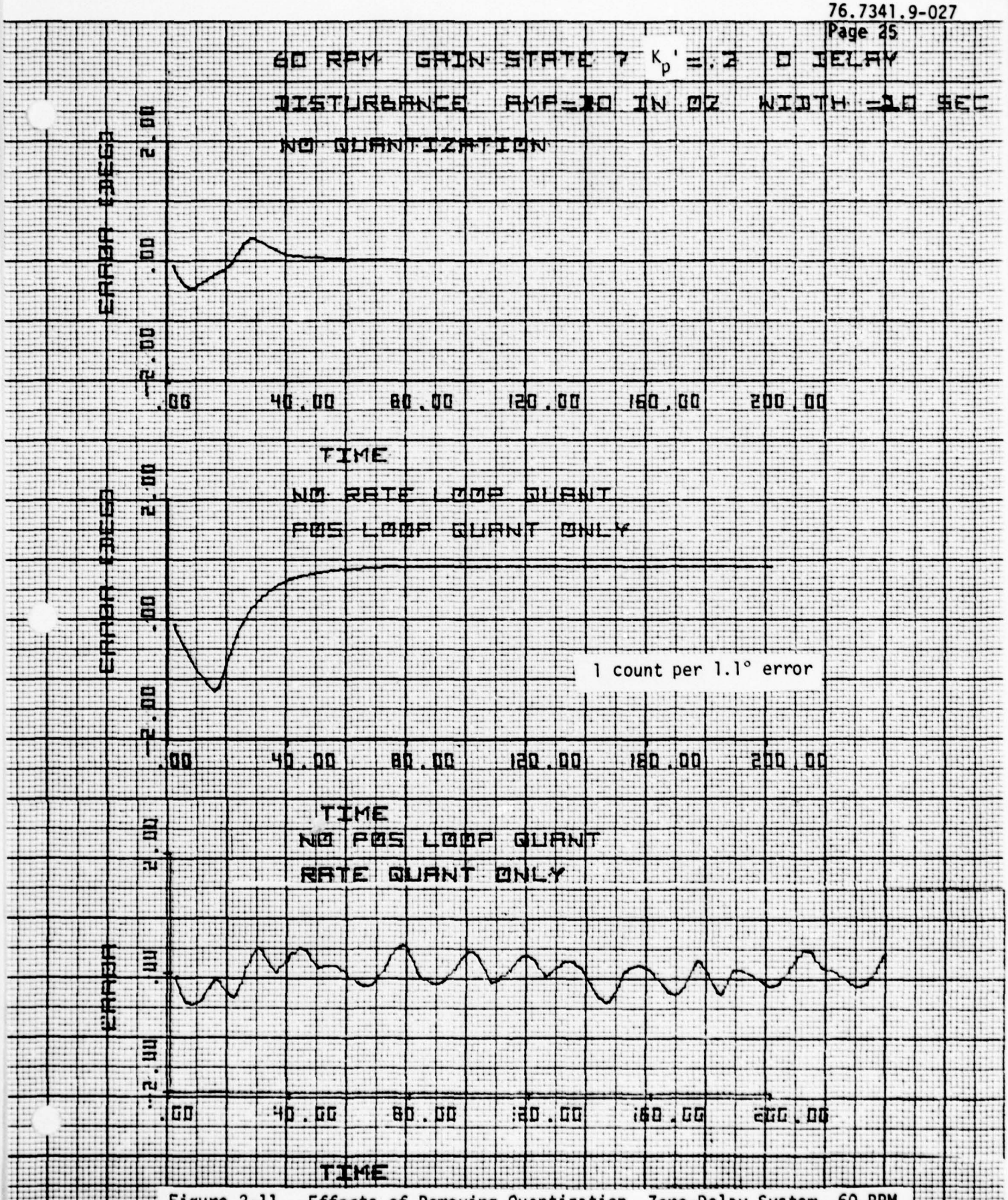

Figure 2-11. Effects of Removing Quantization, Zero-Delay System, 60 RPM

if the ground position loop (consisting of a gain) were ideal, i.e., no delay and no quantization, it would still be impossible to get the steady-state error to settle down.

Figure 2-12 shows the pointing error response with all quantization in (i.e., both rate loop and ground position loop) but still no delay in either loop. After an initial transient, the error oscillates between $\pm$ 1/4.56 K_p', or $\pm$ 1.1 degrees for the case of K_p' = .2. Also shown in this figure are the ground loop commands, the rate, and the rate/error commands due to the rate loop in the spacecraft.

In Figures 2-13 and 2-14, the effect of increasing the position gain is examined, and as predicted, the limit cycle amplitude decreases with increasing gain, so that in Figure 2-14, the limit cycle is .43 degree at 60 RPM, for K_p' = .5 (zero-delay system).

Consider now the case of 40 RPM, where the rate quantization in the spacecraft is smaller (1 count per .10 deg/sec rate error). Figure 2-15 shows the effects of removing quantization from both loops and then each loop separately, and the effect of the smaller rate quantization can be seen in the lower plot in Figure 2-15, where the limit cycle is somewhat smaller than the corresponding case at 60 RPM (Figure 2-11). In Figure 2-16, with quantization in both loops, the pointing error oscillates between $\pm$ 1/4.56 K_p' ($\pm$ 1 deg for K_p' = .2) as in the case at 60 RPM. The effect of increasing the gain, in the lower limit cycle, is again shown in Figure 2-17.

At 75 RPM, the effects of the larger rate quantization are clearly seen in the third plot of Figure 2-18, where the position quantization has been removed. Typical responses of the system showing the effects of increasing the gain on the limit cycle behavior are illustrated in Figures 2-19 and 2-20.

The purpose of this section on the zero-delay system has been to illustrate the effects of the rate and position quantization on the system, and show that even if the ground loop were ideal, i.e., no delay, it would be impossible to get a convergent response of the pointing

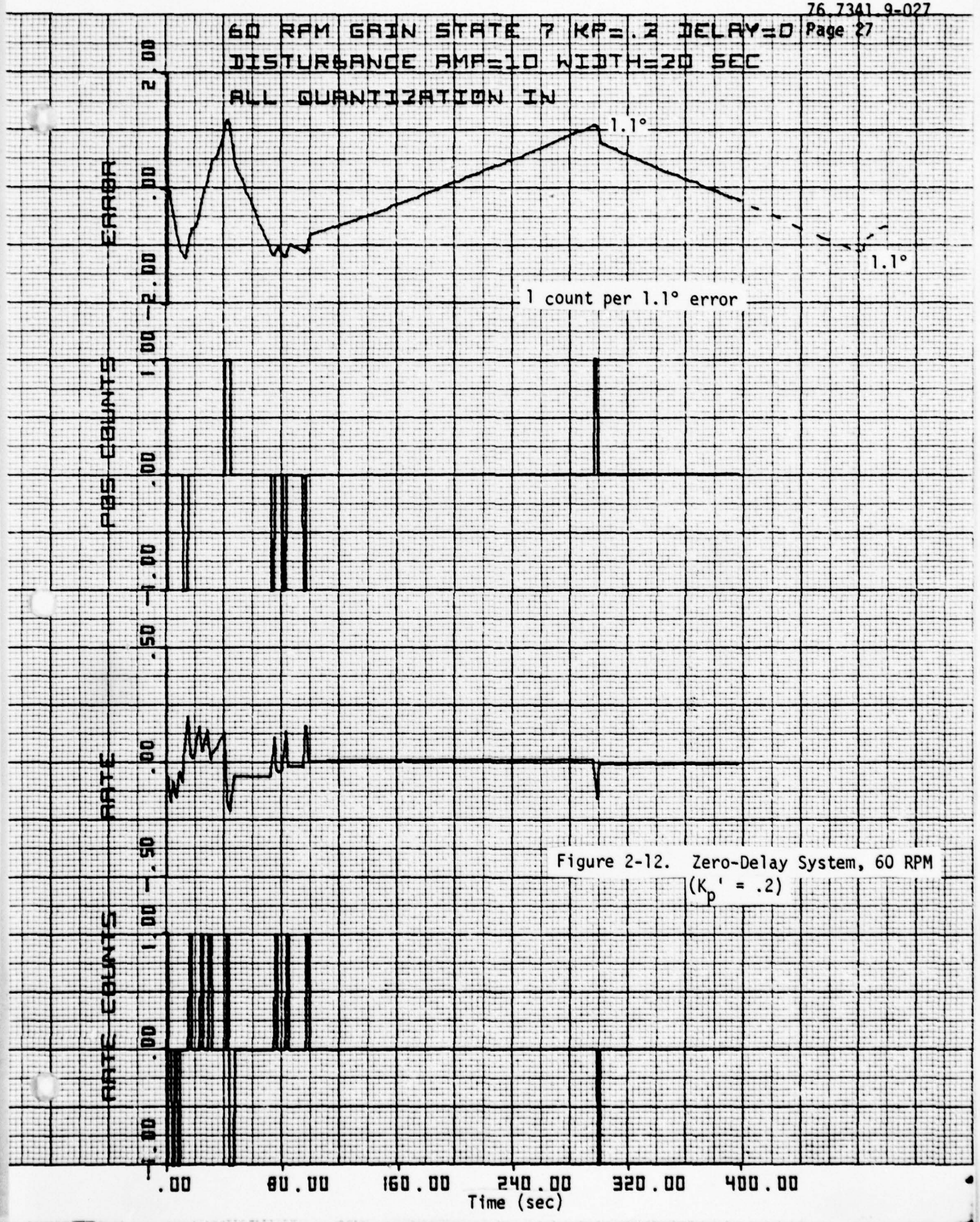

Figure 2-12. Zero-Delay System, 60 RPM ($K_p' = .2$)

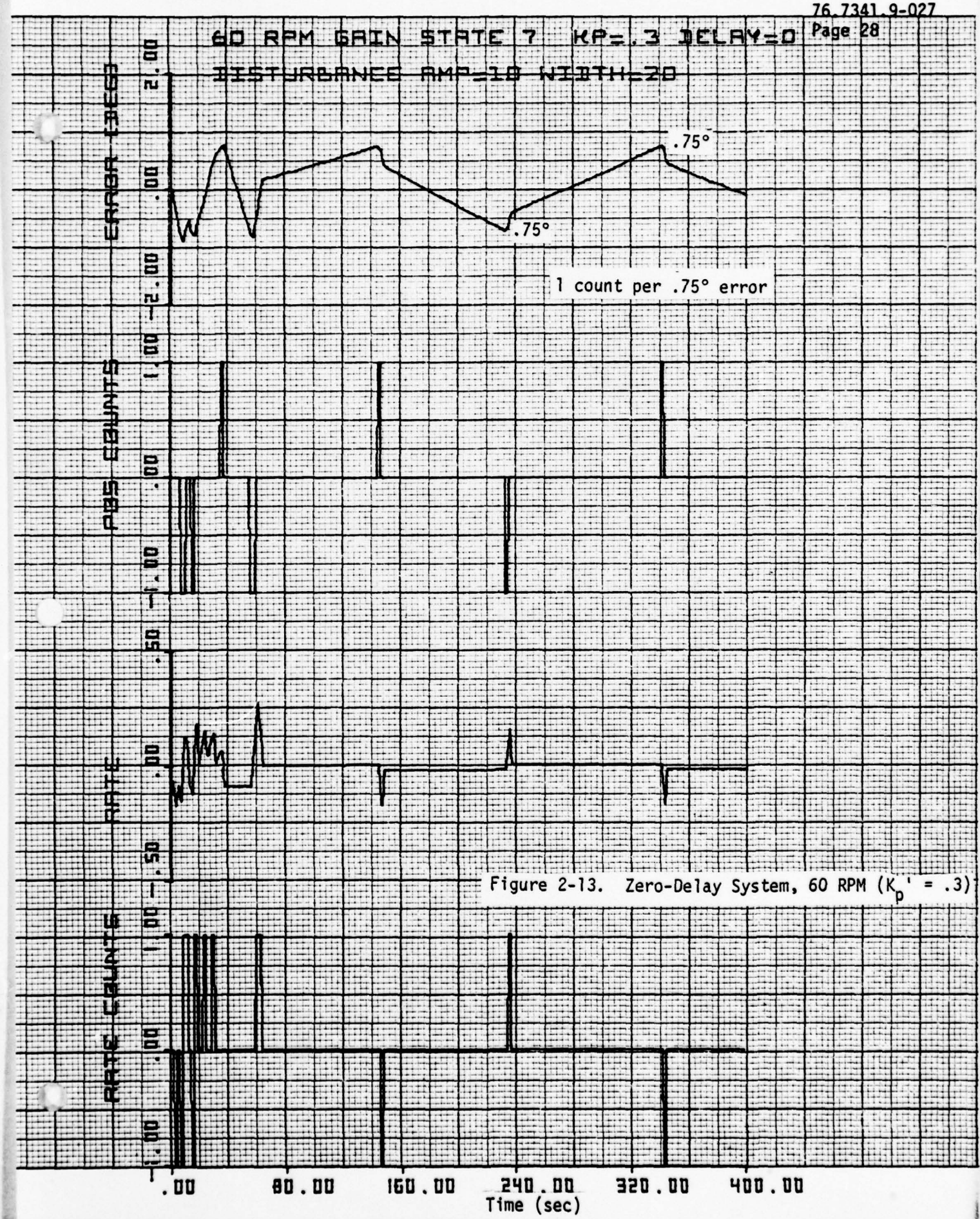

Figure 2-13. Zero-Delay System, 60 RPM ($K_p' = .3$)

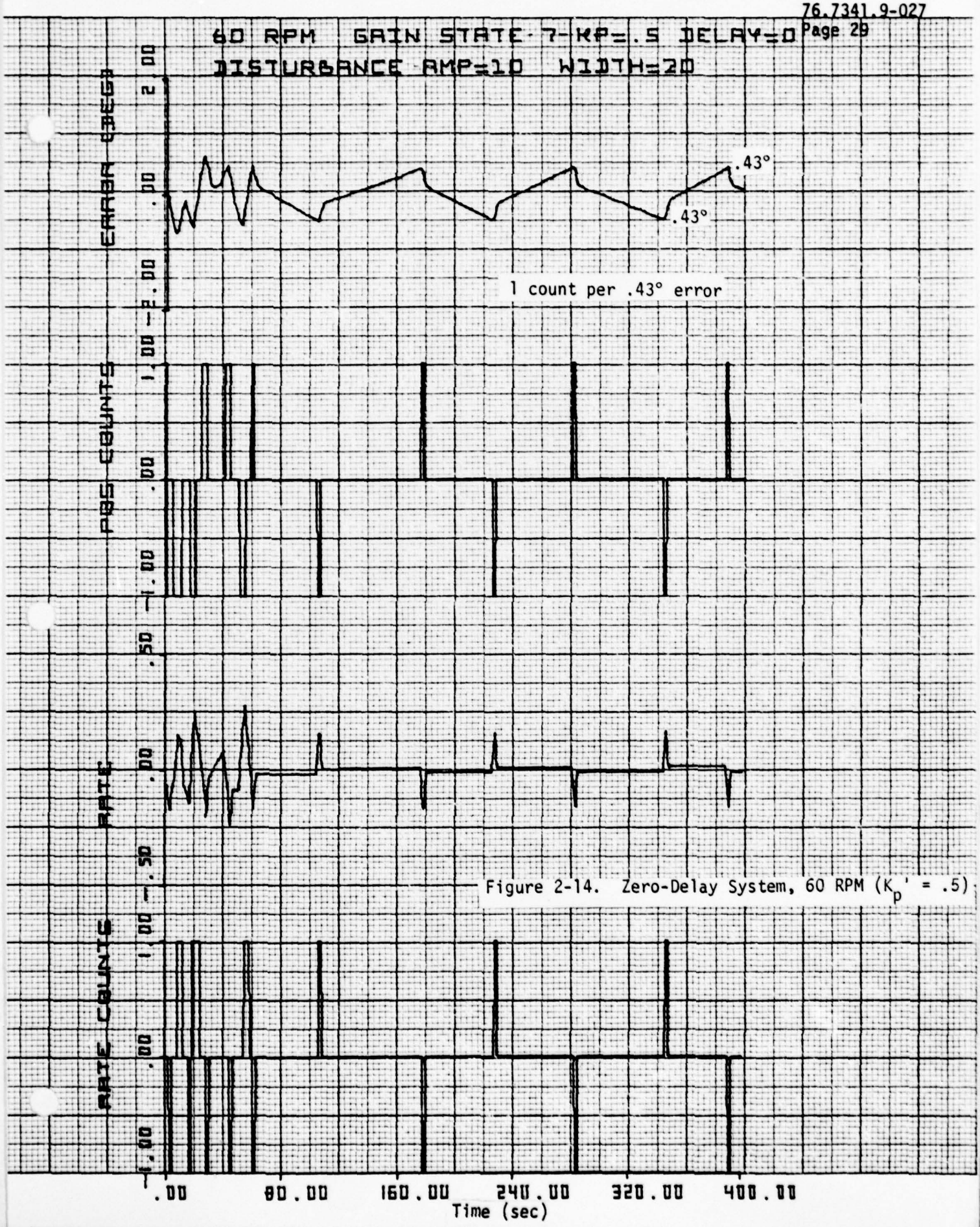

Figure 2-14. Zero-Delay System, 60 RPM ($K_p' = .5$)

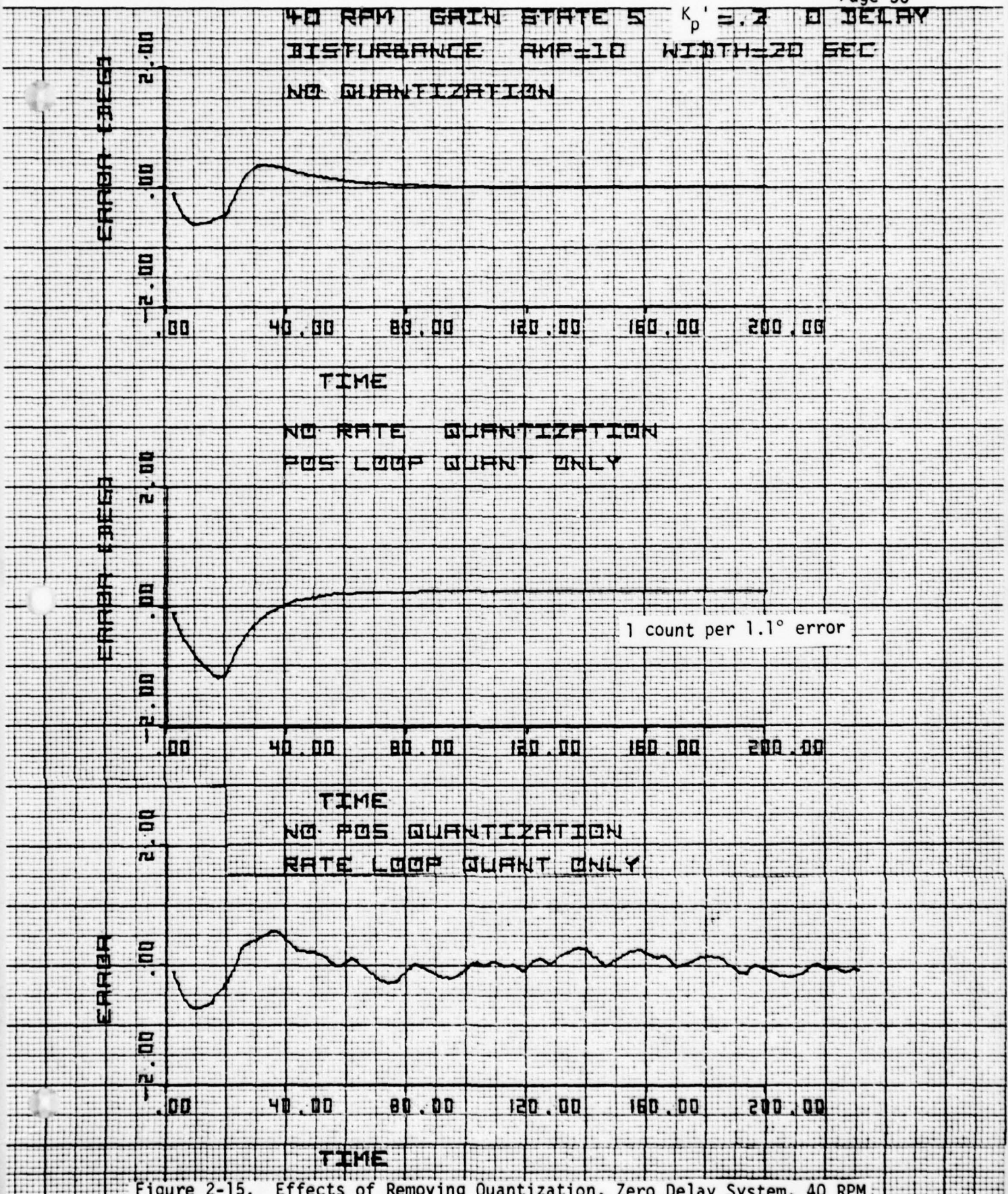

Figure 2-15. Effects of Removing Quantization, Zero Delay System, 40 RPM

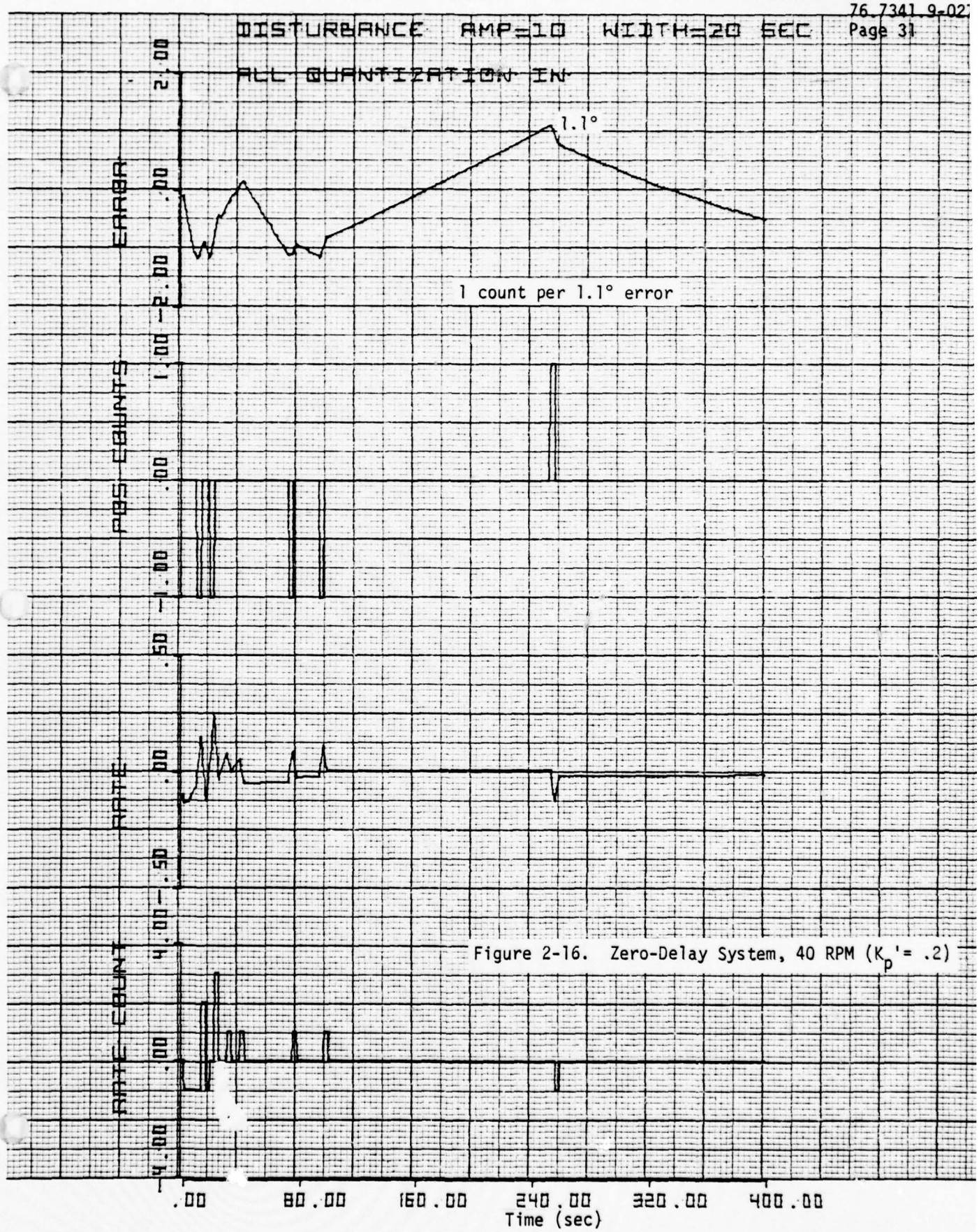

Figure 2-16. Zero-Delay System, 40 RPM (K_p'= .2)

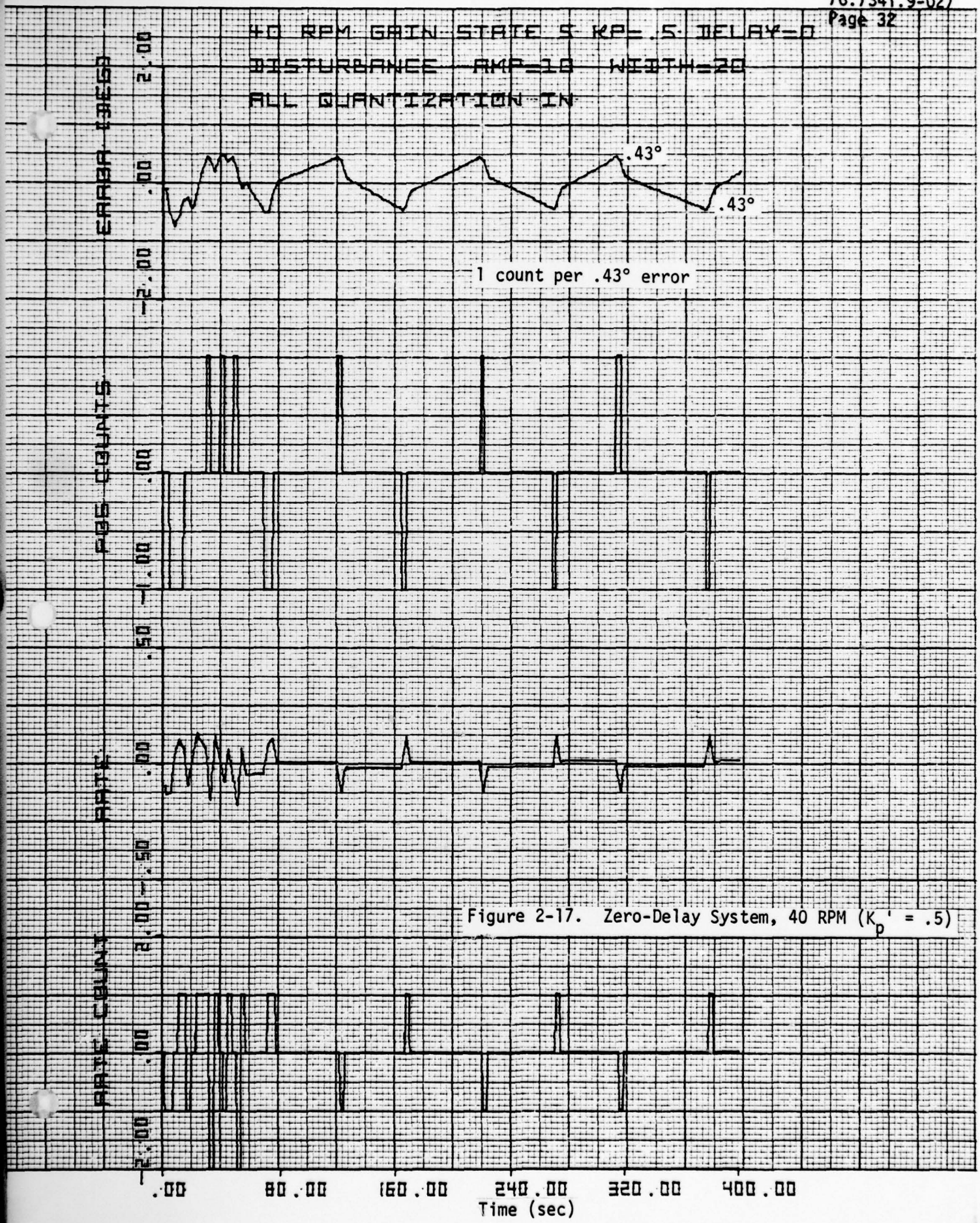

Figure 2-17. Zero-Delay System, 40 RPM ($K_p' = .5$)

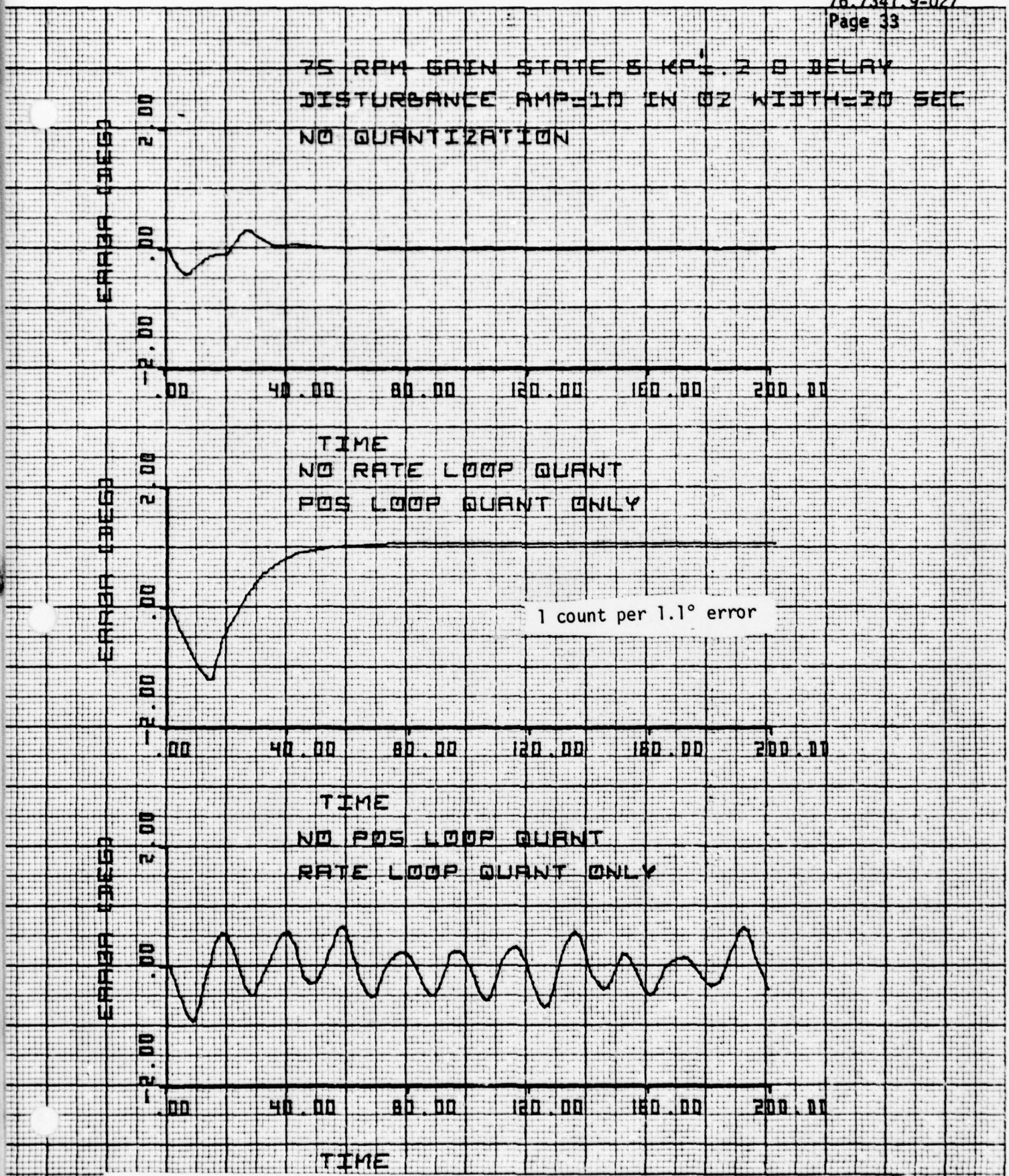

Figure 2-18. Effects of Removing Quantization, Zero-Delay System, 75 RPM

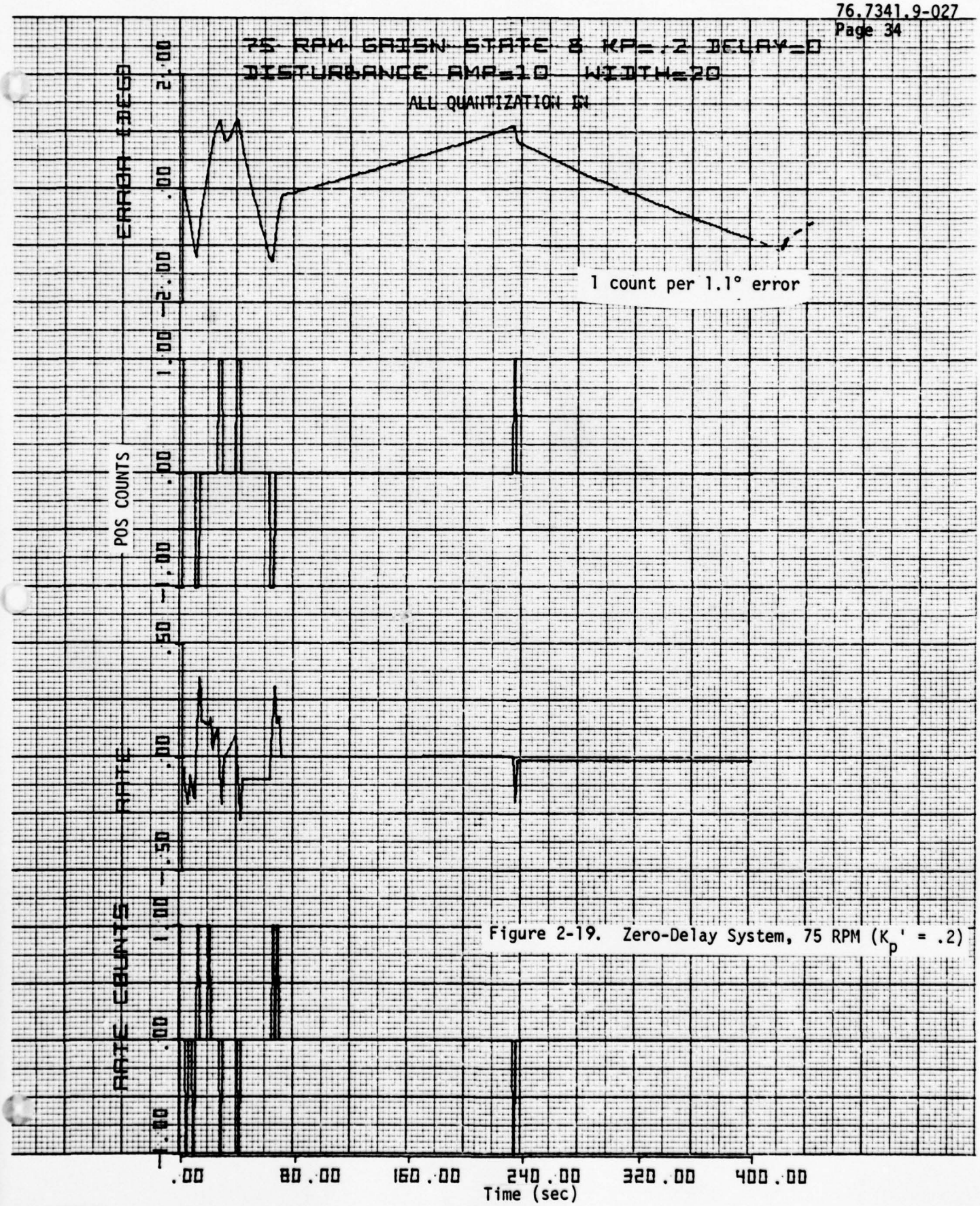

Figure 2-19. Zero-Delay System, 75 RPM ($K_p' = .2$)

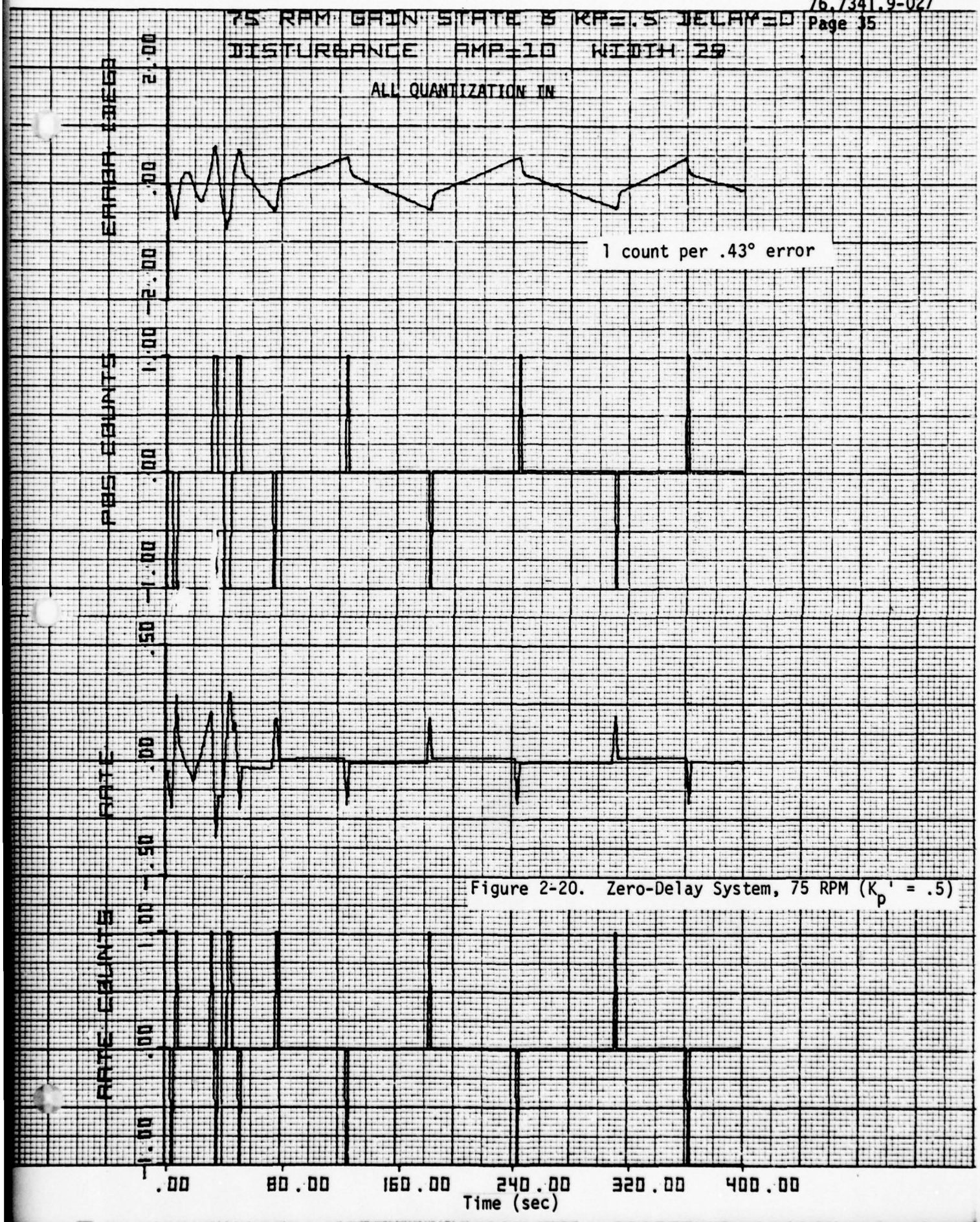

Figure 2-20. Zero-Delay System, 75 RPM ($K_p' = .5$)

error by using the search mode and a ground controller. The steady-state error response is always going to be oscillatory, and the next section will show that, when the effects of the delay are considered, the minimum limit cycle to be expected will be about 1 deg. It will also show that the lower RPM's (a range of 40 to 75 was considered) provide somewhat better limit cycle response due to the fact that a higher value of the ground position gain is possible at the lower RPM's, and also somewhat due to the decreased rate quantization at the lower RPM's. (The former fact was indicated by Figure 2-9.)

3.0 DESIGN OF A POSITION LOOP, CONSIDERING THE EFFECTS OF THE DELAY

In this section, the analysis of Section 2 will be repeated, but the delay in both the rate loop (= .5T) and the position loop will be considered. Currently, the position loop delay is estimated to be about 2 - 6 sec., depending on the spin speed. (See Appendix A.)

Before going into the analyses, the main conclusions from Section 2 (zero-delay system) will be repeated because they provide guidelines for the type of behavior to be expected from the system with transport lag included. The main conclusions were:

- Rate quantization is the main obstacle to obtaining a convergent response of the pointing error, and instead leads to an oscillatory response.
- There is less rate quantization at lower RPM's so possibly better performance at the lower spin speeds can be expected.
- The amplitude of the limit cycles of the zero delay system, taking into account quantization, can be predicted by $1/(4.56\ K_p')$ degrees (assuming stable value for K_p'.)
- The linear stability analysis results show that higher values of the position gain $K_p = 4.56\ K_p'$ are possible at lower RPM's, so so perhaps a smaller limit cycle can be obtained.

3.1 Linear Analysis

The open loop Z-plane transfer function of the controller's inner rate loop is

$$L_R(z) = Z\left[K_o T^2 \left(\frac{z-1}{z}\right) e^{\frac{-sT_s}{4}} \frac{(s+B)}{s^3}\right]$$

$$= K_o T^2 \frac{(z-1)}{z} \; Z\left[e^{\frac{-sT_s}{4}} \frac{s+B}{s^3}\right] \qquad (3\text{-}1)$$

The Z-plane transfer function is evaluated by partial fraction expansion and modified Z transforms.

$$L_R(z) = K_o T^2 \left(\frac{z-1}{z}\right) Z_m\left[\frac{1}{s^2} + \frac{B}{s^3}\right] \quad \text{and } m = .75$$

$$= K_o T^2 \left(\frac{z-1}{z}\right)\left\{\frac{mT_s}{z-1} + \frac{T_s}{(z-1)^2} + \frac{B_1 T_s^2}{2}\left[\frac{m^2}{z-1} + \frac{2m+1}{(z-1)^2} + \frac{2}{(z-1)^3}\right]\right\}$$

$$= K_o T^2 \frac{(n_2 z^2 + n_1 z + n_o)}{2z(z-1)^2} \qquad (3\text{-}2)$$

where

$$n_2 = T_s (2m + BT_s m^2)$$

$$n_1 = T_s [2-4m - 2BT_s m^2 + BT_s(2m + 1)]$$

$$n_o = T_s [2m-2 + BT_s(m^2 - 2m+1)]$$

$$= T_s [2(m-1) + BT_s(m-1)^2]$$

The Z-transform of the position loop is

$$L_p(z) = K_o K_p' \frac{z-1}{z} Z\left[\left(\frac{s+B}{s^4}\right) e^{-\tau_D s}\right] \tag{3-3}$$

Because the delay in this position loop is on the order of several seconds, i.e., large compared to the sampling interval, T_s, it is convenient to study cases where the delay is a multiple of the sampling period. If this is done, then the Z-transform, $L_p(z)$ is easily taken by multiplying the z transform of $L_p(z)$ with no delay by $1/z^k$, i.e.,

$$L_p(z) = K_o K_p' \frac{(z-1)}{z} \cdot \frac{1}{z^k} Z\left(\frac{s+B}{s^4}\right) \tag{3-4}$$

where k is the number of sampling periods of the delay in the ground loop. The transform of the position loop without delay has already been evaluated in Section 2. Therefore, the transfer function of the position loop with delay is

$$L_p(z) = \frac{K_o K_p'}{z^k} \left[\frac{\mu_2 z^2 + \mu_1 z + \mu_o}{6 (z-1)^3}\right] \tag{3-5}$$

where

$$\mu_2 = 3T_s^2 + BT_s^3$$
$$\mu_1 = 4BT_s^3$$
$$\mu_o = BT_s^3 - 3T_s^2$$

The transfer function L(z) of the combined system is

$$L(z) = K_p' L_p(z) + L_R(z),$$

or

$$L(z) = \frac{K_p' K_o}{z^k} \left(\frac{\mu_2 z^2 + \mu_1 z + \mu_o}{6(z-1)^3}\right) + K_o T^2 \frac{(\eta_2 z^2 + \eta_1 z + \eta_o)}{2z(z-1)^2} \tag{3-6}$$

The poles of the combined system $K_p' L_p(z) + L_R(z)$ are:

1. three poles at z = 1
2. 1 pole at origin for k = 0, 1
3. k poles at origin for k = 2, ...

The zeros of the combined system are not as easily solved for. One of the zeros is associated with the S-plane filter breakpoint B, or $z = e^{-BT_s}$. The location and number of the other Z-plane zeros is dependent on the ground loop delay, $\tau_D = K T_s$ and the ground loop position gain K_p'.

In order to solve for the value of K_p' to use, which depends on the gain state chosen and the spin speed, the characteristic equation of the system will be rewritten so as to isolate K_p' as the overall system gain, as was done in Section 2.0. That is, if $L_R(z)$ is the transfer function of the inner rate loop, and $K_p'(z)$ is the transfer function of the position loop, the characteristic equation

$$1 + L_R(z) + K_p'(z) = 0 \tag{3-7}$$

will be rewritten as

$$1 + \frac{K_p' L_p(z)}{1 + L_R(z)} = 0 \tag{3-8}$$

and the new open loop transfer function, H(z)

$$H(z) = \frac{K_p' L_p(z)}{1 + L_R(z)} \tag{3-9}$$

will be plotted in the Z-plane.

The transfer function of the inner loop is

$$L_R(z) = \frac{K_o T^2 (n_2 z^2 + n_1 z + n_o)}{2z(z-1)^2} \tag{3-10}$$

and the transfer function of the outer loop is

$$K_p' L_p(z) = \frac{K_o K_p'}{z^k} \left[\frac{\mu_2 z^2 + \mu_1 z + \mu_o}{6(z-1)^3} \right] \qquad (3\text{-}11)$$

When the characteristic equation $1 + L_R(z) + K_p' L_p(z) = 0$ is rewritten as

$$1 + \frac{K_p' L_p(z)}{1 + L_R(z)} = 0 \qquad (3\text{-}12)$$

the result is

$$1 + \left[\frac{K_o K_p' (\mu_2 z^2 + \mu_1 z + \mu_o)}{z^{k-1}(z-1)\left[6z^3 + z^2(3K_o T^2 n_2 - 12) + z(6 + 3K_o T^2 n_1) + 3K_o T^2 n_o\right]} \right] = 0$$

or

$$1 + G(z) = 0 \qquad (3\text{-}13)$$

where $G(z)$ is equal to the expression in brackets in the previous equation.

The root locus of $G(z)$ was considered for different gain states at each RPM with various delays in the ground loop (i.e., different values of k), where the ground loop delay was considered to be multiples of the sampling period. The maximum values of the previous gain K_p' for stability, i.e., those values which cause the roots of the characteristic equation to be on the unit circle, are shown in Figure 3-1.

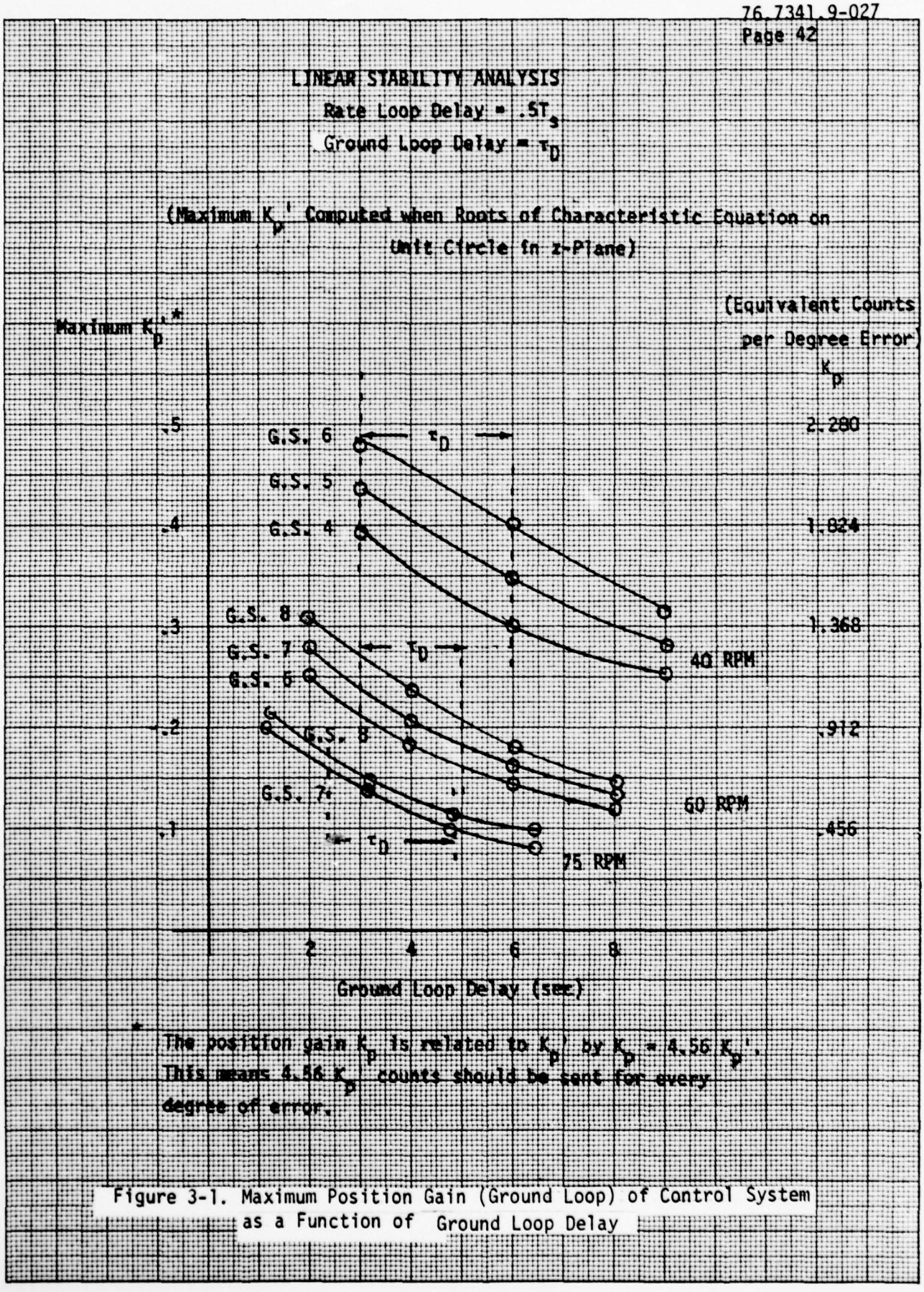

* The position gain K_p is related to K_p' by $K_p = 4.56\ K_p'$. This means 4.56 K_p counts should be sent for every degree of error.

Figure 3-1. Maximum Position Gain (Ground Loop) of Control System as a Function of Ground Loop Delay

3.2 Position Loop Results

The range of the position loop gain K_p for stability of the non-linear system is very nearly predicted by the stability of the linear system as shown in Figure 3-1 if the position loop counter is implemented as follows (Figure 3-2):

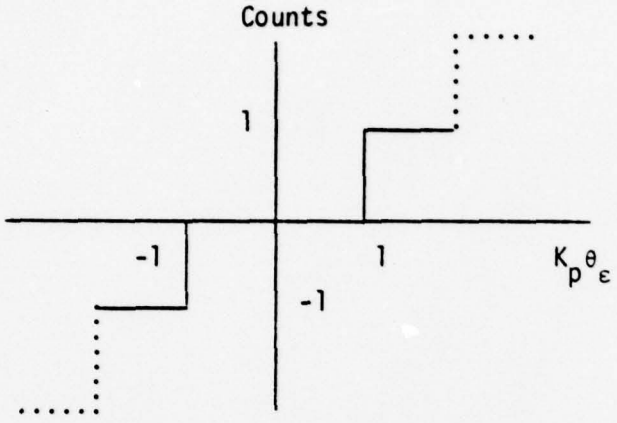

Figure 3-2. Implementation of Ground Loop Counter

The region around the origin, i.e., "0 counts" is of particular importance because it has already been shown in Section 2.0 that the steady state error exhibits a limit cycle behavior oscillating between $\pm 1/K_p$ degrees, with the position loop commanding at most one count in either direction. (The results for Section 2.0 considered a zero-delay system, but the limit cycle of the system with the ground loop delay is only slightly larger than $1/K_p$ degrees, and still only one count is needed in the steady state.) It turns out that it is possible for the control system to command more than one count in response to certain transients; however, even then, there are certain advantages to limiting the counter to $\pm$ 1 count, and these will be presented later in this section. The important point is that any gain selected should be done so with the ground commanded counter implemented as in Figure 3-2.

Simulation results indicate that because the effective gain is somewhat reduced by the quantization, somewhat higher values for the gains could be tolerated than those indicated as being the maximum value in Figure 3-1, especially at the lower RPM. The following values of K_p' were chosen with the idea of picking a higher value of K_p' in order to reduce the limit cycle.

40 RPM $K_p' = .3$

60 RPM $K_p' = .15$

75 RPM $K_p' = .10$

The gain phase plots of the transfer function of the control system, whose open-loop transfer function is L(z),

where

$$L(z) = \frac{z-1}{z}\left[K_o T^2 \quad Z\left(e^{-T_s s/4}\frac{(s+B)}{s^3}\right) + K_o K_p' \; Z\left(e^{-\tau_D s}\frac{(s+B)}{s^4}\right)\right]$$

and $\tau_D = k\ T_s$, k = integer

are shown in Figures 3-3 through 3-10 for various ground loop delays τ_D at each RPM. The final selection of gains in terms of counts per degree, and also the ideal gain state at each RPM is shown in Table 3-1.

Table 3-1. Position Loop Gain Selection

RPM	GAIN STATE	GAIN (COUNTS PER DEGREE)
40 RPM	6	1.368
60 RPM	8	.684
75 RPM	8	.456

The counter should be limited to ± 1 count, with 1 count being sent when the magnitude of $K_p\theta_\varepsilon$ exceeds 1.

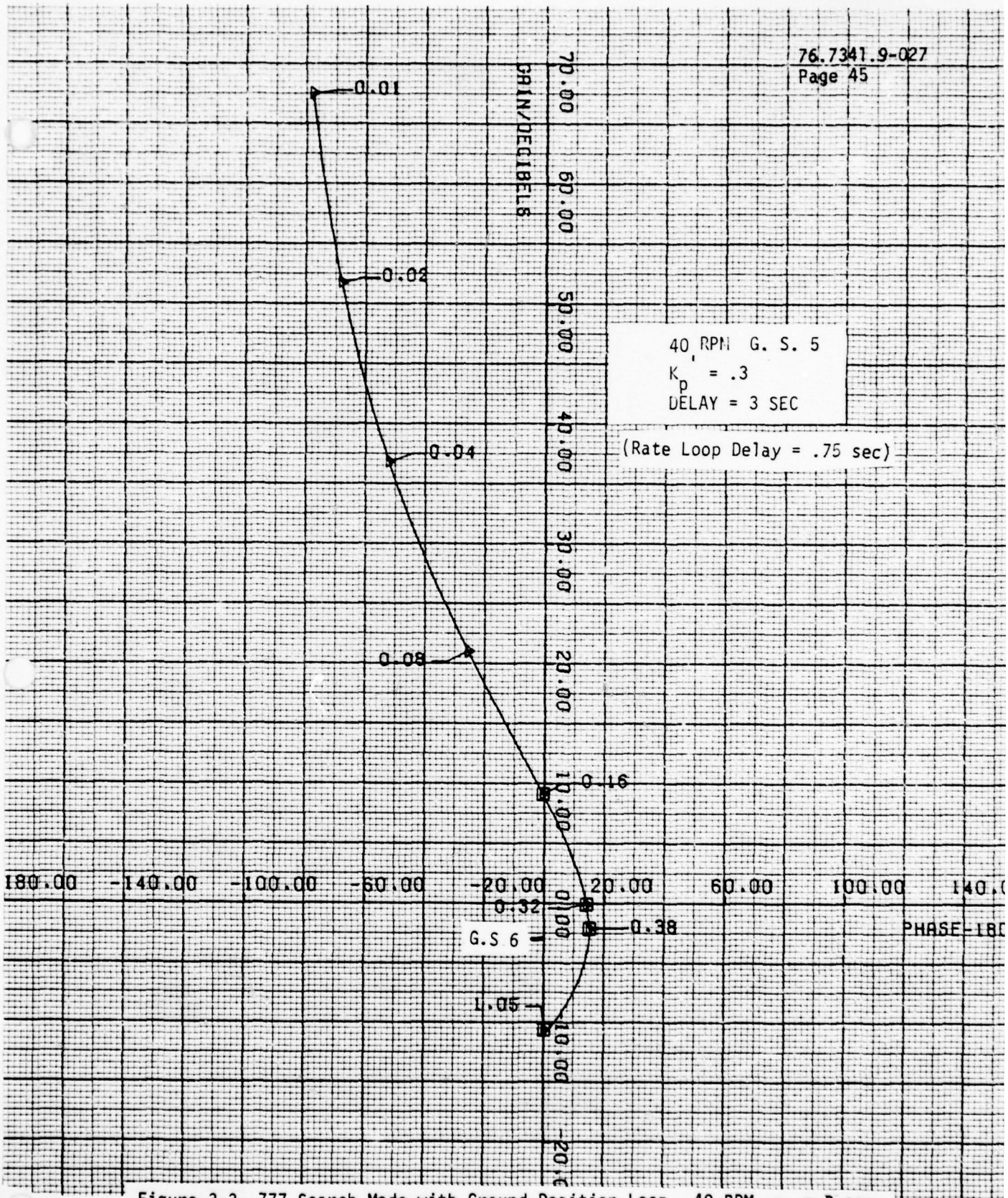

Figure 3-3 777 Search Mode with Ground Position Loop, 40 RPM, τ_D = 3 sec.

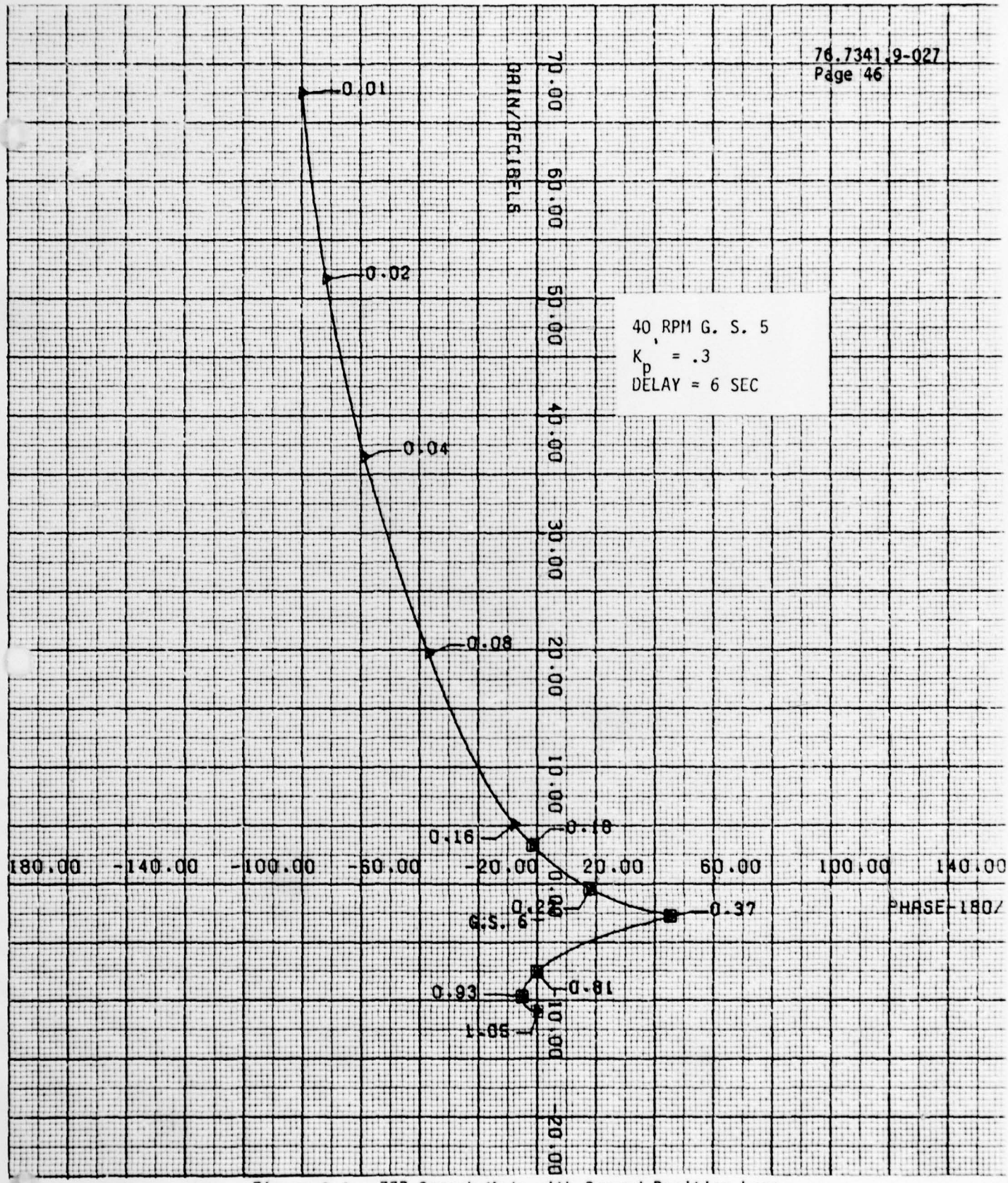

Figure 3-4. 777 Search Mode with Ground Position Loop
40 RPM, τ_D = 6 sec

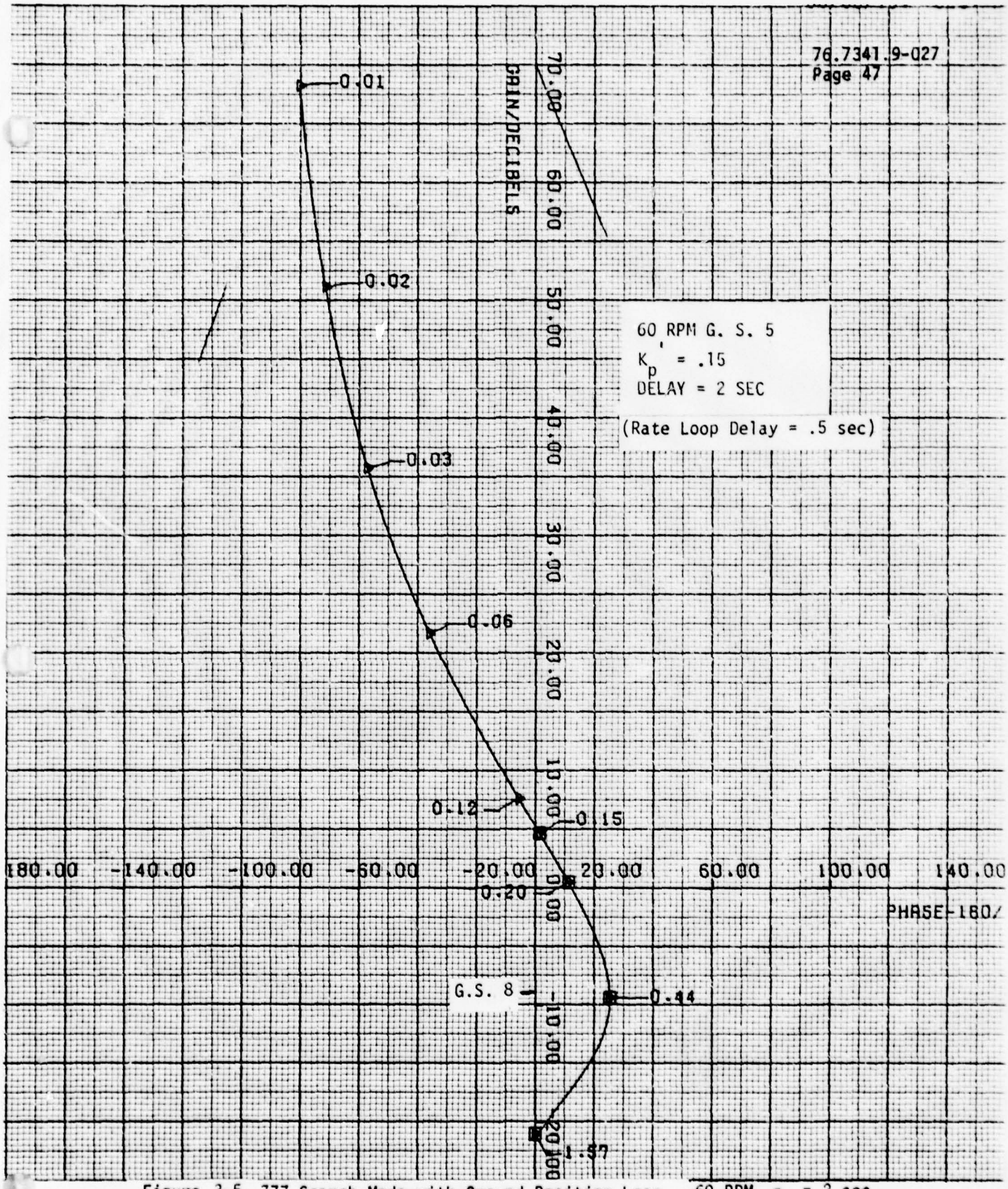

Figure 3-5. 777 Search Mode with Ground Position Loop 60 RPM, τ_D = 2 sec

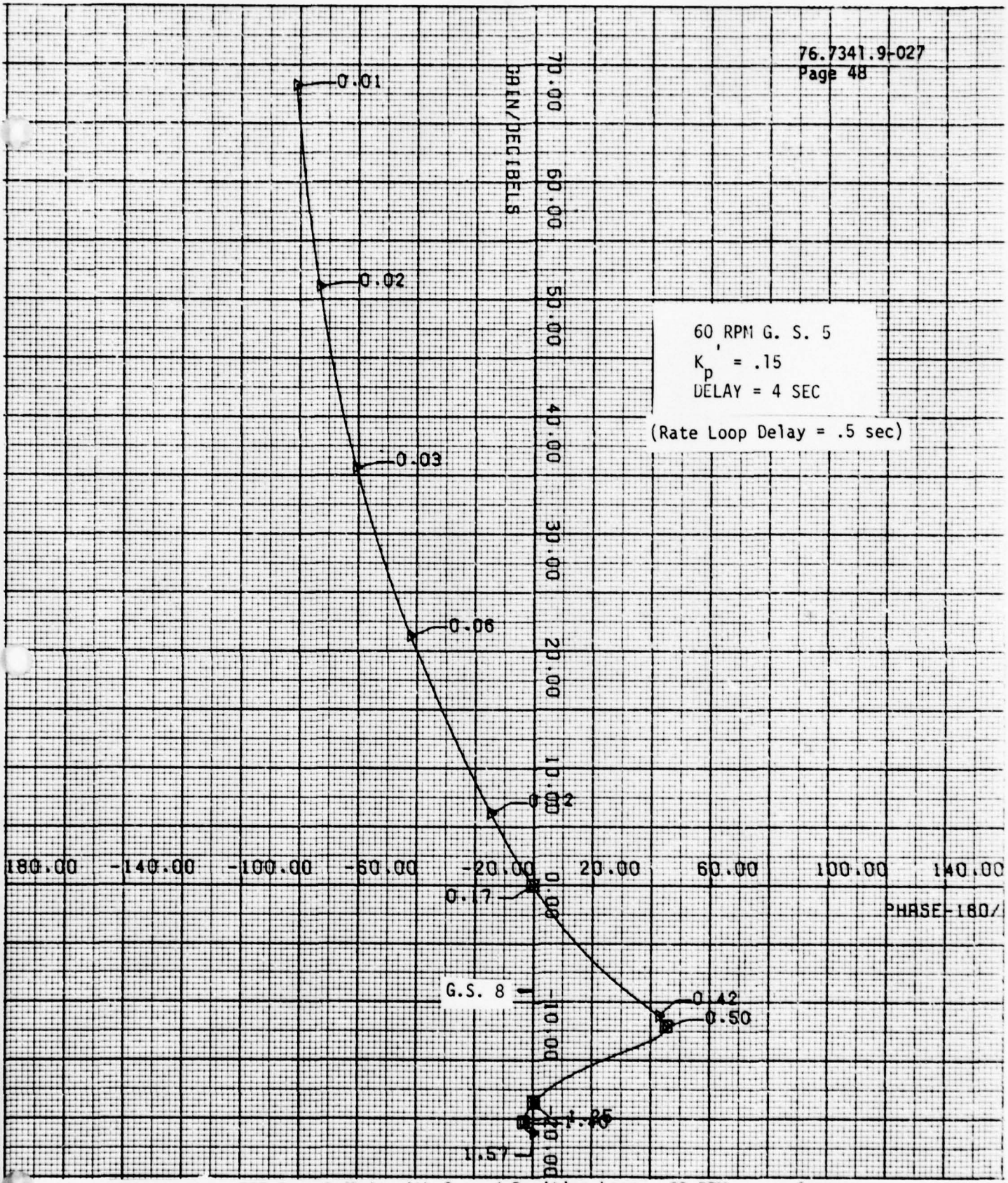

Figure 3-6. 777 Search Mode with Ground Position Loop 60 RPM, τ_D = 4 sec

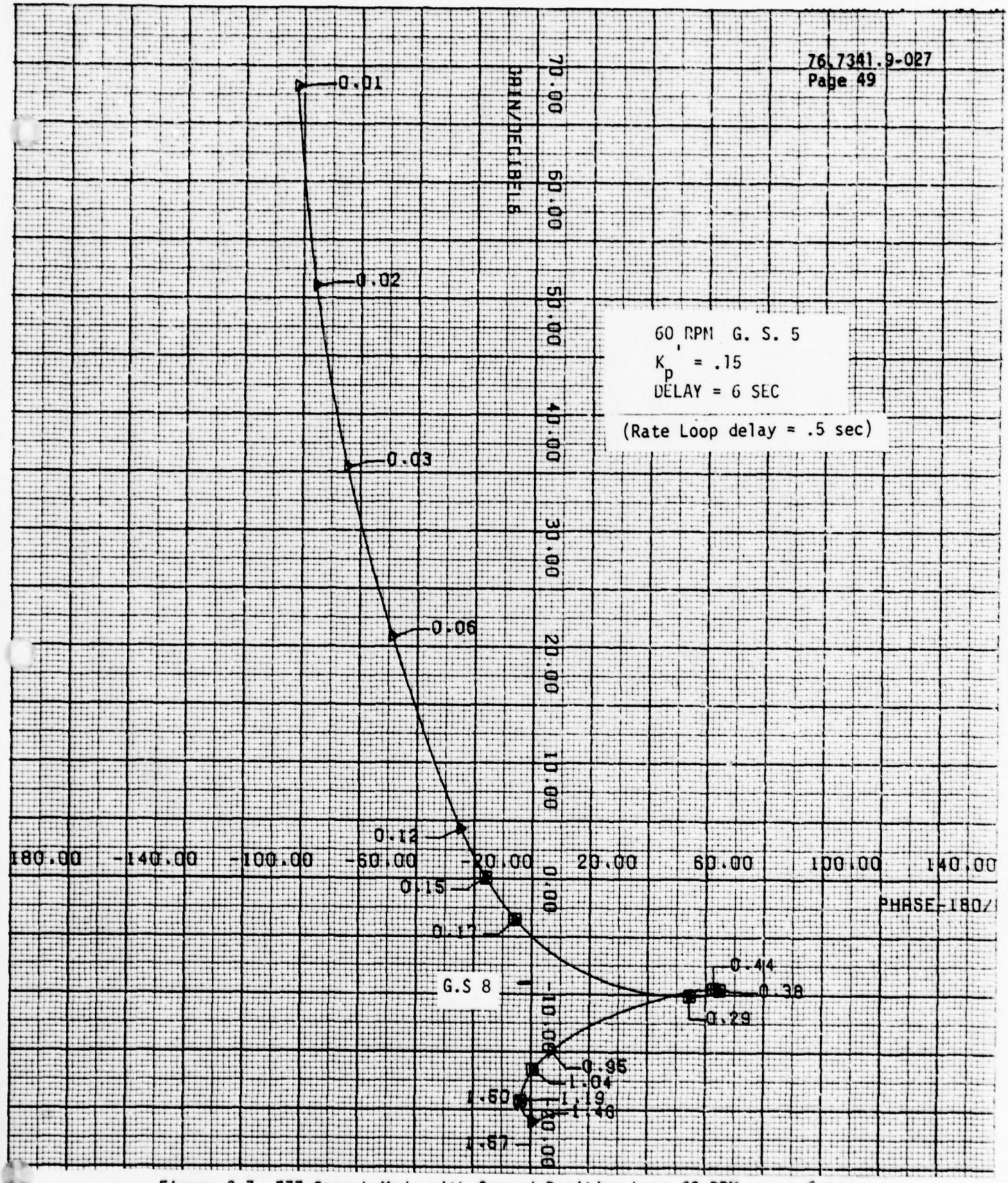

Figure 3-7. 777 Search Mode with Ground Position Loop 60 RPM, τ_D = 6 sec.

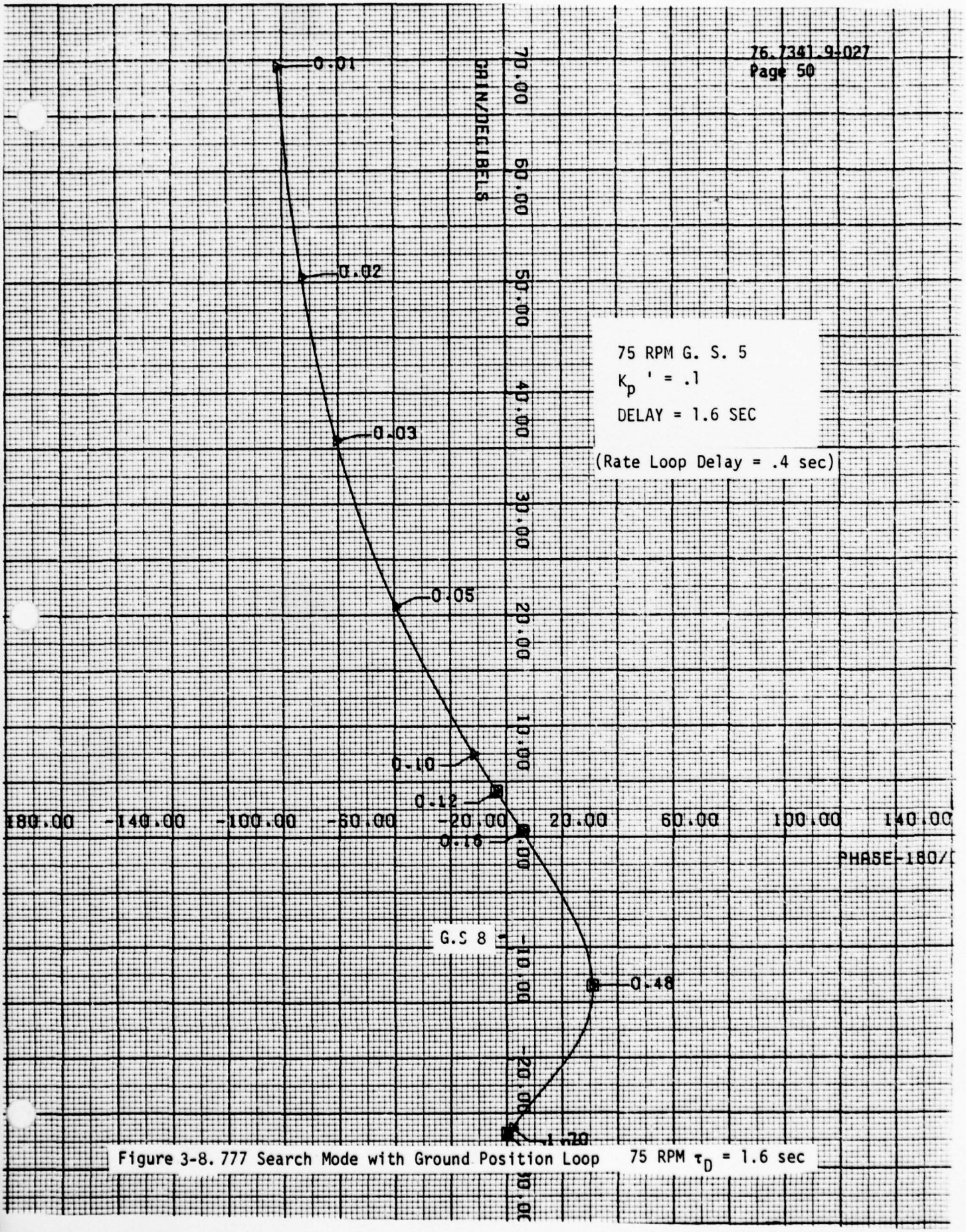

Figure 3-8. 777 Search Mode with Ground Position Loop 75 RPM τ_D = 1.6 sec

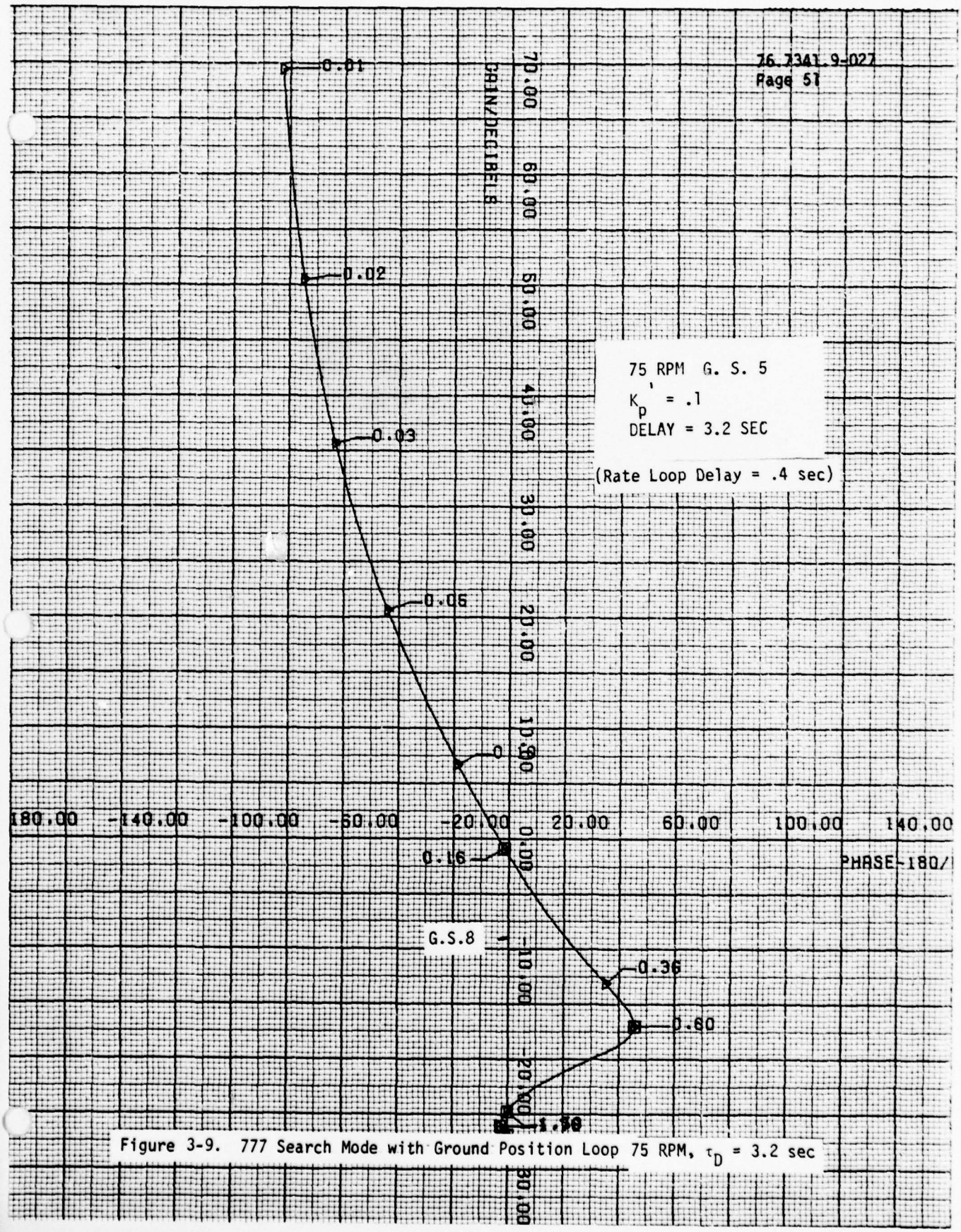

Figure 3-9. 777 Search Mode with Ground Position Loop 75 RPM, τ_D = 3.2 sec

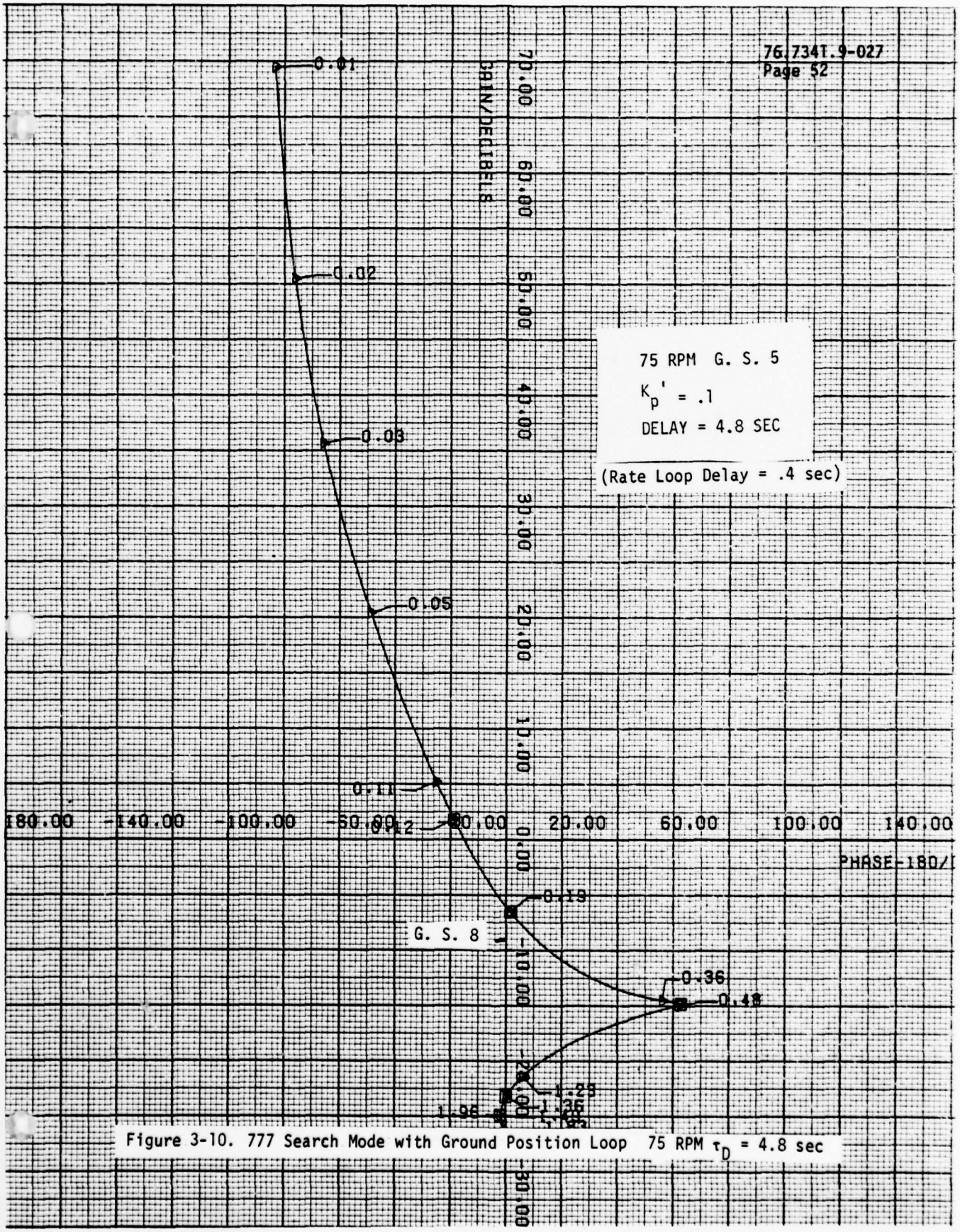

Figure 3-10. 777 Search Mode with Ground Position Loop 75 RPM τ_D = 4.8 sec

3.3 Performance Analysis

In analyzing the performance of the control system, two criteria were examined -- the peak pointing error during a transient, and the limit cycle performance. At each RPM, the worst case delays from Appendix A were assumed.

3.3.1 Steady-State Performance

Figure 3-11 shows the response of the system at 40 RPM using the gains and gain state from Table 3-1 to a simulated disturbance of 10 in-oz for 20 sec. The limit cycle is $\pm$ .8°, with the ground loop commanding at most $\pm$ 1 count. (There was actually a limit on the counter of 5 counts in this case.) Figure 3-12 shows the response of the control system to the same disturbance at 60 RPM, and a limit cycle of under 2° is obtained.

Although in both of the previous cases a true oscillatory response was obtained in the steady-state, i.e., the control system went from one side of the deadzone to the other, it is also possible for the system to stay on only one side of the deadband. This is shown in Figure 3-13, where a different initial condition was used at 40 RPM. In this case, the ground loop is commanding counts on only one side, after the initial transient. (The rate loop in the spacecraft is also issuing counts.) Still, the maximum peaks on the one side are at .8°, as before (40 RPM), and this behavior is what is referred to as "limit cycle" in this report.

3.3.2 Effect of Limiting Counter

A large disturbance (50 in oz for 20 sec) was simulated in Figures 3-14a and 3-14b (60 RPM). In Figure 3-14a, the counter was limited to $\pm$ 5 counts (only $\pm$ 4 counts were actually commanded) and in Figure 3-14b, the counter was limited to $\pm$ 1 count. The important point to notice is that the initial peak pointing error was the same in both cases ($\approx$4.8°) but that in the case where the counter had limits of $\pm$ 5, a large overshoot was seen ($\approx$6°) whereas in the case where the counter was limited, the overshoot was greatly reduced. The large overshoot in the first case was due to the time delay in the system. It seems reasonable, then to limit the counter to $\pm$ 1 count, in order to eliminate these large overshoots especially in light of the fact that in the steady state, 1 count is the

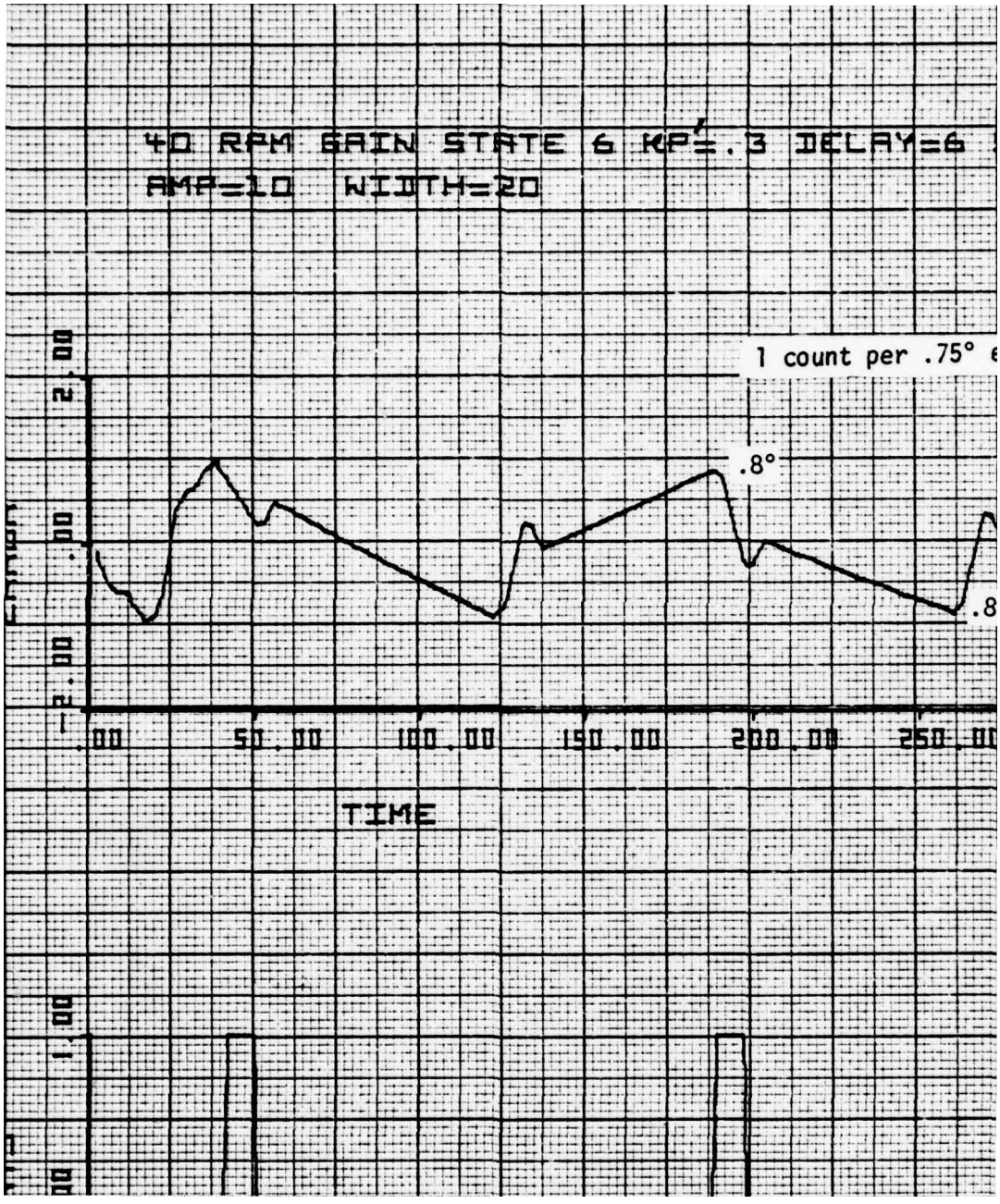
40 RPM GAIN STATE 6 KP'=.3 DELAY=6
AMP=10 WIDTH=20
1 count per .75°
.8°
.8
2.00
.00
-2.00
.00
50.00
100.00
150.00
200.00
250.00
TIME
1.00
.00

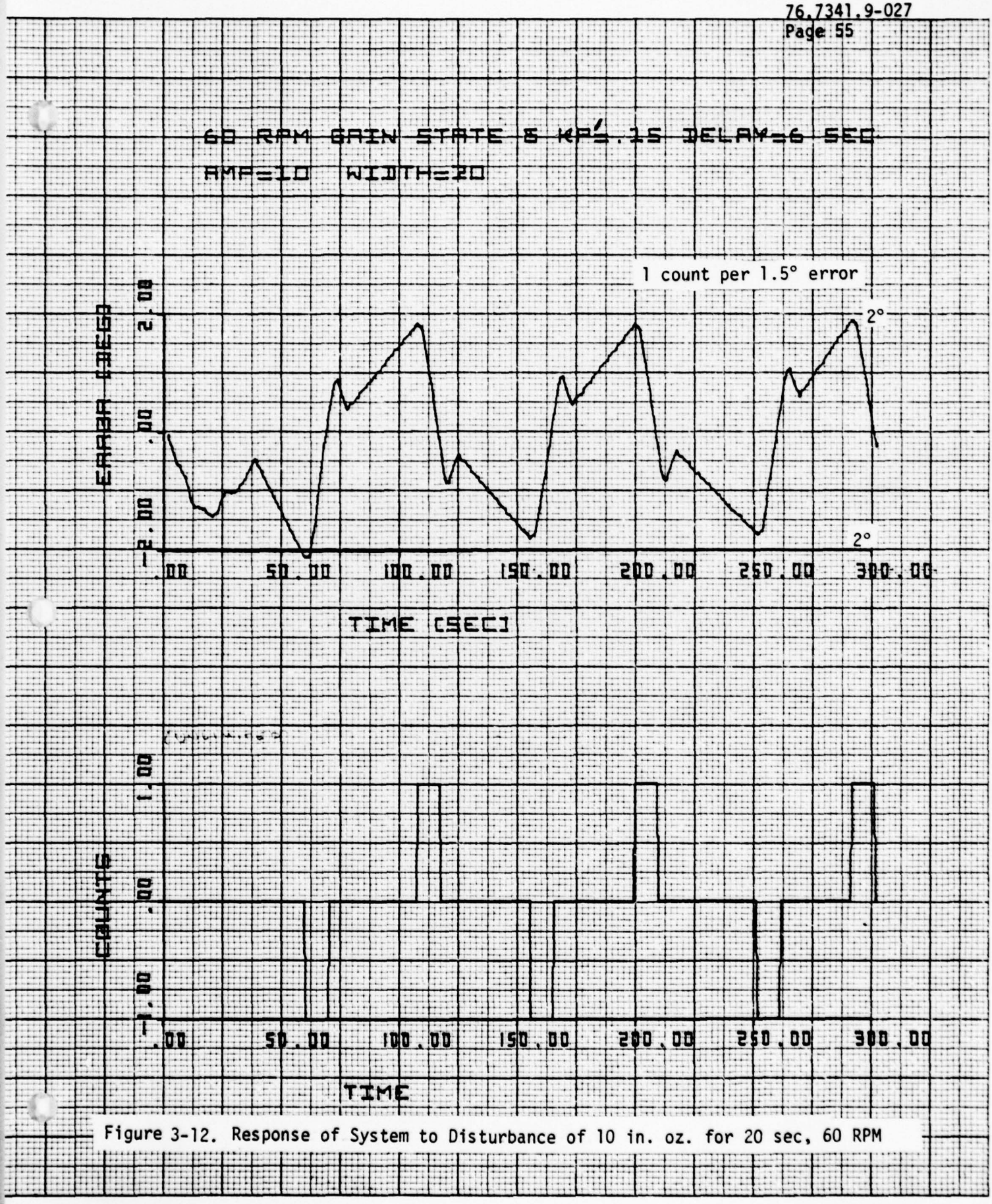

Figure 3-12. Response of System to Disturbance of 10 in. oz. for 20 sec, 60 RPM

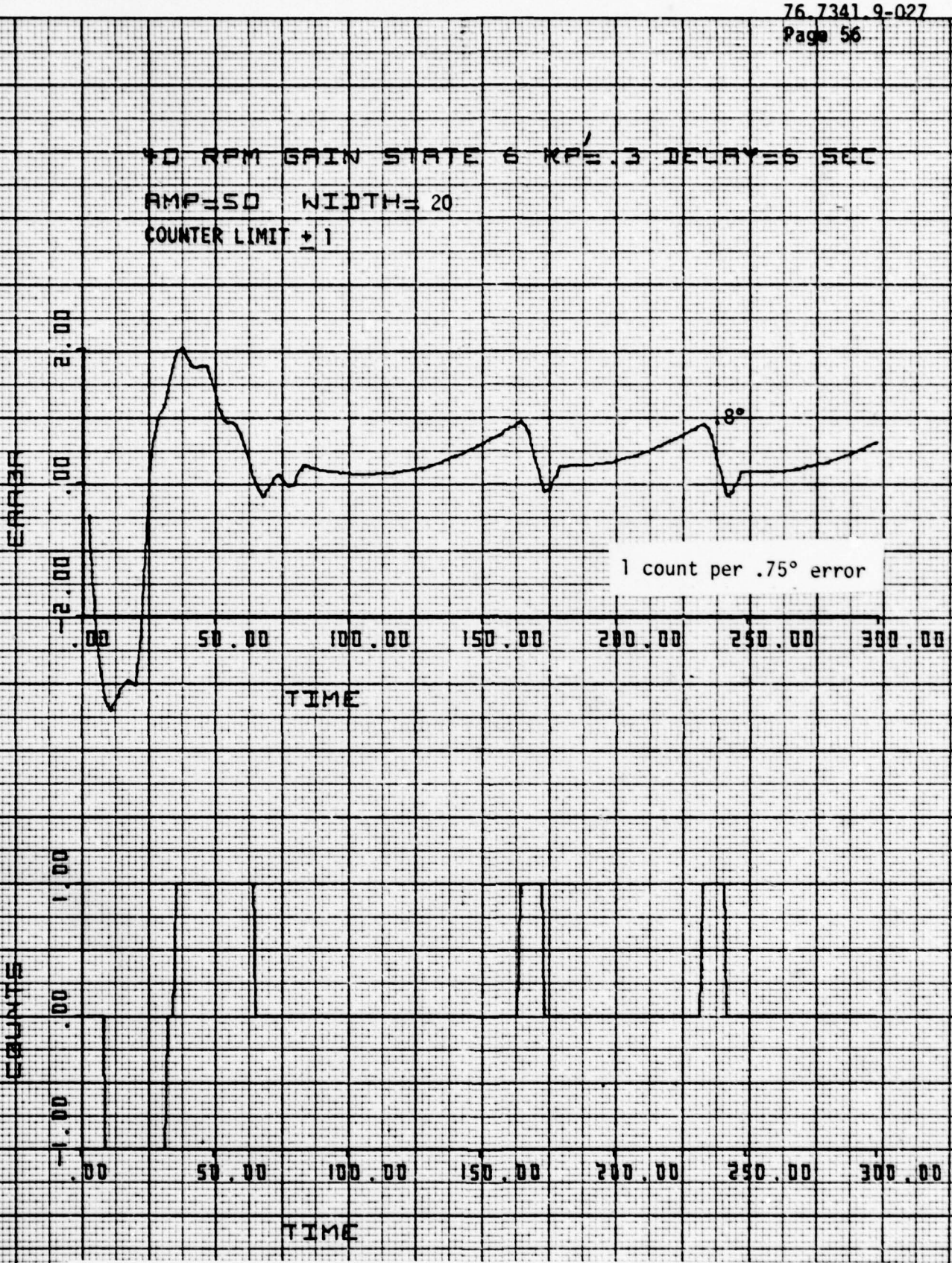

Figure 3-13. Response of System to Disturbance of 50 in-oz for 20 sec, 40 RPM

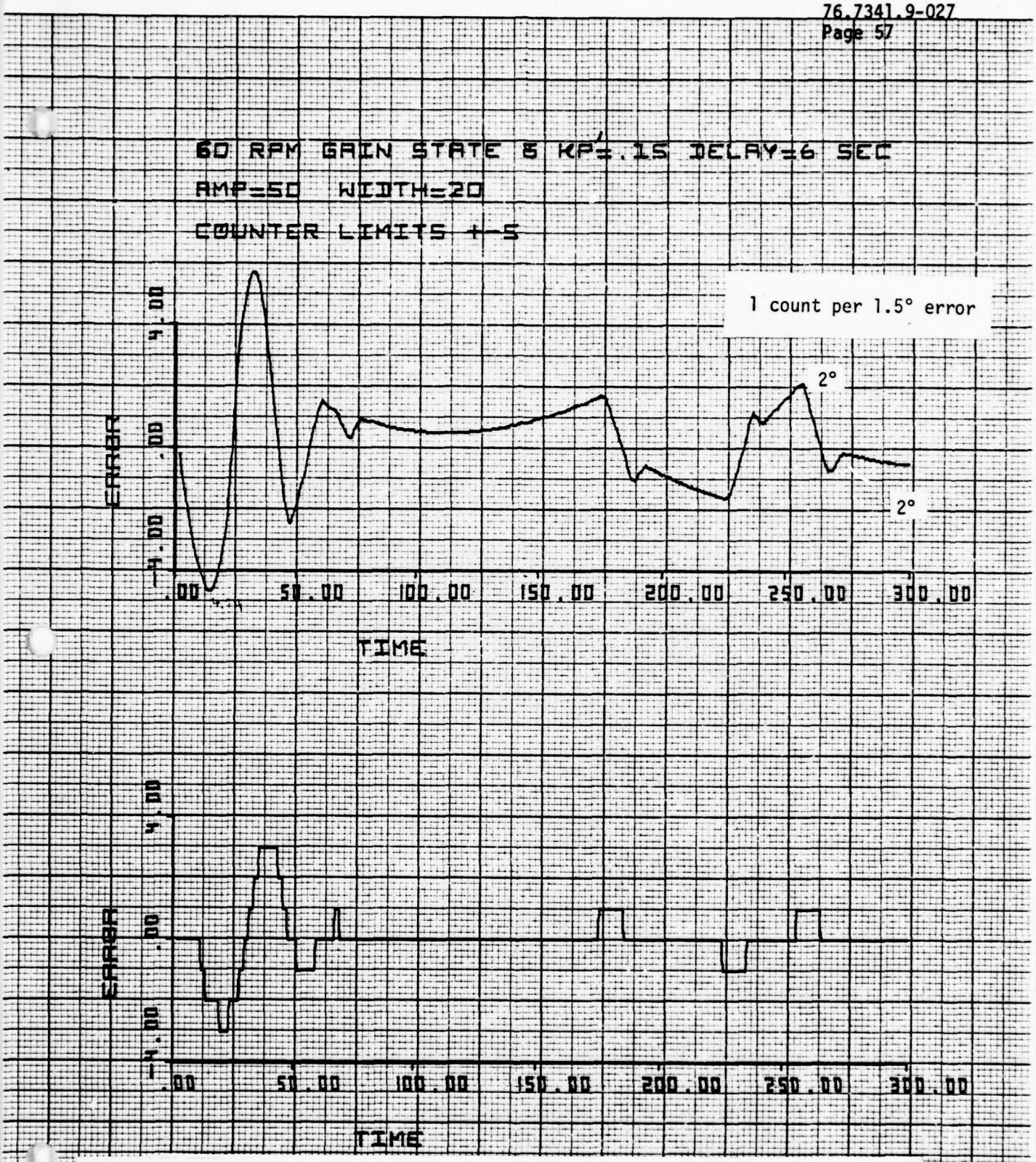

Figure 3-14a. Response of System to Large Disturbance with Counter Limits at ± 5, 60 RPM.

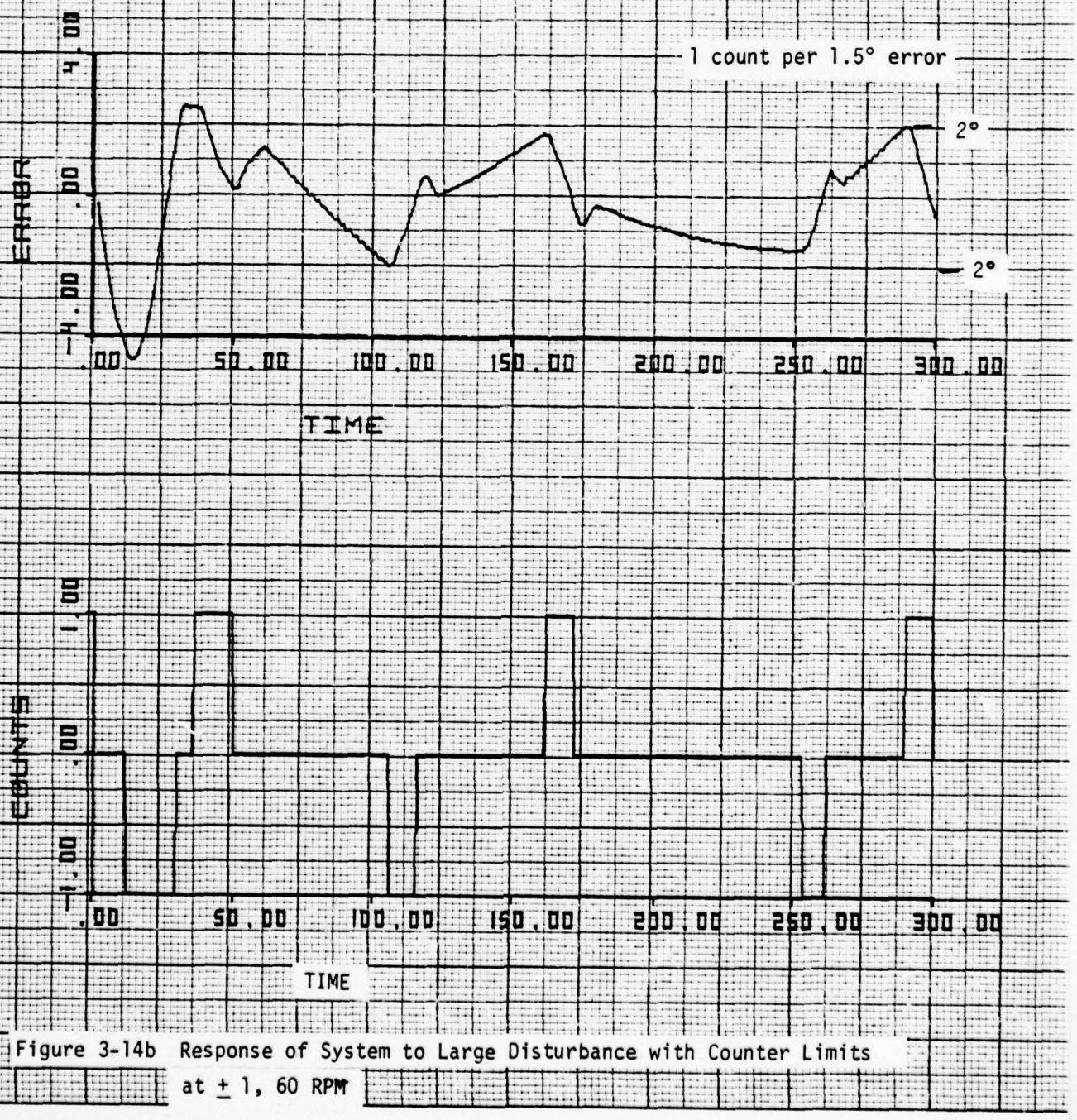

Figure 3-14b Response of System to Large Disturbance with Counter Limits at ± 1, 60 RPM

most needed anyway. Another advantage is that in limiting the counter, if the gain selected is too high, the system will not go unstable, but merely limit cycle at a higher frequency and somewhat higher amplitude than if a stable gain had been chosen. An example of this is provided in the next three figures, which show a test case at 75 RPM.

Figure 3-15 shows the response of the system to the same disturbance used earlier (10 in-oz for 20 sec) and with a stable value of K_p selected, (K_p' = .1 implies 1 count for every 2.2°) and steady-state peaks of about 2.4° are obtained, and the counter commands at most 1 count. (Note in this case that the responses is again "one-sided".) In Figure 3-16 an unstable value of K_p' was purposely selected (K_p' = .2, or 1 count for every 1.1° error) and the counter limits were placed at $\pm$ 5. The system response is obviously unstable, and limit cycles at $\pm$ 16° due to the counter limit. However, if the counter limits had been placed at $\pm$ 1, as shown in Figure 3-17, the error oscillates between $\pm$ 3°. Obviously, this is not optimum either, because better response was obtained in Figure 3-15, where a lower, stable variable of gain was selected, but what should be noted is that limiting the counter sort of "desensitizes" the control system and acts as an insurance policy against the consequences of too high a gain selection.

3.3.3 Effect of Rate Loop Offset

One other effect that can change the character of the steady-state performance is if the counter in the rate loop is not "dead set" around zero. The ideal model for the rate loop counter is shown below in Figure 3-18a, where the point of zero rate is in the center of the 0 count. However, if the rate loop counter is modeled as in Figure 3-18b, this changes both the amplitude and frequency of the pointing error response. This is shown in Figure 3-19, where an offset of .3 was used instead of .5 at 75 RPM. Also shown in Figure 3-19 are the commands issued by the rate loop in the spacecraft.

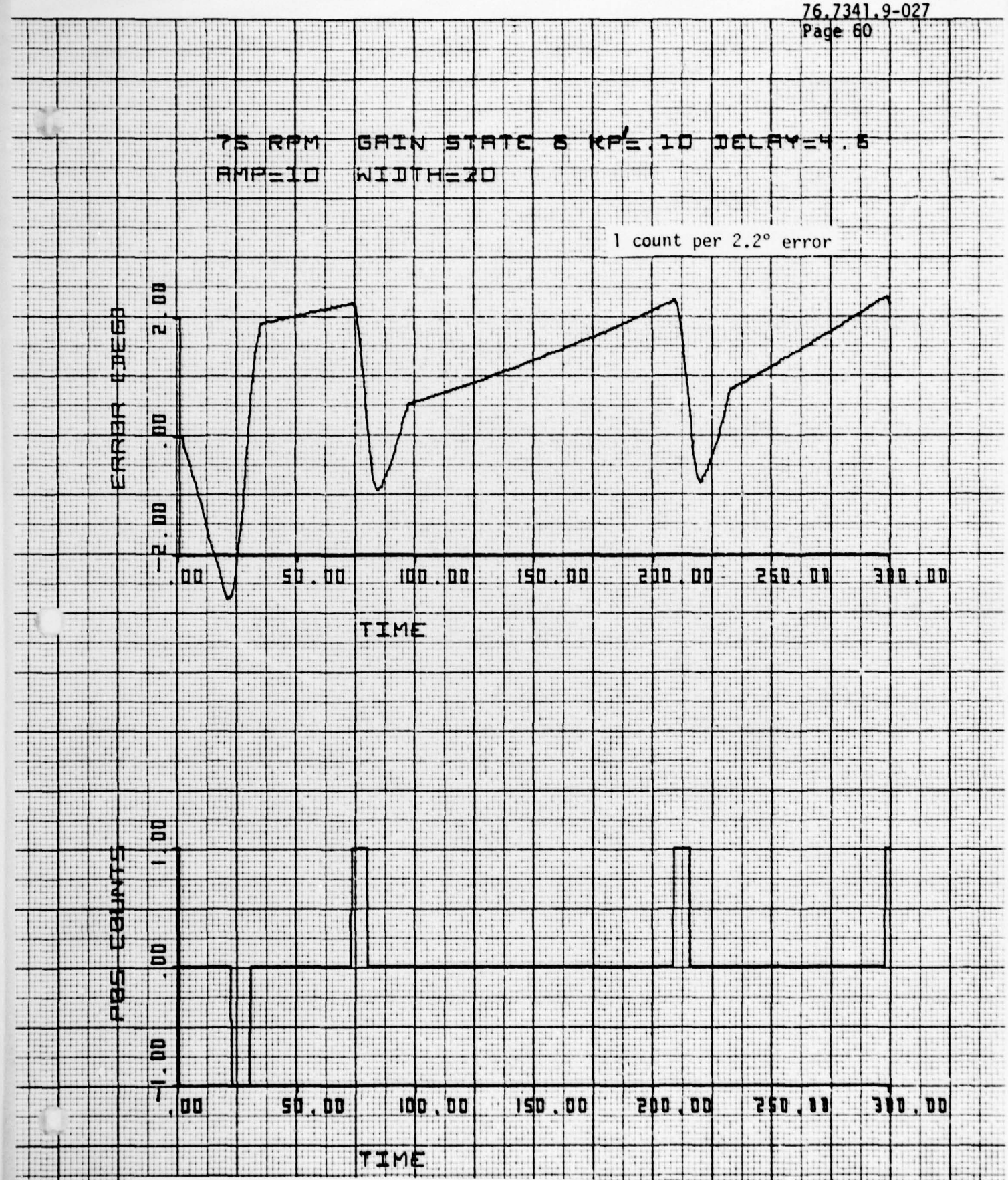

Figure 3-15 Response of Control System at 75 RPM (Stable Value of Gain Selected)

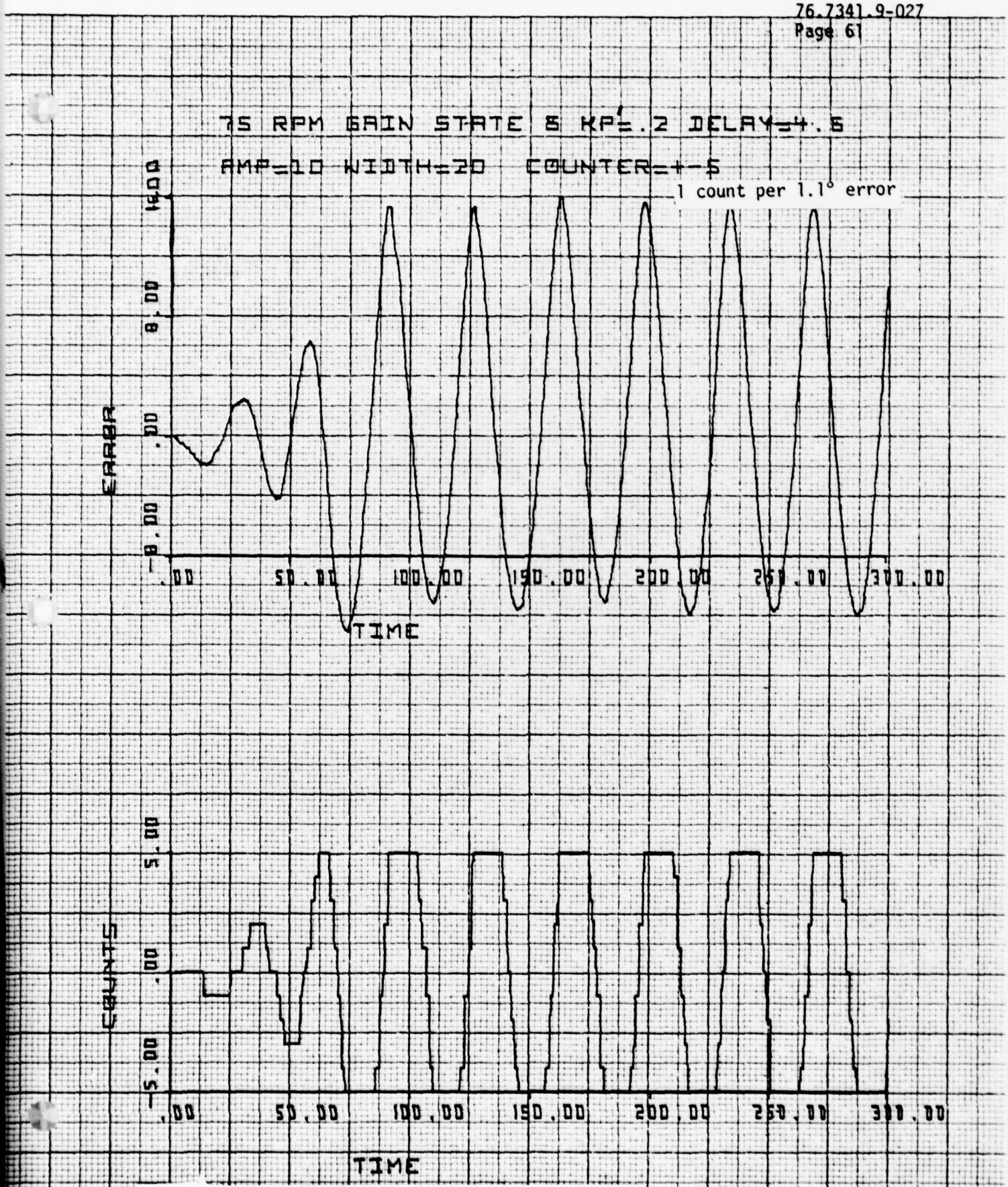

Figure 3-16 Response of Control System at 75 RPM

Unstable Gain Selected and Counter Limits at ± 5

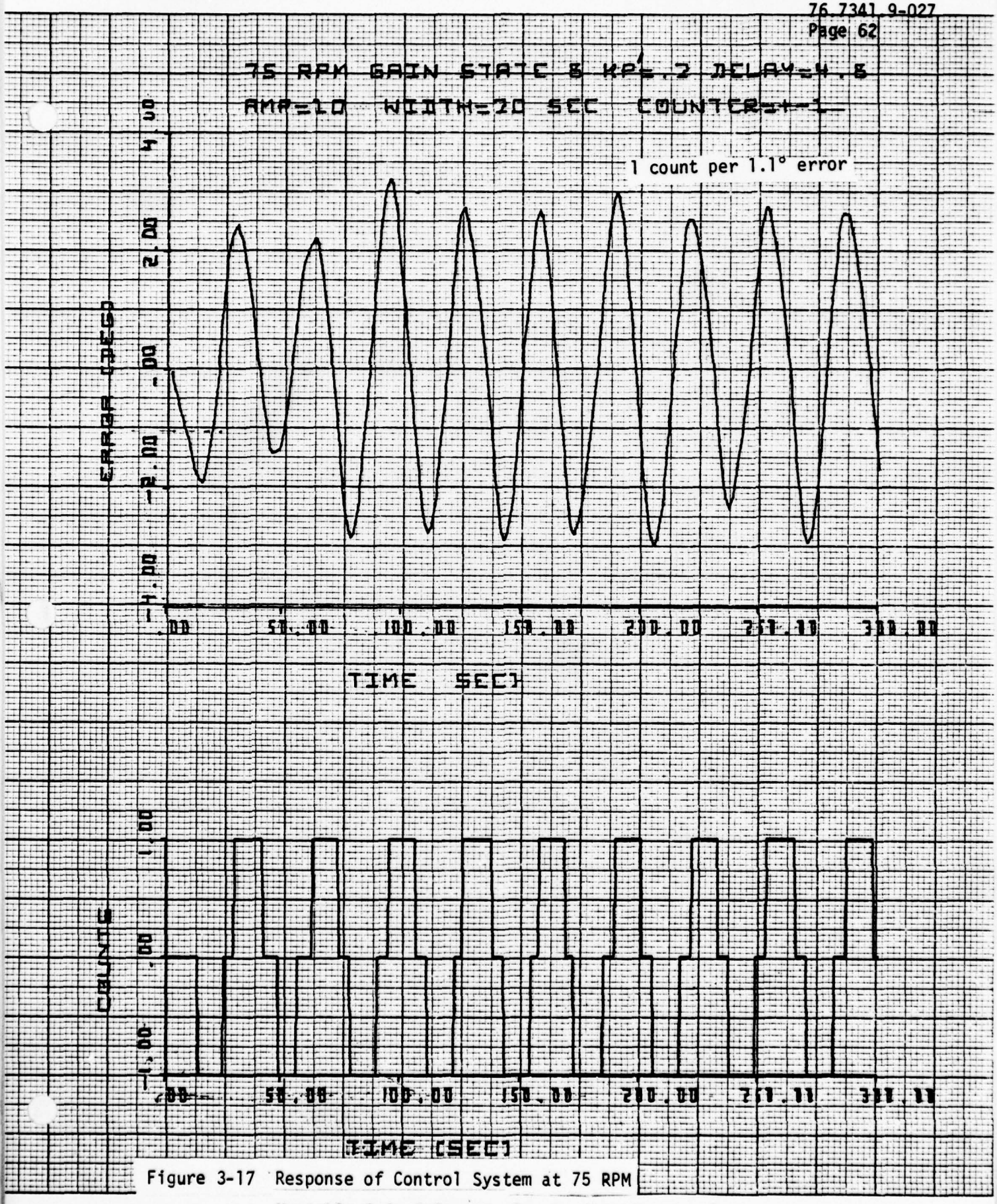

Figure 3-17 Response of Control System at 75 RPM

Unstable Gain Selected, Counter Limits at ± 1

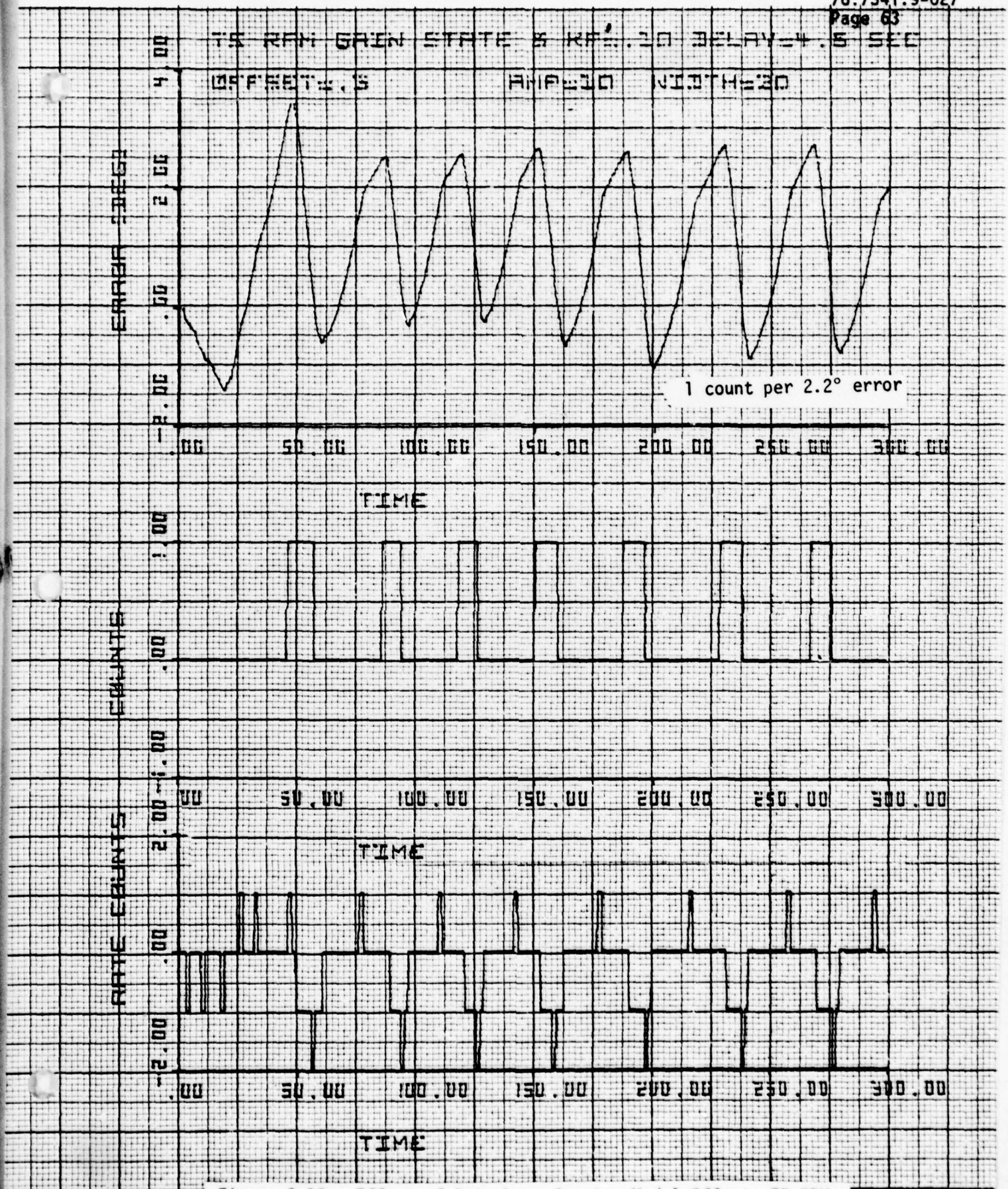

Figure 3-19. Effect of Rate Loop Counter Model Offset, 75 RPM

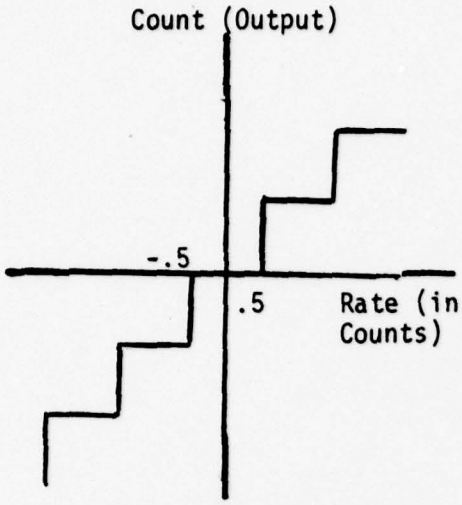

Figure 3-18a. Ideal Rate Counter (Offset = .5)

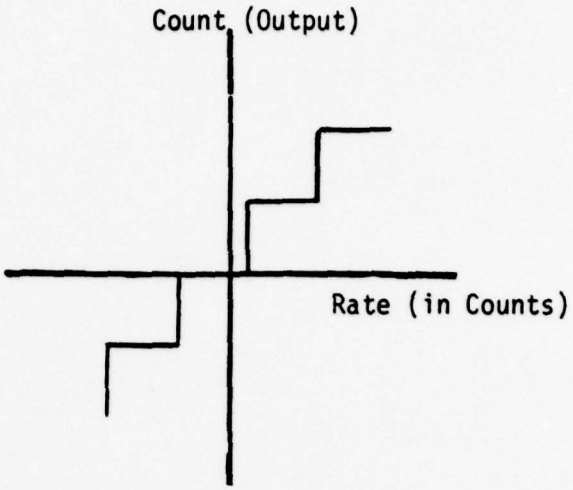

Figure 3-18b. Rate Counter with Offset

3.3.4 Transient Response

The second performance criteria was the peak transient response to sudden disturbances. Figure 3-20 shows the peak pointing errors that serve as a function of the amplitude of the simulated disturbance torque at different RPM's. (The duration of the disturbance was 20 seconds.) The worst case delays errors assumed for each spin speed, and the available motor torque and running friction were assumed to be 170 in-oz and 100 in-oz, respectively. The results show that of the three spin speeds tested, the system is least sensitive to disturbances at 40 RPM. It should also be noted that 40 RPM has the best limit cycle performance.

Figure 3-9. 777 Search Mode with Ground Position Loop 75 RPM, τ_D = 3.2 sec

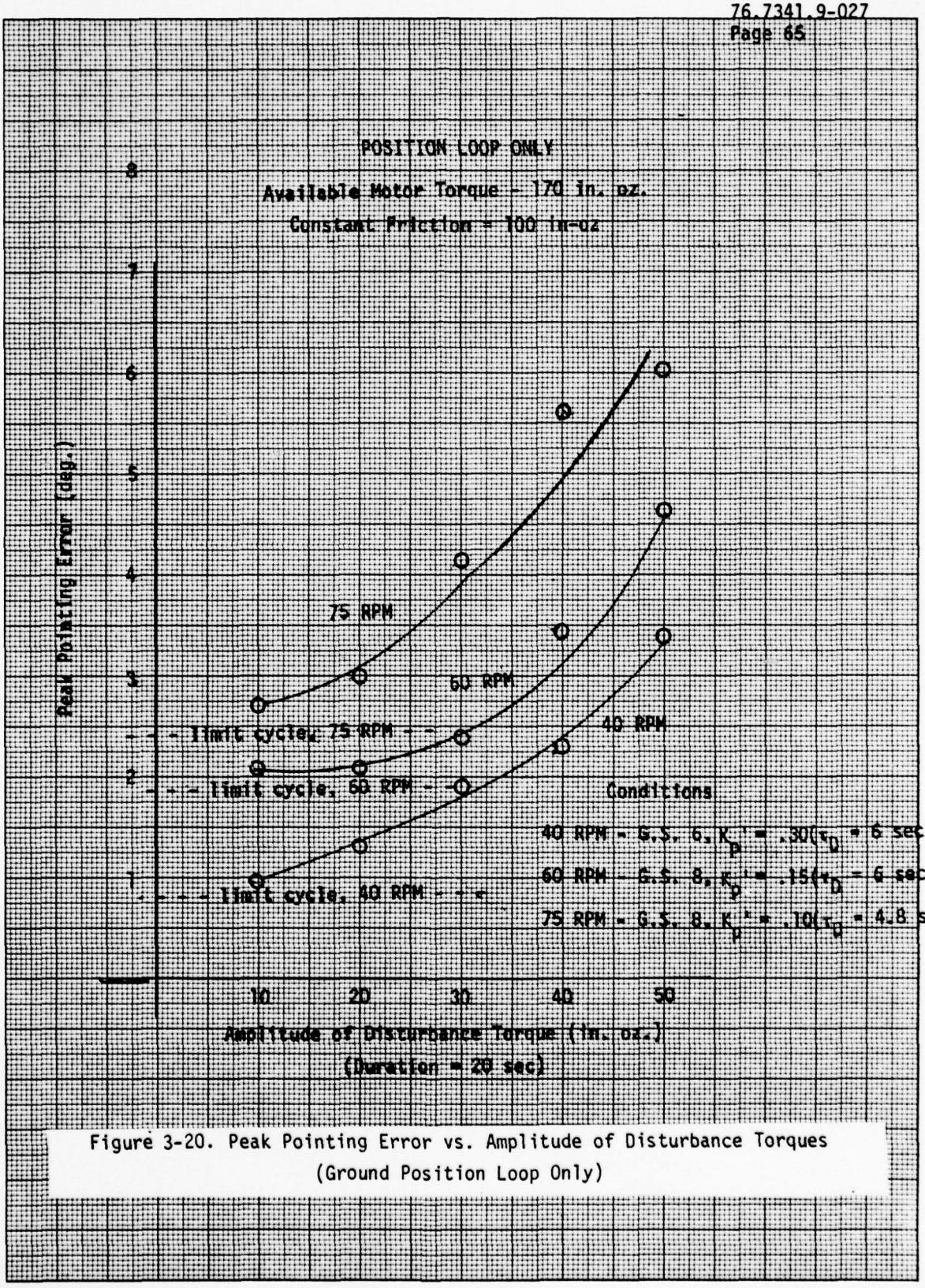

Figure 3-20. Peak Pointing Error vs. Amplitude of Disturbance Torques (Ground Position Loop Only)

Figure 3-10. 777 Search Mode with Ground Position Loop 75 RPM τ_D = 4.8 sec

4.0 DESIGN OF GROUND POSITION AND RATE LOOP

Subsequent to the design of the ground position loop, it was desired to study the effects of implementing a rate loop in the ground path as well, by differencing the position terms. The block diagram of the control system with both a rate term and a position term is the ground loop is shown in Figure 4-1.

4.1 Linear Analysis

Unfortunately, the Z-plane analysis is not so readily done in this case. That is because the rate term is computed by differencing position measurements that are taken at a rate of once per second, regardless of spin speed. However, the spacecraft receives the ground command only once per sampling period ($T_s = 2T$) as before. As a first attempt to analyze the problem, the simplifying assumption will be made that the rate term is computed by differencing position loop measurements taken once per sampling period. Since this is actually less often, i.e., worse, than what is actually happening, any results obtained by this analysis will be conservative.

The open loop transfer function, including delays, is L(z) where

$$L(z) = L_R(z) + K_x L_1(z) + K_p L_2(z) \tag{4-1}$$

where

$L_R(z)$ is the open loop transfer function of the rate loop in the spacecraft,

$$L_R(z) = K_o' K_R K_S \left[\frac{n_2 z^2 + n_1 z + n_o}{2z(z-1)^2} \right] \tag{4-2}$$

and $K_x L_1(z)$ is the rate term in the ground loop

$$K_x L_1(z) = \frac{K_o' K_s K_x}{z^K} \left[\frac{\sigma_2 z + \sigma_1}{2(z-1)^2} \right] \tag{4-3}$$

and $K_p L_2(z)$ is the position term in the ground loop or

$$K_p L_2(z) = \frac{K_o' K_s K_p}{z^k} \left[\frac{\mu_2 z^2 + \mu_1 z + \mu_o}{6 (z-1)^3} \right] \tag{4-4}$$

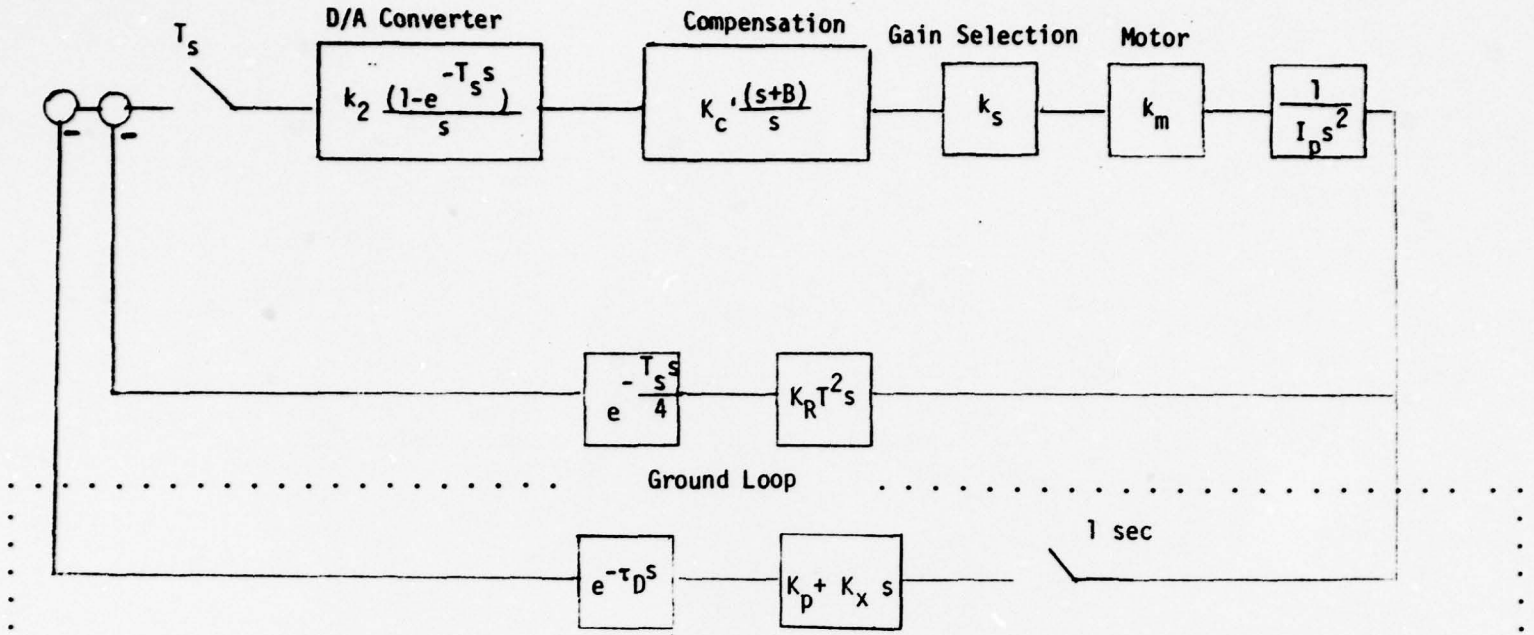

T = spin period
T_s = 2T = sampling period
τ_D = delay in ground loop
K_p = ground position loop gain
$K_R T^2$ = rate loop gain (K_R = 261)
k_s = selectable gain
K_x = ground rate gain

Figure 4-1. Despin Controller - Search Mode with Ground Rate/Position Loop

and

$K_R = 261\ T^2$

$K_o' = .00017938 = \dfrac{K_2\ K_c'\ K_m}{I_p}$

K_s = Selectable gain

K_x = Ground Rate Gain

K_p = Ground Position gain = K_p' x 261

$n_2 = T_s(2m + BT_s m^2)$

$n_1 = T_s[(2 - 4m - 2BT_s m^2 + BT_s(2m + 1)]$

$n_0 = T_s\ (2(m-1) + BT_s(m-1)^2)$

$\sigma_2 = BT_s^{\ 2} + 2T_s$

$\sigma_1 = BT_s^{\ 2} - 2T_s$

$\mu_2 = 3T_s^{\ 2} + BT_3^{\ 3}$

$\mu_1 = 4\ BT_s^{\ 3}$

$\mu_0 = BT_s^{\ 3} - 3\ T_s^{\ 2}$

Then the characteristic equation becomes

$$1 + L_R(z) + K_p L_2(z) + K_x L_1(z) = 0 \qquad (4\text{-}5)$$

In order to determine the range of K_x for stability, (K_x depends on the spin period T, the gain state chosen, and the position gain), the characteristic equation will be rewritten as

$$1 + \frac{K_x L_1(z)}{1 + L_R(z) + K_p L_2(z)} = 0 \qquad (4\text{-}6)$$

The characteristic equation is

$$1 + K_o' K_R K_s \left[\frac{n_2 z^2 + n_1 z + n_o}{2 z(z-1)^2}\right] + \frac{K_p K_o' K_s}{z^x} \left[\frac{\mu_2 z^2 + \mu_1 z + \mu_o}{6(z-1)^3}\right]$$

$$+ \frac{K_o' K_s K_x}{z^k} \left[\frac{\sigma_2 Z + \sigma_1}{2(z-1)^2}\right] = 0 \qquad (4\text{-}7)$$

Multiplying through by $6(z-1)^3 z^k$, we obtain

$$z^k 6(z-1)^3 + 3 K_o' K_R K_s z^{k-1} \left[n_2 z^2 + n_1 z + n_o\right][z-1] + K_p K_o' K_s \left[\mu_2 z^2 + \mu_1 z + \mu_o\right]$$

$$+ 3 K_o' K_s K_x (z-1) (\sigma_2 z + \sigma_1) = 0 \qquad (4\text{-}8)$$

Putting the equation into the form

$$1 + K_x G(z) = 0. \qquad (4\text{-}9)$$

we have

$$1 + \frac{3K_o' K_s K_x (z-1)(\sigma_2 z + \sigma_1)}{z^{k-1}(6 z^4 + \delta_3 z^3 + \delta_2 z^2 + \delta_1 z + \delta_o) + K_p K_o' K_s (\mu_2 z^2 + \mu_1 z + \mu_o)} = 0$$

where

$$\delta_3 = 3K_o' K_R K_s n_2 - 18$$

$$\delta_2 = 18 + 3K_o' K_R K_s (n_1 - n_2)$$

$$\delta_1 = 3K_o' K_R K_s (n_o - n_2) - 6$$

$$\delta_o = -3K_o' K_R K_s n_o$$

40 RPM

Figures 4-2 through 4-4 plot the maximum rate gain K_x for stability as a function of the ground loop delay for various gain states. The graphs are more accurate in predicting the stability of the actual simulation at the higher RPM's. This is to be expected, because in performing the analysis, the assumption was made that the rate term in the ground loop was determined by differencing position measurements taken once per sampling period, rather than once per second, as is done in the simulation. At the higher RPM's, where the sampling period is closer to 1 second, the analysis more closely typifies the actual flight conditions, whereas at the lower RPM's (e.g., 40) the analytical results are conservative. In any case, Figures 4-2 through 4-4 are to be used only as a guide to determine the rate gains, and the final determination must be made by simulation.

4.2 Performance Analysis

The performance analysis will once again be based on two criteria -- limit cycle performance, and the transient response (peak error) due to sudden changes in the friction level. The results will show that there is little improvement in the limit cycles behavior when the rate term is included in the ground loop, but at the higher RPM there is some improvement in the transient response, i.e., the resulting peak errors are not as large.

Figure 4-5 shows the time response of the system at 60 RPM to a simulated disturbance, (10 in-oz for 20 sec) where the ground loop controller has both a rate and position term. As can be seen, the limit cycle is again less than 2 degrees. The response to a larger disturbance (50 in-oz) is shown in Figure 4-6. Figure 4-7 summarizes the peak error responses to disturbance torques of various amplitudes at 60 RPM and compares the resulting peaks to the maximum error when the ground loop controller contained only a position term.

Figure 3-14a. Response of System to Large Disturbance with Counter Limits at ± 5, 60 RPM.

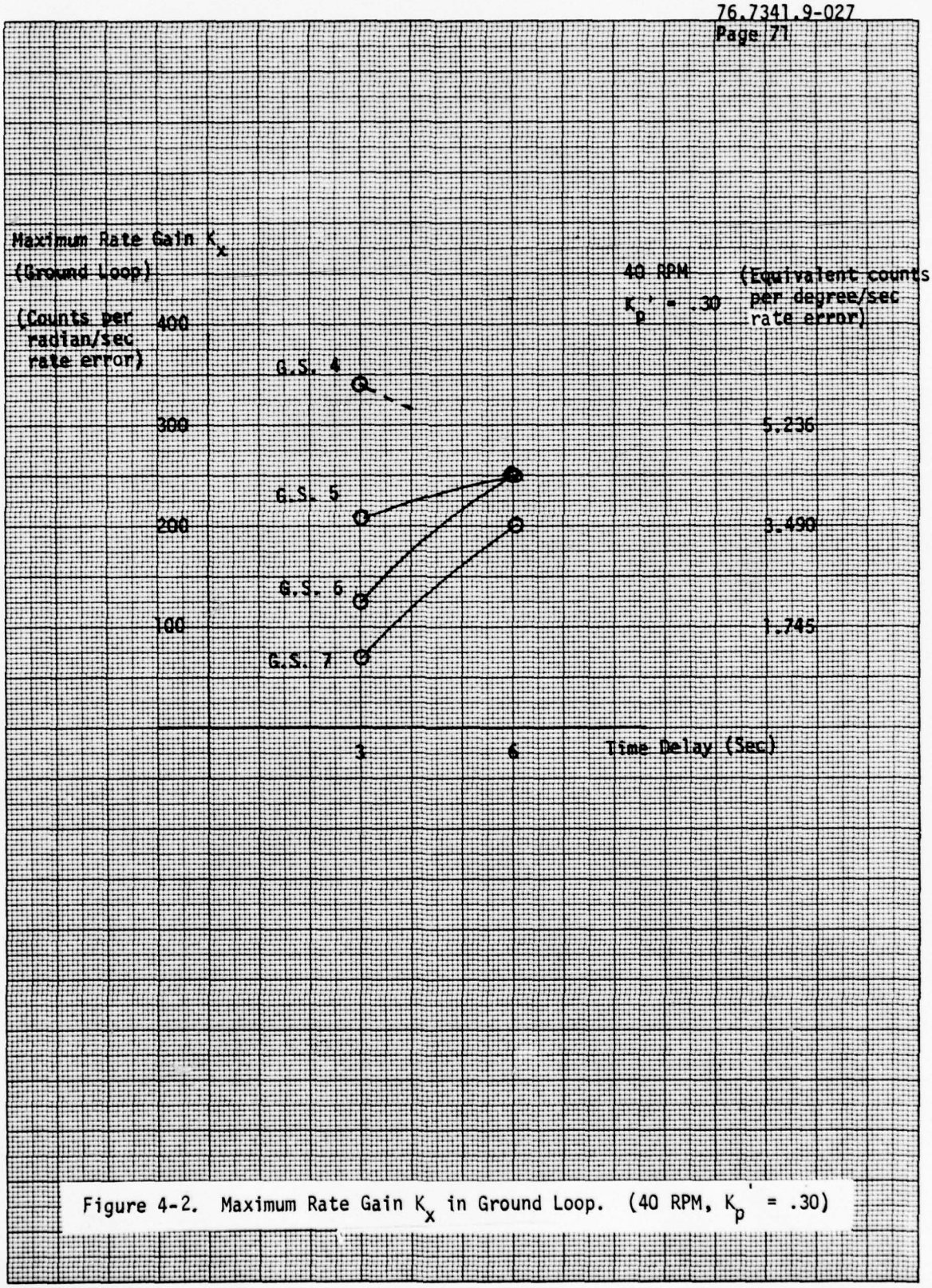

Figure 4-2. Maximum Rate Gain K_x in Ground Loop. (40 RPM, $K_p' = .30$)

Figure 3-14b Response of System to Large Disturbance with Counter Limits at ± 1, 60 RPM

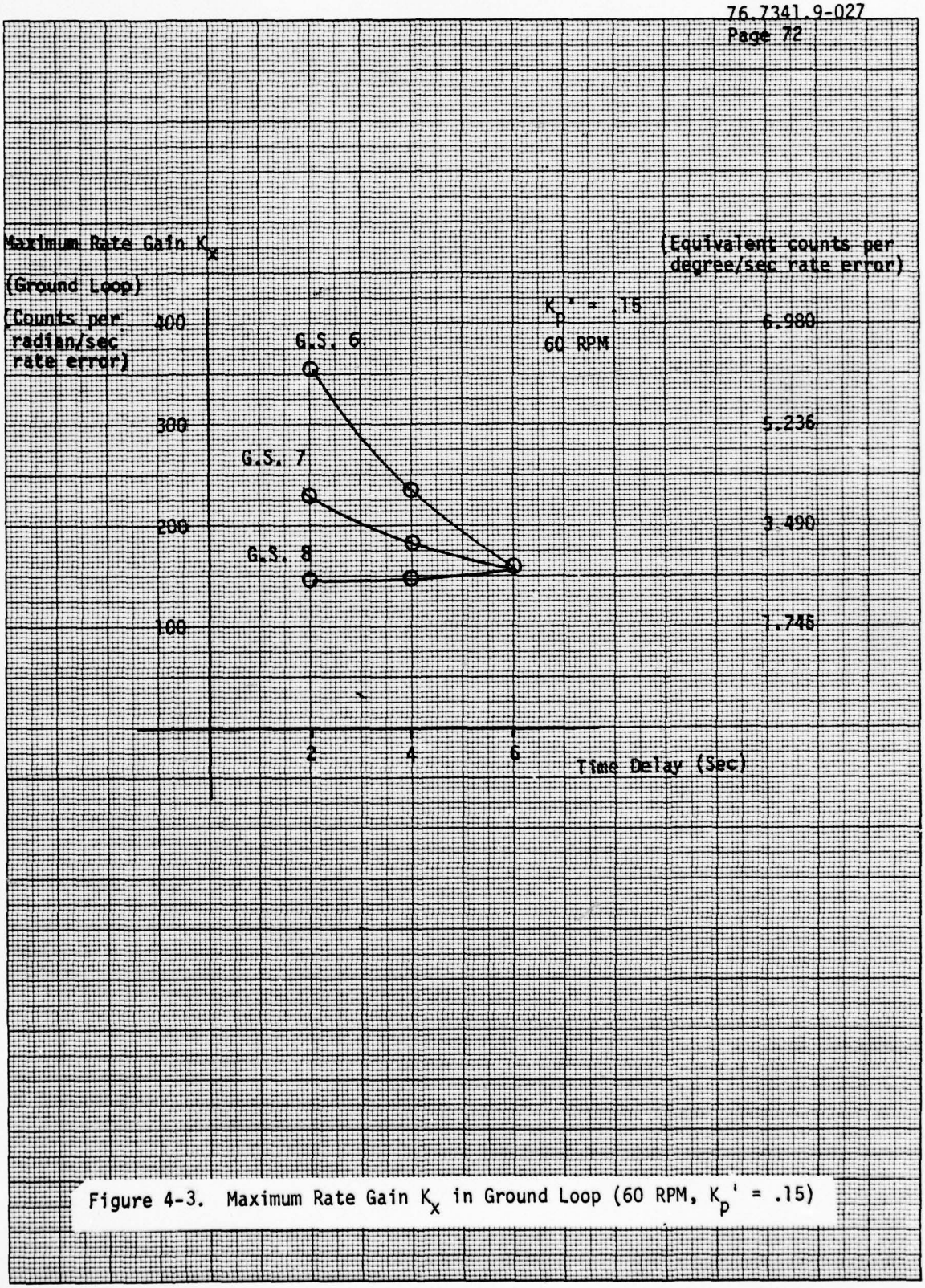

Figure 4-3. Maximum Rate Gain K_x in Ground Loop (60 RPM, K_p' = .15)

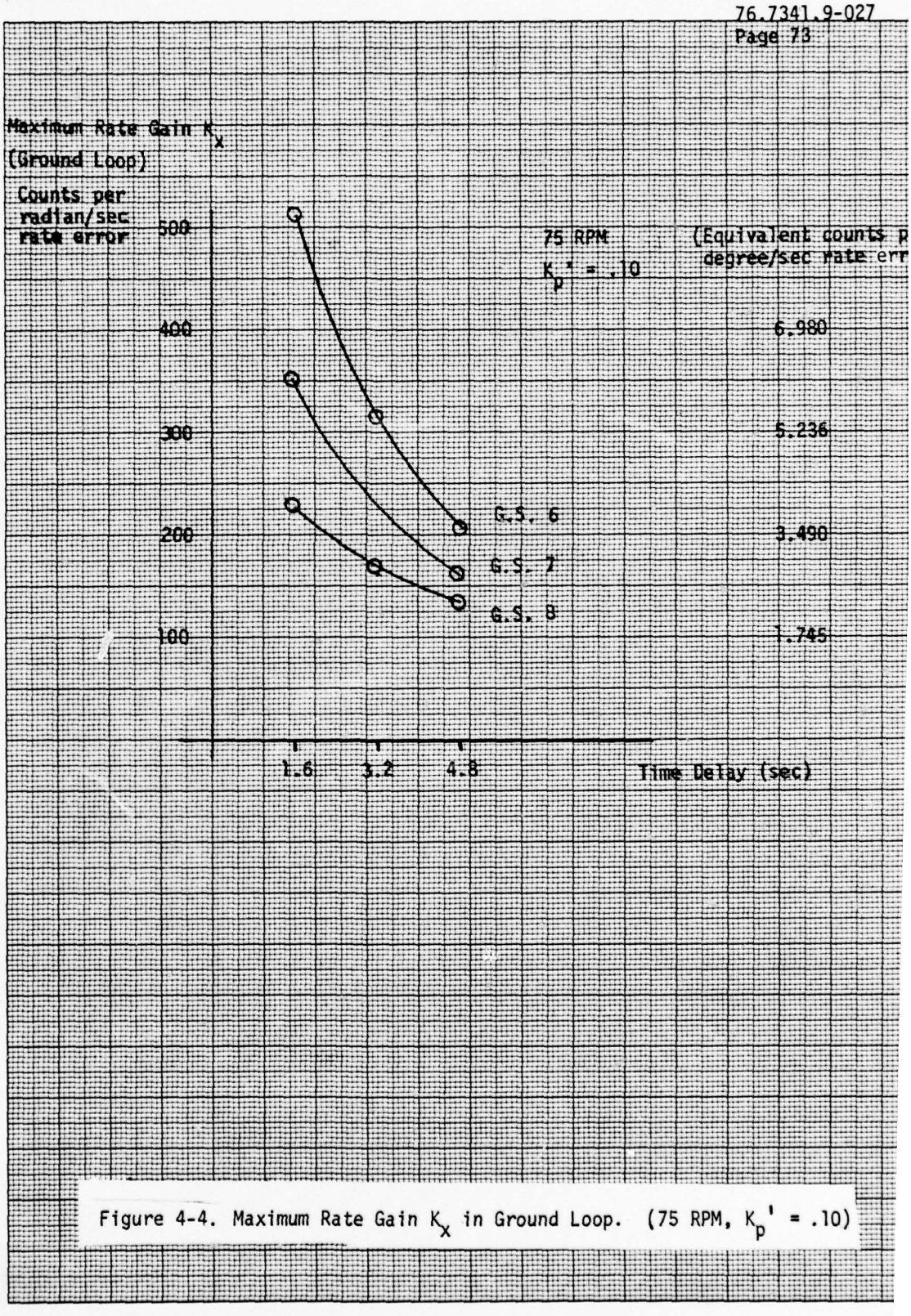

Figure 4-4. Maximum Rate Gain K_x in Ground Loop. (75 RPM, $K_p' = .10$)

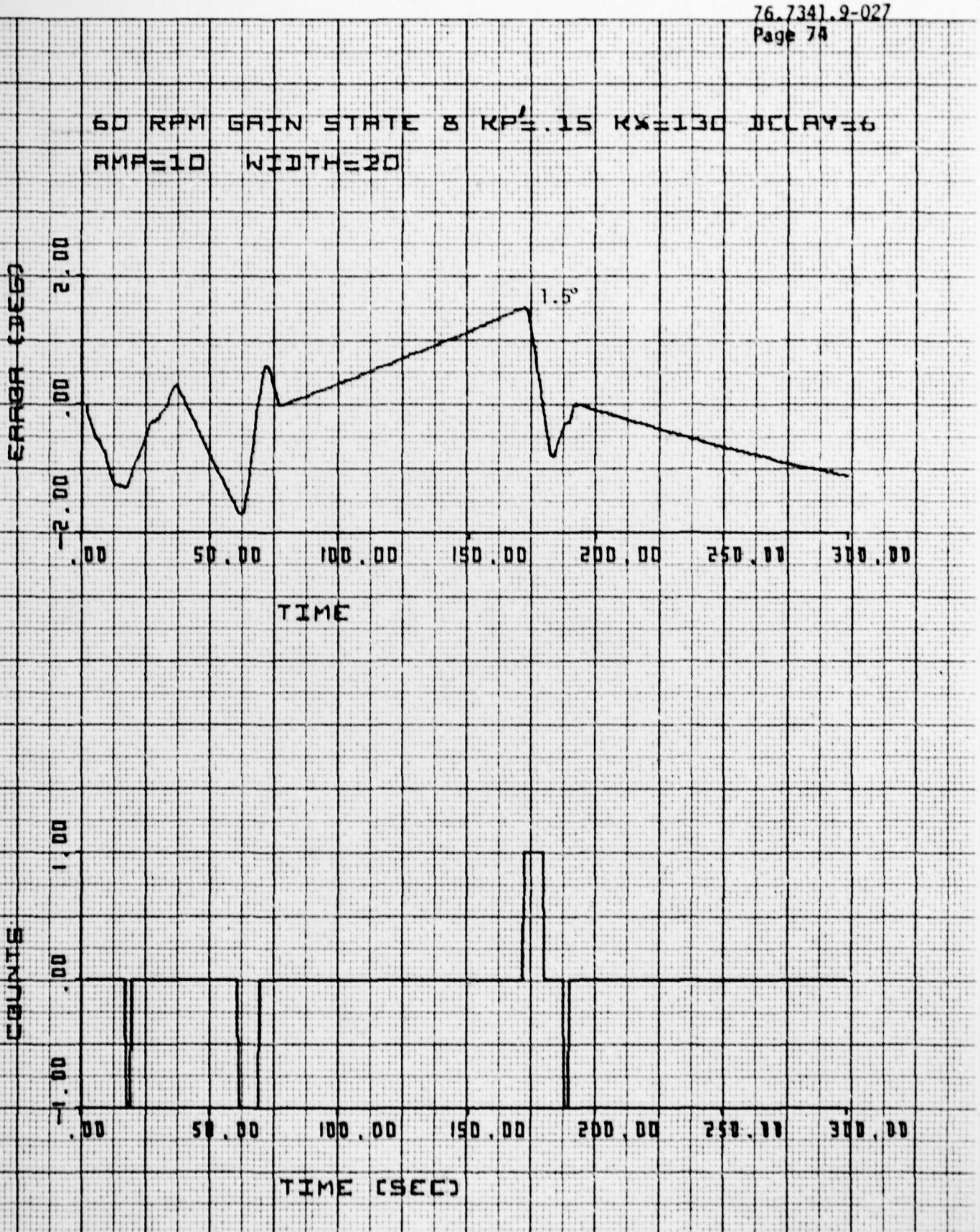

Figure 4-5. Response to Small Disturbance, Ground Position/Rate Loop, 60 RPM

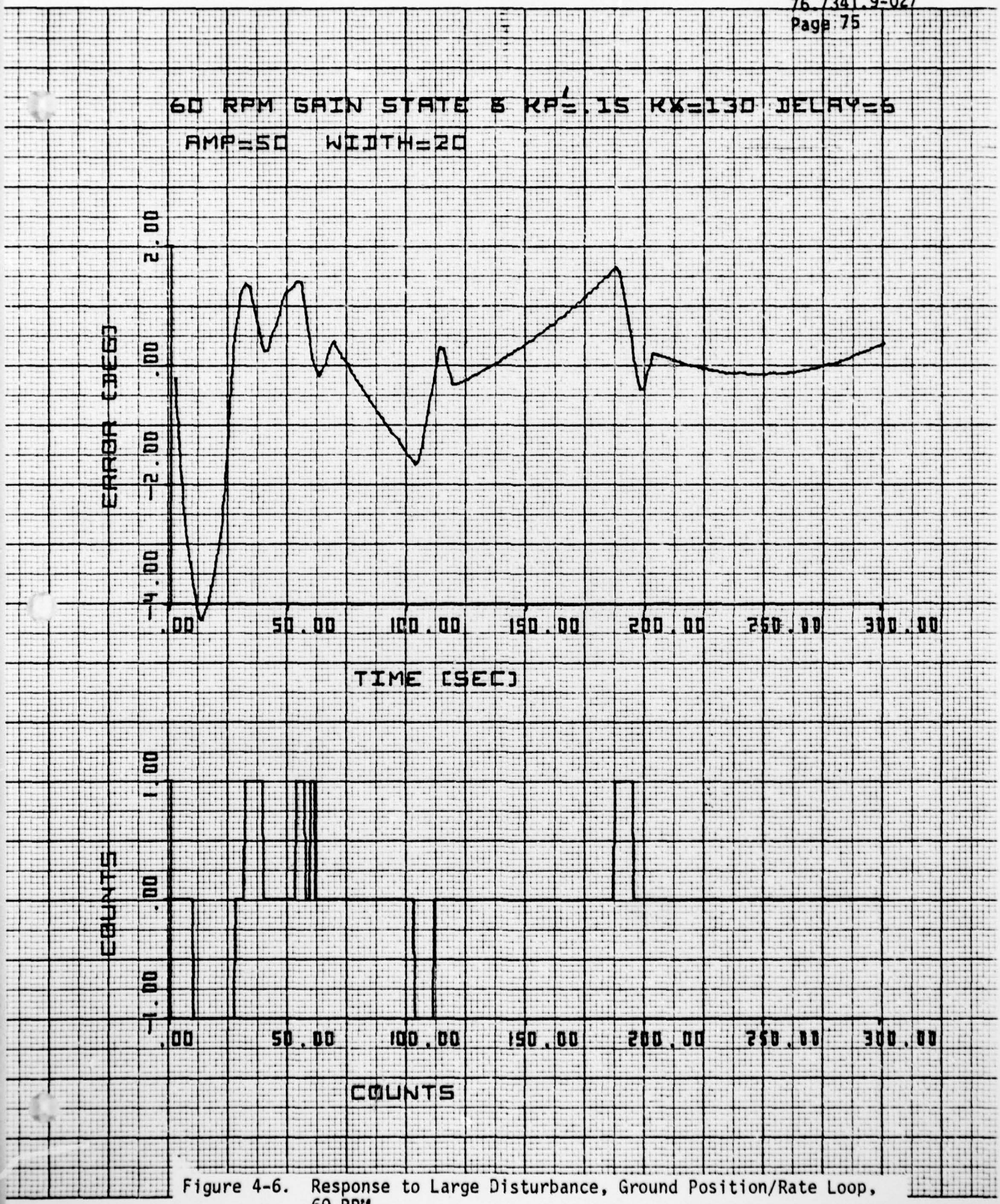

Figure 4-6. Response to Large Disturbance, Ground Position/Rate Loop, 60 RPM

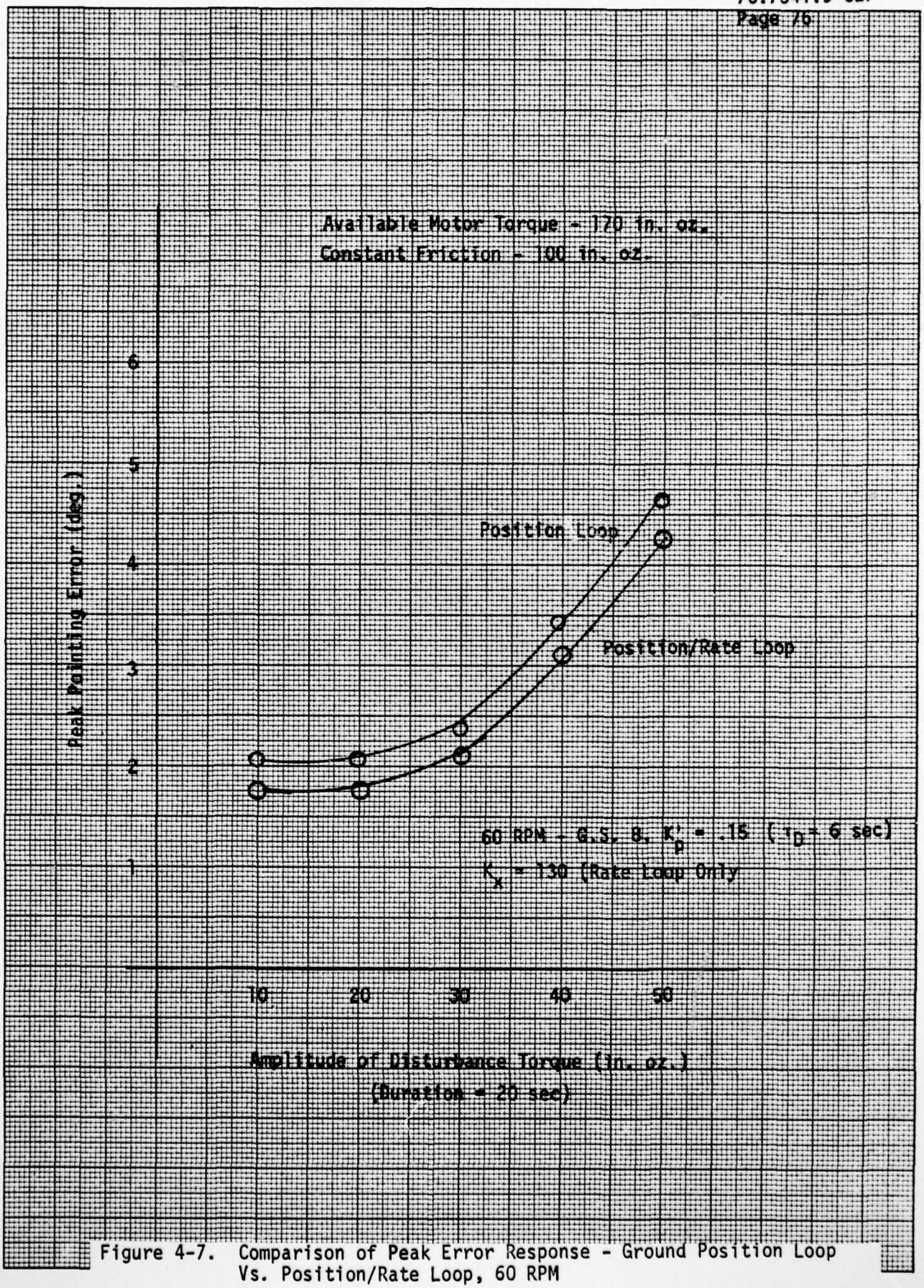

Figure 4-7. Comparison of Peak Error Response - Ground Position Loop Vs. Position/Rate Loop, 60 RPM

At 75 RPM, more improvement in the transient response is shown by the inclusion of the rate term. Typical time traces are shown in Figures 4-8 and 4-9, while the comparison with the performance of the controller with a ground position loop only is shown in Figure 4-10. The reason that more improvement is shown at the higher RPM is that the ground rate gain is larger compared to the spacecraft rate loop gain at 75 RPM than at 60 RPM.

At 40 RPM, there is no improvement in peak performance when the ground rate loop is included, and that is because the ground rate loop gain is almost insignificant compared to the rate loop gain in the spacecraft. This comparison of gains is summarized in Table 4-1.

Table 4.1 Rate Gains

RPM	Spacecraft Rate Gain (counts/rad/sec)	Ground Rate Gain (counts/rad/sec)
40	$261T^2 = 587$	150
60	$261T^2 = 261$	130
75	$261T^2 = 167$	150

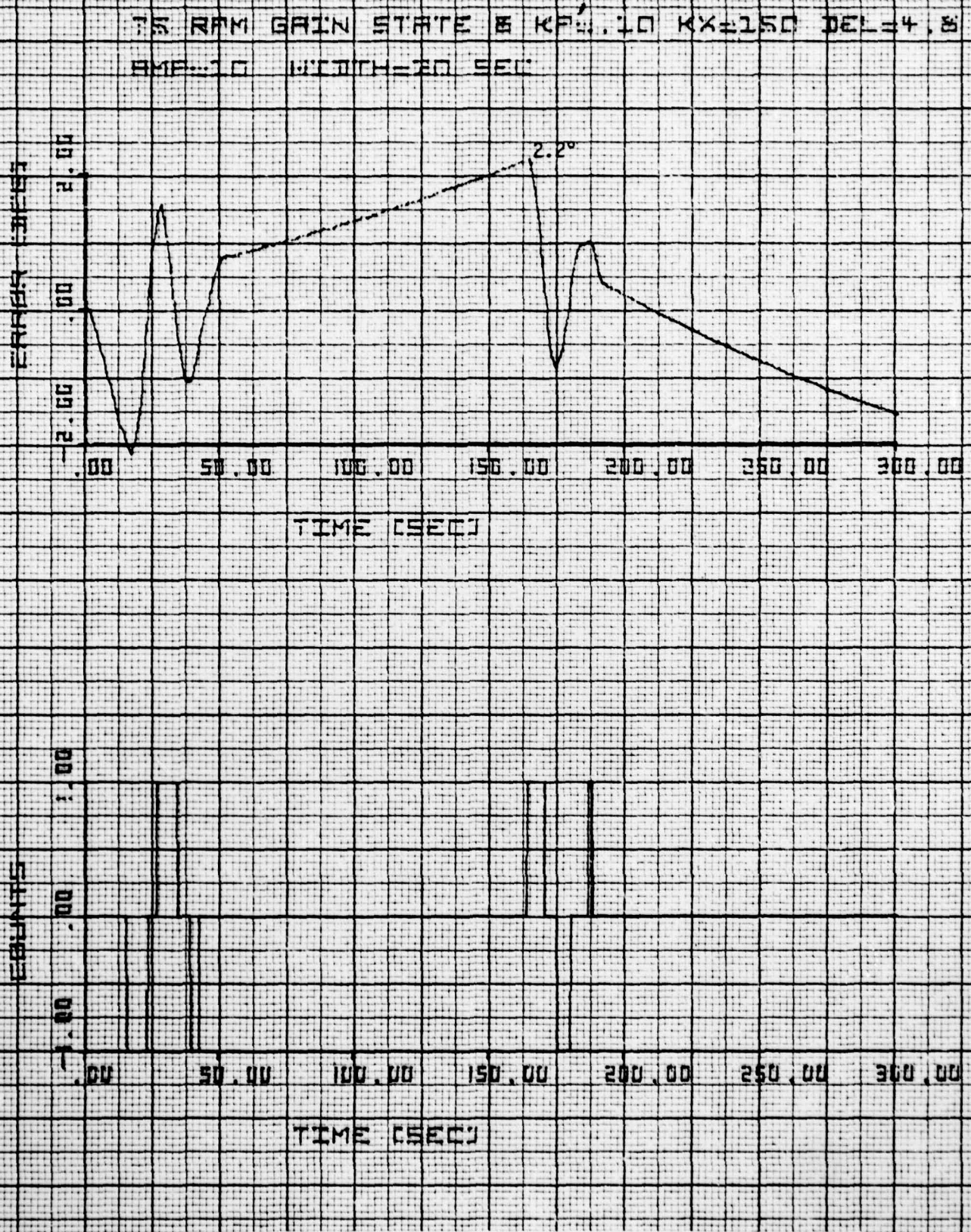

Figure 4-8. Response to Small Disturbance, Ground Position/Rate Loop, 75 RPM

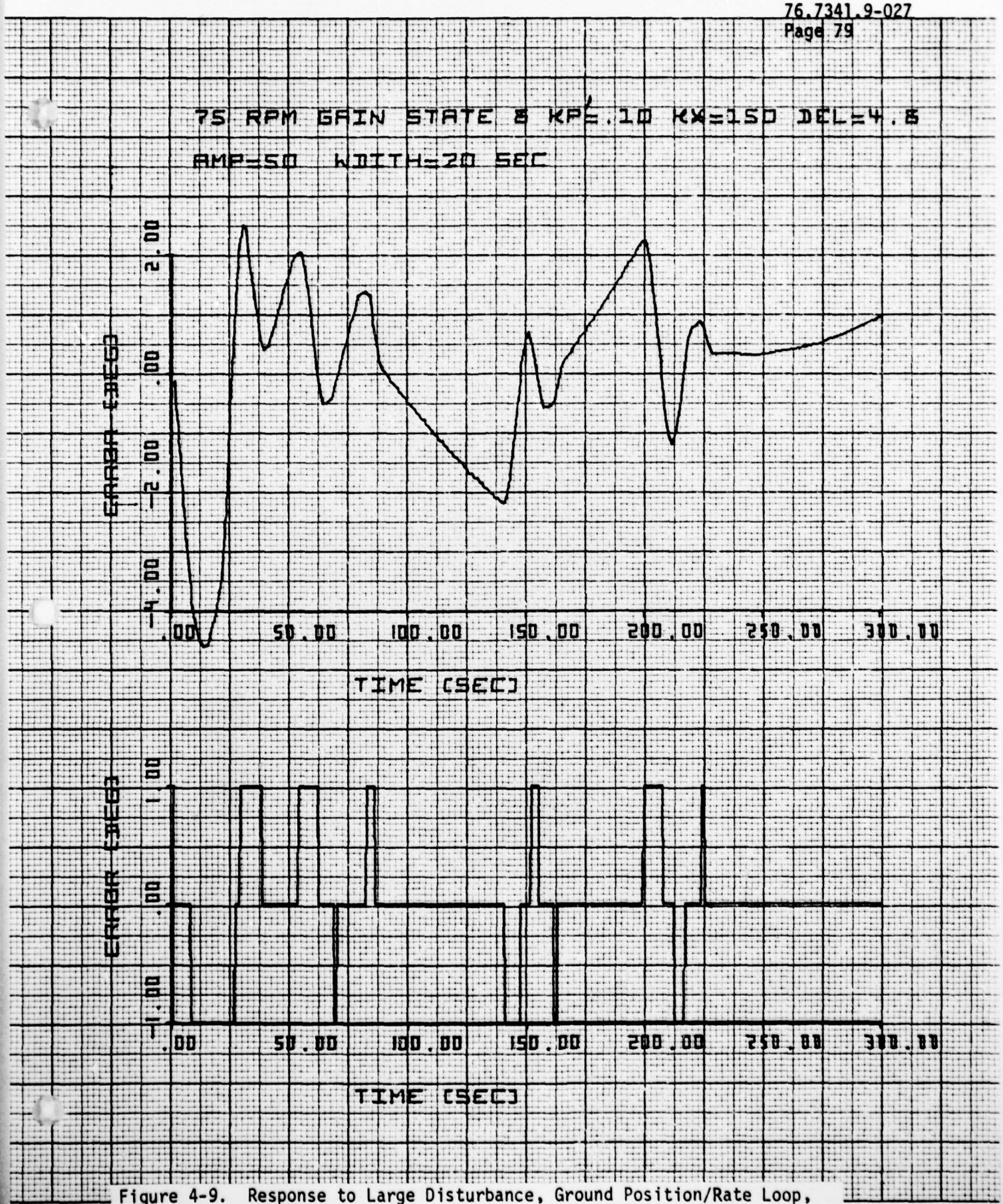

Figure 4-9. Response to Large Disturbance, Ground Position/Rate Loop, 75 RPM

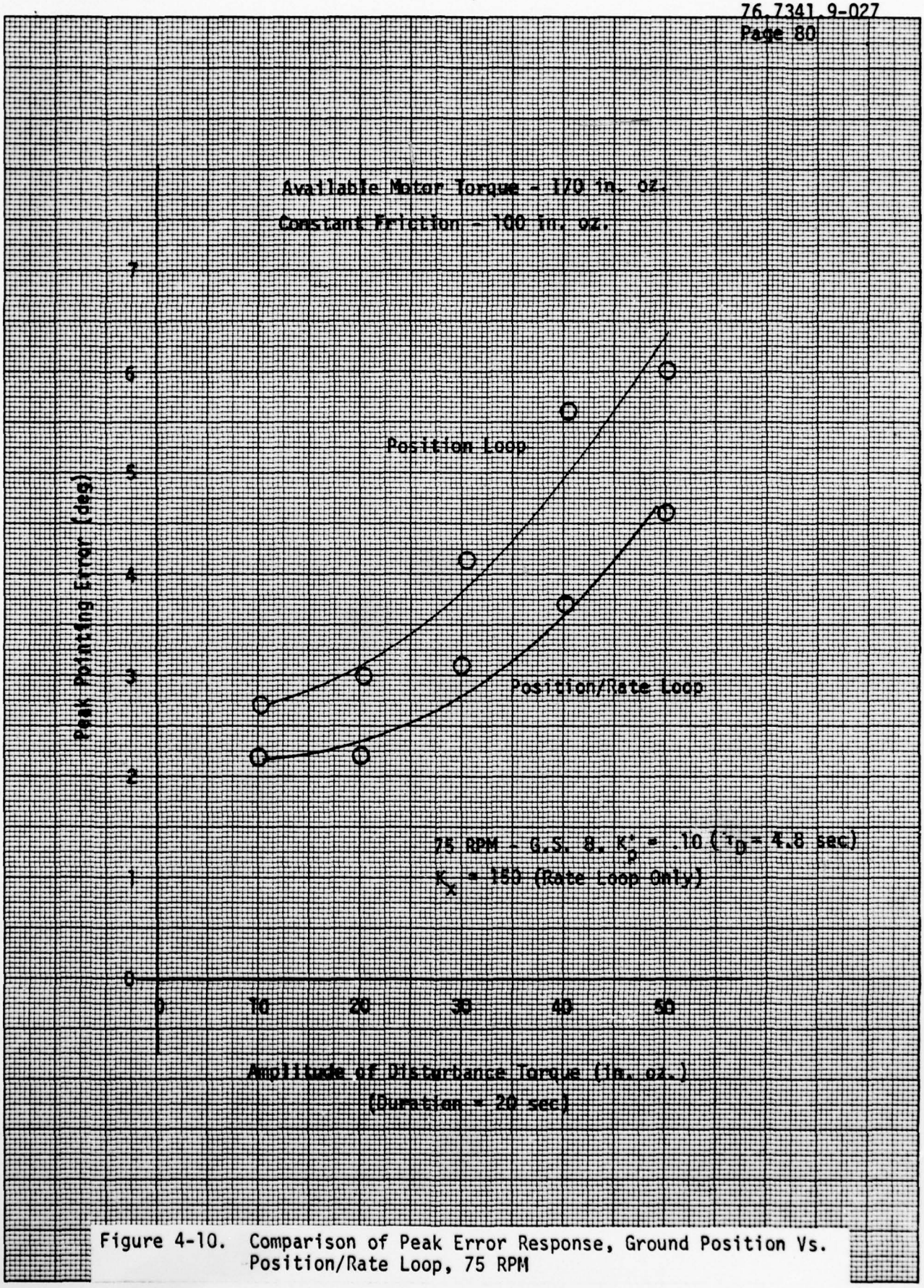

Figure 4-10. Comparison of Peak Error Response, Ground Position Vs. Position/Rate Loop, 75 RPM

5.0 IMPLEMENTATION

The implementation of the ground loop controller, i.e., the criteria for sending a count is very important, because the quantization necessarily produced by the fact that only an integer number of count can be sent is quite large compared to the computed control command. In this report, truncation was used to determine when commands should be sent, while round-off is to be used in the actual implementation of the controller. This is the reason the gains were divided by 2 in column 4 of Table 5-1. In addition, 1 count in either direction is sufficient for controlling the system, so the counter should be limited to $\pm$ 1 count. A diagram of the controller implementation is shown in Figure 5-1.

Some question has been raised regarding performance when the platform has been knocked off the earth, and the telemetered signals are no longer valid, but instead are the saturated value. Since the ground command is limited to 1 count anyway, it makes no difference that the values telemetered to the ground controller are limited to $\pm$ 6° when in reality the error is larger. The ground controller will continue to send 1 count until the error has been reduced sufficiently to bring the command inside the deadzone.

In addition, the question was raised as to how long the error should be off the earth before the control system is inhibited. In the normal mode, the criteria is 3 counts, or 3 seconds, and this was seen to be quite insufficient. It is recommended that the criteria of 60 counts or 1 minute be used in the "fly by wire" design, in order to allow the control system more than sufficient time to recover from large transients.

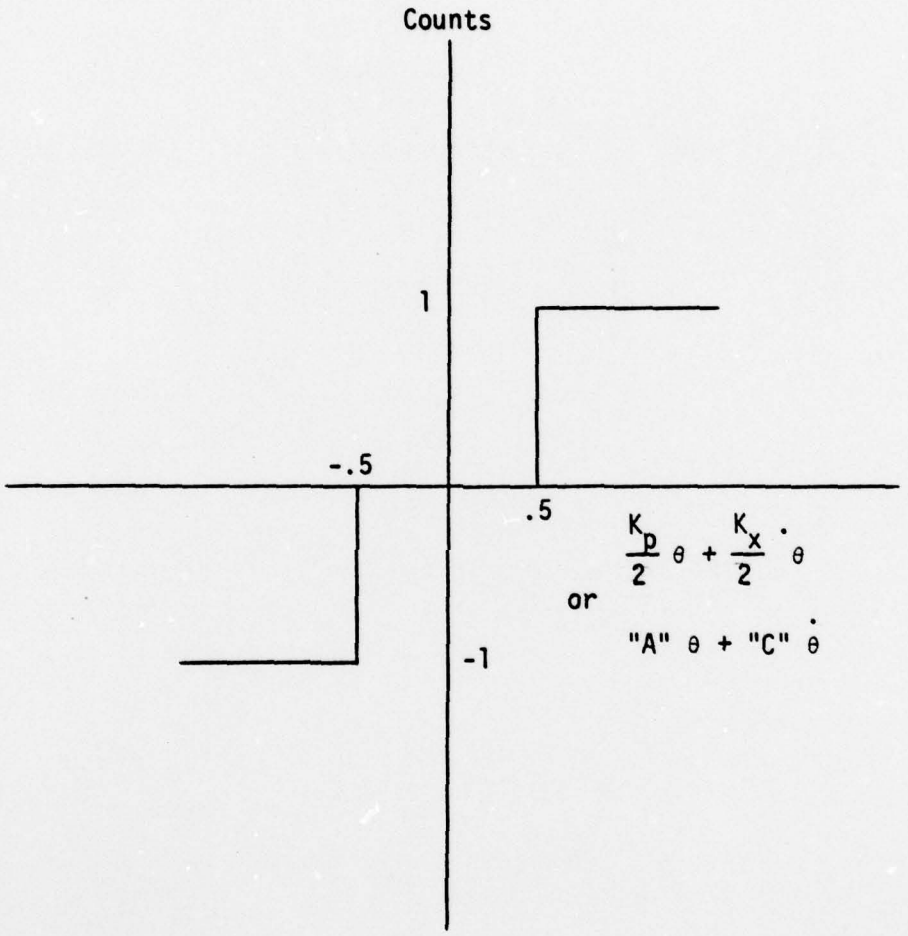

Figure 5-1. Implementation of Ground Loop Controller (Round Off)
(For definition of K_p, K_x, A and C see Table 5-1.)

TABLE 5-1 CONVERSION FACTORS

RPM	GAIN STATE	POSITION GAIN K_P (COUNTS/DEG) (TRUNCATION)	POSITION GAIN $K_P \div 2$ (COUNTS/DEG) (ROUNDOFF)	÷ CONVERSION FACTOR ÷ 16384/SPIN RATE (DEG/SEC)	NEW GAIN "A" (BIAS COUNTS/ TELEMETERY COUNTS	DEGREE ERROR WHEN 1 COUNT SENT = $1/K_P$
40	6	1.37	.685	68.27	.010	.73°
60	8	.68	.340	45.51	.0075	1.5°
75	8	.46	.230	36.41	.0063	2.2°
		RATE GAIN K_X (COUNTS/DEG/ SEC)	RATE GAIN $K_X \div 2$ (COUNTS/DEG/ SEC)		NEW GAIN "C"	
40	6	2.62	1.31	68.27	.019	
60	8	2.27	1.135	45.51	.025	
75	8	2.62	1.31	36.41	.036	

"A" and "C" are the designations being used in other reports to indicate the position and rate gain, respectively

6.0 CONCLUSIONS AND RECOMMENDATIONS

The results of this study indicate that the 777 spacecraft #9433 can be controlled with a reasonable degree of accuracy by operating the spacecraft in the search mode and sending up commands from the ground. It should be realized however, that because of the large quantization in the control system, a convergent response of the pointing error can never be obtained, and even in the steady state the response will be oscillatory.

Two basic ground loop control system designs were considered. The first consisted simply of proportional control, while the second used proportional plus rate control. These controller designs were evaluated using two criteria - limit cycle response (steady state) of the position error, and the transient response due to large torque disturbances (up to 50 in oz). For this study, the designs were tested at 40, 60 and 75 RPM.

In the steady state, the amplitude of the limit cycle oscillations depends on the magnitude of the position gain, and the stability analysis shows that a higher position gain is possible at the lower RPM's (Figure 3-1). Using the gains given in Table 5-1, the simulation results show, using proportional control only, that both the best limit cycle performance and transient response is obtained at the lower RPM's. At 40RPM, a limit cycle of about 1° can be expected compared to about 2 1/2° at 75 RPM. The peak errors in response to transients were summarized in Figure 3-20. When the rate loop is included, some improvement is seen in the transient response at the higher RPM's but at 40 RPM there is no difference.

It is thus recommended that the spacecraft be operated at the lower RPM's. In addition, it is recommended that the control system first be tested using only the position loop, and if this is satisfactory, that the rate term not be included.

REFERENCES

1. 28600-AR-010-01, Final Report, "9433 Despin Pointing Anomaly, dated 30 January 1976.

2. DSCS-FX-004, "Time Delays for Ground Loop Control Software Development," W. P. Carey, 23 February 1976.

3. 69.7231.9-70, 777-F2-282, "Design and Analysis of Program 777's Despin Control System," T. R. Bierma, December 1969.

4. 75.7341.9-47, "Simulation and Analysis of Abnormal Pointing Behavior on Spacecraft #9433," H. C. Osborne, dated December 30, 1975.

APPENDIX A. GROUND LOOP TIME DELAYS

Reference: DSCS-FX-004, "Time Delays for Ground Loop Control System Development," W. P. Carey, 23 February 1976

The above reference contains a detailed analysis of the various time delays associated with the 777 Command and Telemetry lines and on-board despin controller measurement logic. Table A-1, which is taken from the reference, presents the minimum and maximum delays associated with each RPM. The overall minimum value for the delay is 2.4 sec, and occurs at 75 RPM, and the maximum is 6.4 sec, occurring between 47 and 50 RPM.

The delays are plotted as a function of spin rate in Figure A-1.

Table A-1
Time Delays

RPM	T	τ_D MIN	τ_D MAX
75	.8	2.4	4.8
70.4	.852	Not Given	5.11
70	.857	2.57	14.29
65	.923	2.77	4.62
60	1.0	3.0	5.0
55	1.091	3.27	5.46
50	1.2	3.6	6.0
46.97	1.279	Not Given	5.11
45	1.333	4.0	5.33
44.7	1.342	2.64	Not Given
40	1.5	3.0	6.0

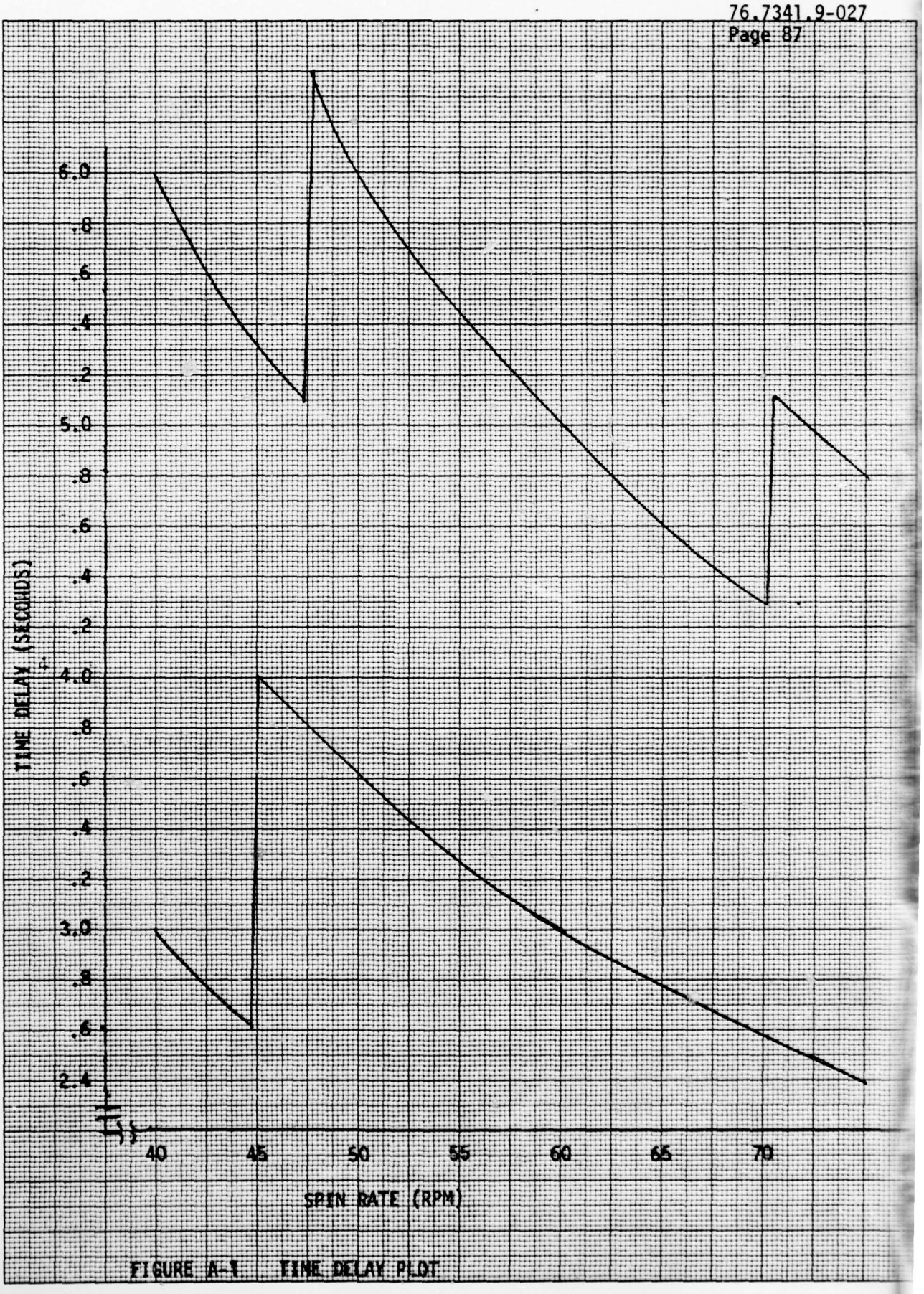

FIGURE A-1 TIME DELAY PLOT

AD-A073 342 TRW DEFENSE AND SPACE SYSTEMS GROUP REDONDO BEACH CA F/G 17/2
DESIGN AND ANALYSIS OF 777 'FLY-BY-WIRE' CONTROL SYSTEM.(U)
APR 76 H C OSBORNE F04701-75-C-0257
UNCLASSIFIED TRW-TR-28600-AR-011-01 SAMSO-TR-79-14 NL

2 OF 2
AD A073842

END
DATE FILMED
9-79
DDC

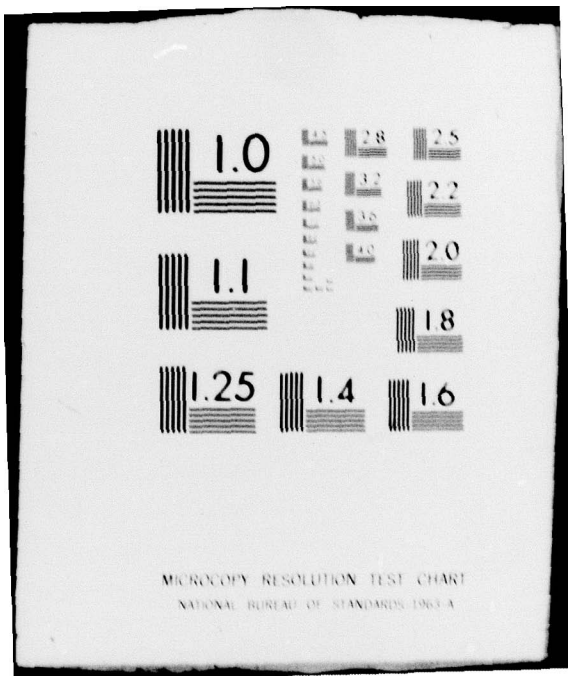
1.0
1.1
1.25
1.4
1.6
2.8
3.2
3.6
4.0
2.5
2.2
2.0
1.8
MICROCOPY RESOLUTION TEST CHART
NATIONAL BUREAU OF STANDARDS-1963-A

APPENDIX B. SIMULATION DESCRIPTION

The simulation results presented in this document were obtained from the Tymshare digital simulation briefly described in this appendix. This simulation (as well as this description) is based on the same 777 simulation used in Reference 3, with some modifications. The capabilities and limitations of the simulation are discussed in the following paragraphs, as well as the main differences between this simulation and the one of Reference 3.

B-1 Simulation Model, Saturation Limits

The simulation model is shown in Figure B-1. The simulation is patterned closely after the hardware limitations in order to realistically evaluate the effect of hardware non-linearities. For example, each of the saturations shown in the simulation represent saturation levels in the hardware. These saturation limits were often reached when the simulation was operated in the search mode. However, in the "fly by wire" mode of operation, where at most a few counts are being commanded from the ground loop and spacecraft rate loop combined, these can be neglected for the most part. For example the number counts needed to reach some of the saturation limits is shown below:

I_1 (= 14 volts)

$k_2 k_1 H_1 > 14$ or $H_1 > 1942$ counts, for saturation

I_2 (= 14 volts)

$k_1 k_9 H_1 > 14$ or $H_1 > 14$ counts, for saturation

A more complicated model of the integrator in the rate mode (denoted by levels I_5, I_6) showing the saturation effects was introduced in Reference 4, and this model has been retained in the simulation, although only the behavior in the linear region is indicated in the diagram.

B-2 Rate Measurement Logic and Relay

The measurement logic is a functional representation of the hardware. The platform rate error signals are not obtained in this simulation as they are in the hardware, by processing the earth sensor and platform reference

FIGURE B-1: PROGRAM 777 DESPIN CONTROLLER SIMULATION, "FLY BY WIRE"

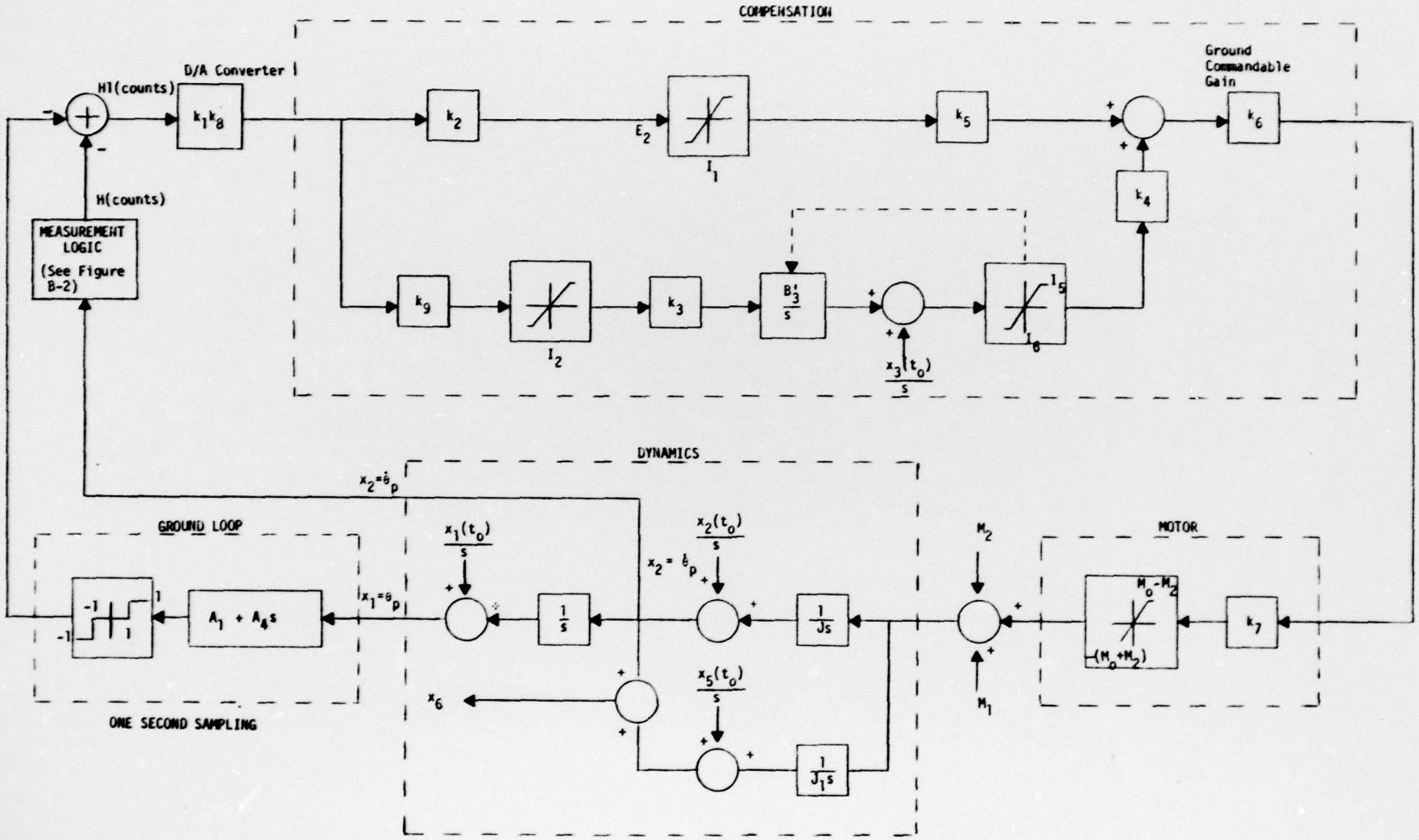

89

pipper signals. Instead, the up-down counter contents are calculated from the platform's instantaneous rate using appropriate scale factors.

The model of the measurement logic in the rate loop of the spacecraft is given in Figure B-2. This model is different than that of the simulation of Reference 3, which was incorrectly modeled with a double sided deadband, as in Figure B-3a. (For the mode of operation for which Reference 3's simulation was intended, this inaccuracy is insignificant.) For the "fly-by-wire" design, when the rate loop is at most putting out a few counts, and very often only one count, the modeling of the counts around zero is very significant. A provision has been made to study the effects of an asymmetric quantization model, (see Figure B-2) since in reality the counter is not "dead set" around 0.

The measurement delay of one quarter of a sampling period in the spacecraft rate-loop is implemented by saving the necessary variables 3/4 of the way through the integration subroutine, to be used in the next sampling period.

B-3 Ground Loop Model

The gound loop consists of both a position and rate term. The position gain A1 is scaled the same way as K_p" in the analysis presented in the body of the report. That is, the actual position gain will be 4.56 A1 counts/degree. This scaling can be changed by amending line 845 if the user finds some other units more convenient.

The rate term is computed by differencing position terms taken once per second, regardless of spin speed. The rate gain, A4, is in units of counts/radian/sec, but this can also be changed by altering line 843.

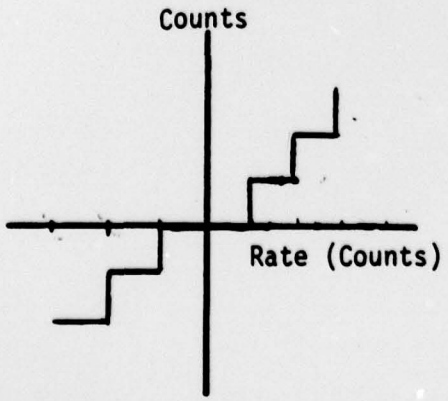

Figure B-3a. Incorrect Model - Double Deadband at Origin

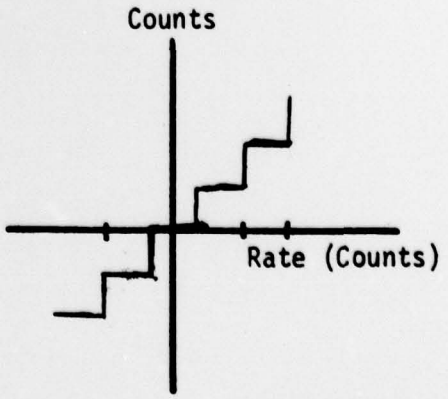

Figure B-3b. Correct Model - All Counts "Even"

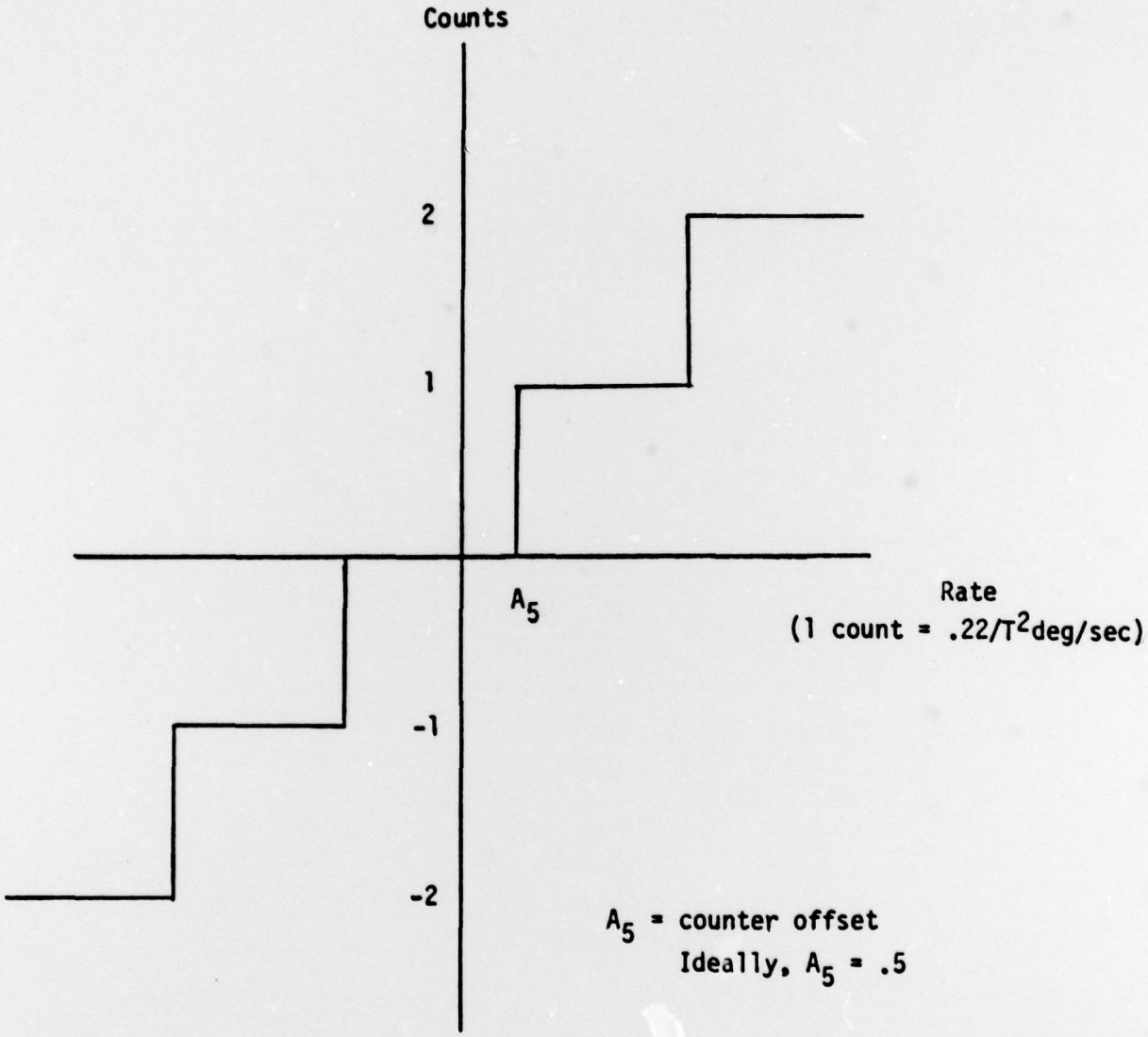

FIGURE B-2. Rate Quantization Model

The method of quantization (truncation) has already been indicated in Section 2.0, and one count is sent when the magnitude of the ground command exceeds 1. If it is desired to change this to round-off, the position and rate gains presented in the analysis should be halved.

B-4. Implementation of Ground Loop Delay

When this study of the "fly-by-wire" design first began, and only a position loop was considered, the ground loop delay τ_D was simply modeled as an integer number of sampling periods, or τ_D = D6 T_s, where D6 is an input to the program. (If D6 = 0, the ground loop delay was that of the rate loop, or $T_s/4$.) The following diagram shows how this was done.

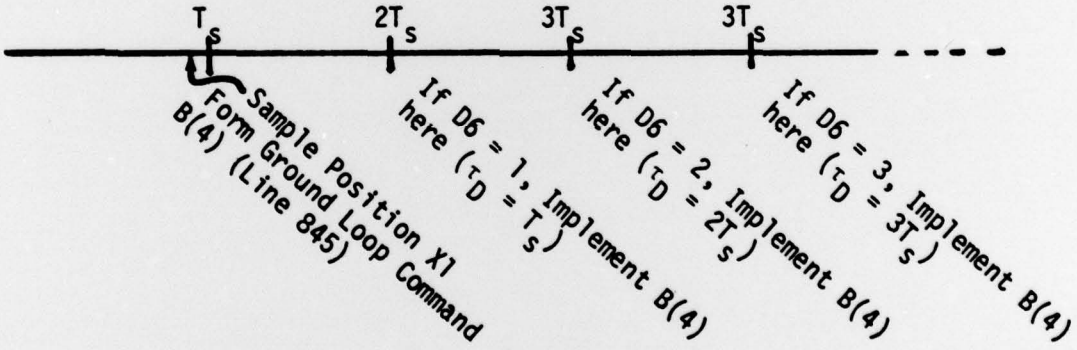

Figure B-4. Implementation of Ground Loop Relay in Simulation (Position Loop)

The fact that X1 was sampled "immediately before" T_s is indicated by the use of the variable X1 in line 845. The range of values of D6 to be used were taken from Appendix A. The fact that position measurements were taken only once per second was not modeled, since any delays associated with this could be accounted for by an appropriate choice of D6.

When the rate term in the ground loop was added, it was necessary to model the fact that the samples were taken only once per second since the rate term is computed by differencing position measurements. Figure B-5 shows the implementation of the delay under those conditions.

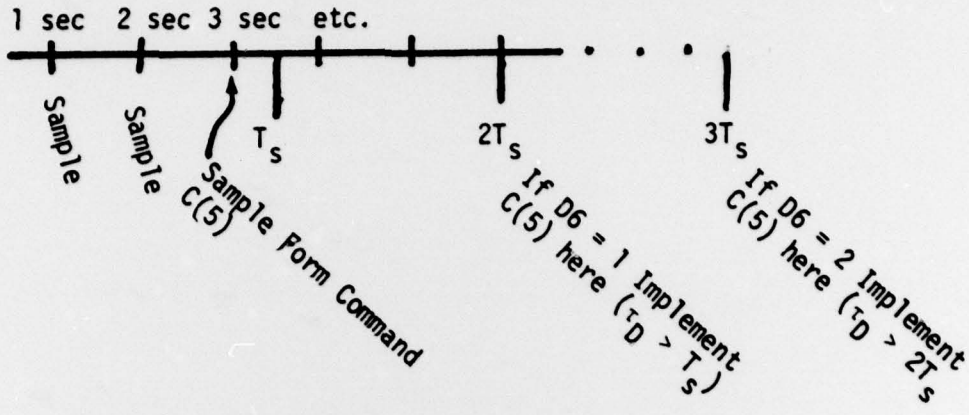

Figure B-5. Implementation of Ground Loop Delay - Measurements Taken Once/Sec

The important point to notice is that the resulting delay τ_D will be greater than D6 T_s. (For many of the simulation results the position term in the ground loop was still taken as shown in Figure B-4, i.e., for the position term only, the fact that measurements were taken only once per second was not used. This can be easily fixed by replacing X1 by X(1) in line 845, and any future simulation work should be done with this change made.)

B-5. Dynamics

The platform dynamics are simply modelled in the Tymshare simulation as rigid body, single axis linear dynamics, i.e. there is no cross coupling with the rotor or other platform rates. Nutation cross-coupling and damper dynamics are ignored. However, comparison between the dynamics of this simulation at the time it was originally written, and design verification runs, indicate that satisfactory results were obtained from using the simplified model.

B-6. Motor Model

One aspect of the simulation model that has recently come under close scrutiny is the motor model. Presently, the maximum motor capability is modeled as being constant, or the same for all spin speeds. However, recent studies have indicated that the motor capability might be greatly reduced at the higher RPM's. At this time no more definite model has been presented, and so this limitation has not been taken into account in the simulation.

TABLE B-1

PARAMETER DEFINITIONS FOR PROGRAM 777's

"FLY-BY-WIRE" TYMSHARE SIMULATION

PROGRAM SYMBOL	NOMINAL VALUE	DEFINITION
F	1	Mode control F = 1 - inhibit transfer from rate/search mode to normal control
P1	1	Number of sample periods between printout
N7	20	Number of integration steps per sampling interval
X1	variable	Platform position error (deg)
X2	variable	Platform rate error (deg/sec)
X4	variable	Integrator voltage in lead-lag filter (volts)
X5	360	Spacecraft rotor spin rate (deg/sec)
X6	variable	Relative rate between platform and rotor (deg/sec) X6 = X5 - X2
B(1)	0	Measurement voltage offset during rate/search mode
B(3)	0	Platform rate bias during serach mode (counts)
R	0	Spacecraft rate error (deg)
N0	0	Initialization of random number sequence
N1	variable	Measurement noise during serach mode
I1	14	Saturation level (volts)
I2	14	Saturation level (volts)
I5	5	Saturation level (volts)
I6	-14	Saturation level (volts)
B3	.0667	Integrator gain during rate/search mode
F1	1643	Measurement clock frequency during rate/search mode (counts/sec)
K1	5.86×10^{-3}	D/A converter gain (volts/count)
K2	1.23	Gain during rate/search mode which replaces the lead/lag network (volts/volt)
K3	.131	Integrator gain (volt/volt)
K4	.2286	Relative integrator gain (volt/volt)
K5	4.48	Relative lead-lag gain (volt/volt)
K6	variable	Ground commandable controller gain (volt/volt)

PROGRAM SYMBOL	NOMINAL VALUE	DEFINITION
K7	.4	Motor gain (ft-lb/volt)
K8	1	Measurement scaling gain (not really used in simulation)
K9	183.9	Integrator input path gain (volt/volt)
M0	170	Motor saturation (in-oz)
M1	100	Motor friction (in-oz)
M2	.14 X6	Motor back emf (in-oz)
J	69	Platform pitch inertia (slug-ft^2)
J1	339	Rotor pitch inertia (slug-ft^2)
D6	variable	Delay in ground loop (number of sampling periods) (see Appendix A) (if D6 = 0, Delay is same as spacecraft rate loop delay, i.e., .5T)
A1	.15	Ground loop position gain (K_p')
A4	130	Ground loop rate gain, counts/radian/sec
L1	1	Ground loop counter limit
A5	.5	Offset bias in simulation spacecraft rate loop counter (see Figure B-2)
T0	variable	Simulation run time (sec)
S(1)	variable	Sample period during rate/search mode
M9	variable	Number of torque pulses to be simulated
D(I)	variable	Amplitude of i-th pulse (in-oz)
U(I)	variable	Time i-th pulse begins (sec)
G(I)	variable	Time i-th pulse ends (sec)

```
4 SIGNIFICANCE 4
5 READ F , P1 ,  N7
6 OPEN =DATA=,OUTPUT,2
10 DATA 1,1,20
15 READ X1,X2,X4,X5,D6,A1,A4,L1,A5
20 DATA 0,0,0,450,3,.10,0,1,.5
22 X6=X5-X2
23 M2=.14*X6
25 READ B(1) , B(3) , R
30 DATA 0,0,0
35 READ N0 , N1 , N2 ,  I1 , I2,I5,I6
40 DATA 0,0,0,14,14,5,-14
45 READ  B3 ,  F1
50 DATA   0.0667 , 1643
55 READ K1 , K2 , K3 , K4 , K5
60 DATA 5.86E-3 , 1.23 , 0.131 , 0.2286 , 4.48
64 READ K7,K8,K9
65 DATA .4,1,183.9
69 READ K6,M1
70 DATA 11.32,100
71 READ M9
72 DATA 1
73 FOR I=1 TO M9
74 READ D(I),U(I),G(I)
75 NEXT I
76 DATA 35,0,20
78 READ M0,J,J1
80 DATA 170,69,339
85 READ M$,F$
90 DATA 0,0
91 B(4)=0
92B(5)=0
93 B(6)=0
94 B(7)=0
95 B(8)=0
96 B(9)=0
97 B(10)=0
98 X(1)=0
99 X(6)=X6
100 X(5)=X5
101  X(2)=X2
102 C(4)=0
```

PROGRAM INPUTS

INITIALIZATION

```
103 T3=0
105 C(5)=0
106 X(7)=0
107 X3=-(M1+M2)/(192*K4*K6*K7)
108 K$=M1,N$=0
120 PRINT ≡TIME(SEC)≡,≡X2(DEG/SEC)≡,≡X6(RPM)≡,≡X3(VOLT)≡,≡COUNTS≡
125 PRINT
127 F8=0
128 C8=1/114
130 TO = 0
131 E1 = K8*B(1)
132 E2 = E1 + X4
133 E3 = X3
134 E4=K9*E1
135 IF ABS(E4)>E2 THEN E4=SGN(E4)*E2
138 X7=K3*B3*X4
140 PO = 0
142 M3=0
145 PRINT TO , X2 , X6/6 , X3 ,
155 IF F = 2 THEN 380
160 N(1) = (RND(0) + RND(0) + RND(0) -1.5)*(N1/1.5)
180 S(1) = 720/X6
182 T=S(1)/N7
184 T1=T/2
186 T2=T1*T1
188 C9=EXP(-C8*T)
190 H=360*F1*(N(1)-X(2))/(X(5)*X(6))
195 B(5+D6)=B(5+D6)
197 IF ABS(B(5+D6))>L1 THEN B(5+D6)=L1*SGN(B(5+D6))
198 C(4)=B(5+D6)
199 H2=INT(ABS(H+30+A5))-30
200 H1 = INT(ABS(H+30 +A5))-30 + B(3)-INT(B(5+D6))
210 IF ABS(H1) < 511 THEN 230
212 IF H1 > 0 THEN 225
215 H1 = -511
220 GOTO 230
225 H1 = 384
230 E1= (K1*H1 + B(1))*K8
231 E2=K2*E1
232 IF ABS(E2)>I1 THEN E2=SGN(E2)*I1
233 E4=K9*E1
234 IF ABS(E4)>I2 THEN E4=SGN(E4)*I2
```

```
235 X8=X7
236 X7=K3*B3*E4
244 PRINT H1 IF T0=0
260 P0 = P0 + 1
270 IF P0<P1 THEN 295
280 PRINT ON 2: T0 ,-X1,-X2,-INT(B(5+D6)),INT(H2)
282 IF T0>298 THEN 1300
290 P0 = 0
295 IF F = 1 THEN 450
450 N9=.75*N7
480 IF D6=0 THEN GOSUB 700
481 IF D6=1 THEN GOSUB 699
482 IF D6=2 THEN GOSUB 698
483 IF D6=3 THEN GOSUB 697
484 IF D6=4 THEN GOSUB 696
485 IF D6=5  THEN GOSUB 695
486 IF D6=6 THEN GOSUB 694
490 GO TO 160
694 B(11)=B(10)
695 B(10)=B(9)
696 B(9)=B(8)
697 B(8)=B(7)
698 B(7)=B(6)
699 B(6)=B(4)
700 F(1)=1
705 FOR N8=1 TO N9+.5
710 T0=T0+T
712 T3=T3+T
713 IF T3>=1.0 THEN F3=1 ELSE F3=0
714 IF F3=1 THEN T3=0
715 X3=X3+(X7+X8)*T1 IF F8=0
720 X3=X3*C9+(E9+E4)*(1-C9) IF F8>0
725 X3=X3*C9+(E9+E4)*(1-C9) IF F8<0
730 E9=X3
735 F8=0
740 IF E9<I5 THEN 760
745 E9=I5
750 IF(E4+E9-X3)>=0 THEN F8=1
755 IF(E4+E9-X3)<0 THEN F8=-1
760 IF E9>I6 THEN 780
765 E9=I6
770 IF(E4+E9-X3)<=0 THEN F8=1
```

PRINTOUT

INTEGRATION UPDATE

INDICATES 1 SEC INTERVALS

```
775 IF(E4+E9-X3)>0 THEN F8=-1
780 M=192*K6*K7*(K5*E2+K4*E9)
785 FOR I=1 TO M9
790 IF TO>U(I) AND TO<G(I) THEN 795 ELSE 805
795 D$=D(I)
800 GO TO 815
805 D$=0
810 NEXT I
815 M1=K$+D$
820 IF M>M0-M2 THEN M=M0-M2
825 IF M<-M0-M2 THEN M=-M0-M2
830 M4=M3
835 M3=(M+M1+M2)/192
840 X1=X1+X2*T+57.3*(M3+M4)*T2/J
841 IF F3=1 THEN X(7)=X(1)
842 IF F3=1 THEN X(1)=X1
843 C(5)=A4*(X(1)-X(7))/57.3
845 B(4)=X1*(261)*A1/57.3
846 B(4)=B(4)+C(5)
850 X2=X2+57.3*(M3+M4)*T1/J
855 X5=X5-57.3*(M3+M4)*T1/J1
860 X6=X5-X2
865 IF F(1)=1 THEN X(6)=X6
870 IF F(1)=1 THEN B(5)=B(4)
875 IF F(1)=1 THEN X(2)=X2
880 IF F(1)=1 THEN X(5)=X5
885 M2=.14*X6
890 NEXT N8
895 IF F(1)=0 THEN GO TO 930
900 F(1)=0
905 N9=.25*N7
910 PRINT ON 2:TO,-X1,-X2,-INT(C(4)),INT(H2)
915 GO TO 705
930 RETURN
1300 CLOSE ALL
1400 END
```

Position measurements taken every sec

(Replace X1 by X(1))

Ground rate term

Ground position term

Total ground command

Implementation of Ts/4 Delay

Print out